Torbjørn Heimvik

Battery for Capacity Expansion

A Techno-Economic Case Study in Trøndelag

◙ NTNU

Norwegian University of
Science and Technology

Torbjørn Heimvik

Battery for Capacity Expansion

A Techno-Economic Case Study
in Trøndelag

NTNU
Norwegian University of
Science and Technology

Preface

This master's thesis marks the end of the two-years master's program in Energy and Environmental Engineering (*Energi og miljø, MIENERG*) at NTNU (*Norges teknisk-naturvitenskapelige unversitet*) in Trondheim. The work started in the end of August, 2022, and has been ongoing until the end of January 2023. It constitutes 30 ECTS of the master's degree.

The project of this thesis is about battery energy storage systems (BESSs) for capacity expansion, for a specific case in Fosen (Trøndelag, Norway), where there are congestion issues in the power grid. FosenKraft and GETEK AS have provided the problem description, and data has been made available by Nettselskapet AS (DSO). The approach has been to investigate the technical and economical feasibility of a solution with BESS, by building and solving optimization models. This has required knowledge and experience from several courses on, for instance, electric power engineering and economics, in additional to practice in logical reasoning.

The last year of study, starting with the specialization project during the spring of 2022, has been both rewarding and challenging. I have gained valuable insight and more in-depth knowledge about optimization of the power system, and the complexity of the required control strategies. However, it has also been a challenging process within a demanding field of subject. I would like to thank my supervisor, Associate Professor Mohammad Amin (NTNU), for his guidance throughout the specialization and master's project. In addition, a thank is given to co-supervisor Yusuf Shankar Gupta (NTNU), for his inputs and support throughout the master's project.

Furthermore, I want to thank Christian Eidsaune, Rune Otterstad and Helge Engebø, from Nettselskapet AS, FosenKraft and GETEK AS, for providing an exciting case and a substantial amount of data. Finally I would also like to express my gratitude to my family, friends and especially to my girlfriend. Your support have been of utmost importance.

Torbjørn Heimvik

Abstract

To cope with climate change and population growth, electrification and new renewable energy generation are suggested as important measures. However, this causes challenges for the power grids as the peaks of power production and demand become higher. A solution to this can be the use of battery energy storage systems (BESSs), which can support the power grid with stability services and the end users with demand side management.

For the case of this study, an end user in Fosen (Trøndelag, Norway) wants to increase its power consumption. But, as there are capacity limitations in the power grid, the grid customer is not allowed to increase its consumption of grid power before grid reinforcements are in place. Therefore, this thesis aims to investigate how a BESS can be a solution, making it possible to cover an increased demand, and if it can prove to be technically and economically feasible.

Li-ion batteries are the basis for the energy storage system in the case. It represents a versatile type of battery, that can be used for many purposes, and are known to have long life spans and high efficiencies. Although the investment cost of a Li-ion battery is high, the prices of the battery packs have reduced considerably the last decade, making it a feasible solution for several other projects. The technical principles and limitations of a Li-ion battery, based on the LMO-NMC chemistry, are included in the models of this thesis. This also comprises degradation.

Optimization models for sizing and operation of the BESS have been made and solved using the Julia programming language with JuMP and Ipopt. The optimization problem for sizing includes a simple model of the power grid, with relevant constraints such as available power, operating costs and BESS investment costs. The unit costs of 2 500 NOK/kWh and 3 200 NOK/kW are the basis for the this. The optimal sizing parameters are found to be 12 500 kWh and 1330 (1500) kW. Further, these are taken as inputs for the operation model, which aims to simulate optimal operation for a period of four years, by minimizing operating costs. Degradation is also taken into account, with the results showing an aging of around 20 % after four years.

The most significant results for BESS operation are found for variations in electricity spot prices. For highly varying prices, such as for the elspot of NO5 in 2022, the net present costs of operation are found to be 2.41 % lower than a hypothetical scenario with only grid power. But for low prices with little variations (NO3 elspot, 2020) the costs are found to be 3.64 % higher. In other words, the potential costs savings from a BESS, for the case of this thesis, are quite low or none. Therefore, the feasibility of the investigated solution is mostly dependent on the investment cost, assumed to be above 54 MNOK, and the estimated revenue from increasing the power consumption. The load profile of the end user, representing few opportunities for reduction in peak power, is pointed out as a main factor of why the BESS is not generating more savings.

It is concluded that a BESS is probably not an economically feasible solution for the case of this thesis.

Sammendrag

Elektrifisering og ny, fornybar, kraftproduksjon er viktige tiltak for å imøtekomme befolkningsvekst og redusere klimagassutslipp. Dette medfører imidlertid utfordringer for kraftnettet, på grunn av økte effekttopper på både forbruks- og produksjonssiden. Batterisystemer (BESS på engelsk) kan benyttes for å håndtere dette, ved å sikre stabil nettdrift og bidra til reduksjon i effekttopper hos forbrukere.

Denne case-studien baserer seg på en sluttbruker på Fosen (Trøndelag), som ønsker å øke strømforbruket sitt for å øke en næringsaktivitet. Men på grunn av kapasitetsutfordringer i overliggende kraftnett må strømkunder på Fosen i utgangspunktet begrense effektøkninger fram til at strømnettet er oppgradert. Denne masteroppgaven ønsker derfor å undersøke om det er mulig å benytte batterier som en løsning, slik at energiforbruket kan økes. Det vurderes om en slik løsning kan være teknisk gjennomførbar og mulig innenfor visse, økonomiske, rammer.

Energilagringssystemet baserer seg på Li-ion-batterier, som har vist seg å være en allsidig batteriteknologi som kan benyttes for de fleste formål. Selv om investeringskostnadene for slike batterier er relativt høye, så har prisene sunket vesentlig det siste tiåret, noe som har gjort flere batteri-prosjekter lønnsomme. Teknisk data og begrensninger for et Li-ion-batteri basert på LMO-NMC er utgangspunktet for denne oppgaven. Dette inkluderer også degradering (batteriets aldring).

Programmeringsspråket Julia er tatt i bruk for å løse optimeringsmodeller for både dimensjonering og drift av et batterisystem. Modellen for dimensjonering inkluderer også et enkelt oppsett av distribusjonsnettet, som sluttbrukeren er koblet til, med relevante restriksjoner på blant annet tilgjengelig effekt, samt drifts- og investeringskostnader. Enhetskostnadene som er tatt i bruk for batteridimensjoneringen er 2 500 NOK/kWh og 3 200 NOK/kW. Den første optimeringen resulterte i en batterikapasitet på 12 500 kWh og en installert effekt på 1330 (oppjustert til 1500) kW. Dette benyttes videre i driftsmodellen, med mål om å simulere optimal drift av batterisystemet for fire år, med lavest mulige driftskostnader. Her er også degradering av batteriet tatt hensyn til, og det viser seg at batterisystemets kapasitet reduseres med omtrent 20 % etter fire år.

Det er variasjoner i elektrisitetspriser (spotpriser) som gir de mest betydelige resultatene. Basert på spotprisene for NO5 fra 2022, som var høye og svært varierende, er netto nåverdi for driftskostnader 2.41 % lavere når batterisystemet benyttes, i forhold til et hypotetisk scenario hvor sluttbrukeren kun får kraft fra strømnettet. Men for tilfellet med lave og lite varierende spotpriser (NO3, 2020), vises det at kostnadene er 3.64 % høyere. Med andre ord så er de potensielle kostnadsbesparelsene med et batterisystem relativt små eller negative for casen i denne studien. Følgelig er de økonomiske fordelene ved et slikt system mest avhengig av investeringskostnadene, som er antatt å være omtrent 54 millioner NOK, og de potensielle inntektene som kan forventes ved et økt energiforbruk. Lastprofilen til sluttbrukeren, som er preget av et jevnt strømforbruk med få muligheter for effektreduksjoner, pekes på som en viktig årsak til at besparelsene ikke er større.

Det konkluderes med at et batterisystem antakeligvis ikke er en økonomisk gunstig løsning for den aktuelle casen.

List of Symbols

Symbol	Unit	Description
B	-	Battery, or point B (label).
C	*NOK*	Cost or cash flows.
c	*NOK/...*	Cost per unit (e.g. per unit of energy or power).
$cos(\phi)$	-	Power factor.
E	*Wh, Ah*	Energy, capacity.
f	*Hz*	Frequency.
G	-	Generator (label).
I	*A*	Electrical current.
I_0	*NOK*	Investment cost.
L	-	Load (label).
m	-	Month.
N_{eq}	*#*	Number of equivalent cycles.
P	*W*	Power.
Q	*Wh, Ah*	Capacity, energy.
R	Ω	Electrical resistance.
r	-	Decimal number: rate (discount rate).
S	*VA*	Power capability (apparent power).
t	*s, h*	Time.
T	°C, *K*	Temperature.
U	*V*	Voltage.
y	-	Year.
α_r	-	Discount rate.
γ	[%]	Battery degradation.
Δ		Delta. Indicating difference.
η	-	(eta). Efficiency, number between 0 and 1.0.
ϕ	°, *rad*	(phi). Phase displacement (voltage ↔ current).

List of Terms and Abbreviations

Term	Description
Anode	The electrode of which an oxidation process occurs. For a discharging battery cell, it is the negative electrode.
Arrhenius relationship	A certain temperature dependence of reaction rates (chemistry).
Balance of system	Referring to all components, structures and parts that are necessary for a system, in addition to the *main parts*.
Battery management system	Any electronic system that monitors and controls a rechargeable battery, for protection and balancing of charging and discharging.
Cathode	The electrode of which a reduction process occurs. For a discharging battery cell, it is the positive electrode.
Calendric aging	(Calendar aging). The reduction of capacity (mostly) and power capability (somewhat) of a battery, while the battery is at rest.
Converter	(Power converter). An electrical device for converting the characteristics of electrical energy. This involves changing voltage levels, currents and waveforms.
c-rate	A measure on the rate of charging and discharging of a battery, based on its capacity.
Current carrying capacity	Maximum continuous operating current (stationary) allowed for a specific conductor. Also known as thermal loading limit.
Cycle	(Charge cycle). The process of charging a rechargeable battery to a certain state, and discharge it back to initial state.
Cycle life	The number of cycles that a battery can undergo before its aging reaches certain limit.
Cyclic aging	(Cycle aging). The reduction of capacity and power capability of a battery, caused by the battery usage.
Demand side management	A strategy/process where the consumption of electric power, at the end users, are controlled, influenced and/or adapted. E.g. peak shaving.
Distribution system operator	Institutions or companies that operate and manage the distribution grids. They can also own the grid, which is the case of DSOs in Norway.
Energy arbitrage	The concept of buying and/or selling energy and taking advantage of price difference, in order to save or earn money.
Energy density	The amount of energy that can be stored, produced or distributed per unit of volume.
Inverter	A power converter that converts DC to AC. It is often used interchangeable with *power converter*, in cases where it can also convert AC to DC.
Load shifting	A strategy to shift load from periods of high power peaks to periods of lower power.

Peak shaving	A strategy to avoid power peaks by reducing consumption. Sometimes also called *load shedding*.
Power factor	The ratio of real power to the apparent power.
Round-trip efficiency	The relationship between the energy that is added to an energy storage system, and the energy that is retrieved from the same system.
Secondary battery	A rechargeable battery.
Second life battery	A battery that have been used, typically for transport/mobility, but are considered to be at its EOL for its purpose. However, having some more capacity left, it can be used for other purposes.
Specific energy	The amount of energy that can be stored, produced or distributed per unit of mass.
Spinning reserve	Extra generating capacity that is on-line but not in use.
State of charge	The energy level of a battery at a certain time, related to its nominal capacity. The opposite of *depth of discharge.*
State of health	A measure on the available capacity of a battery at a certain time, relative to the original capacity (of a new battery).

Abbreviation	Description
AC	Alternating current.
Avail.	Available. (E.g. available power).
BESS	Battery energy storage system.
BOS	Balance of system.
BMS	Battery management system.
BTM	Behind-the-meter (battery location in relation w/ the electrical meter).
Ch.	Charge.
DC	Direct current.
Dch.	Discharge.
DoD	Depth of discharge.
DSO	Distribution system operator.
Elspot	Electricity spot price.
EOL	End of life.
FEC	Full equivalent cycle (factor of equivalent cycles).
FTM	Front-of-meter (battery location in relation w/ the electrical meter).

Abbreviation	Description
HSE	Health, safety and environment.
HV	High voltage.
HVAC	Heating, ventilation and air conditioning.
IEA	International Energy Agency.
IEEE	Institute of Electrical and Electronics Engineers.
LFP	Lithium iron phosphate (battery type).
Li-ion	Lithium-ion (battery).
LMO-NMC	Li-ion battery with the Manganese Oxide/Nickle-Manganese-Cobalt blend.
MNOK	Million NOK.
NaS	Sodium-sulfur (battery).
NEK	The Norwegian Electrotechnical Committee.
NOK	The Norwegian krone (currency).
NO3, NO5	Price zones for electrical energy in Norway (west and mid-Norway).
NPV, NPC	Net present value, net present cost.
NREL	The National Renewable Energy Laboratory (the USA).
NVE	The Norwegian Water Resources and Energy Directorate.
OPEX	Operating expenses (operation and maintenance costs).
Pb	Lead (chemical element).
PV	Photovoltaic (technology for extraction of solar energy).
RMS	Root mean square. (Standard measure for currents and voltages).
RV	Residual value.
SoC	State of charge.
SoH	State of health.
s.t	Subject to.
T2	(This thesis:) Transformer connecting the regional grid with the distribution grid.
T3	(This thesis:) Substation connecting the end user to the distribution grid.
VAT	Value added tax (Norwegian tax on all goods and services).
VRFB	Vanadium redox flow battery.

List of Figures

List of Tables

Contents

1   Introduction and Background

High energy demand, especially in the form of electric power, represents a great challenge today and for the years to come. The challenge is present both globally, nationally and locally, due to population increase, higher loads and the need for replacing fossil fuels in order to reduce greenhouse gas emissions and global warming. Within 2050, the energy production from fossil fuels are predicted to fall to 31 %, from being more than 80 % today, while renewable energy sources (e.g. hydro, wind and solar) are predicted to constitute more than 62 % of the mix [1, 2]. This mix of resources represent highly intermittent power supplies which, in addition to higher loads from electrification, entails challenges for the power grids.

The increased amount of power that needs to be transferred from producer to user will require substantial upgrades of the power grids. However, grid reinforcements are expensive and may take long time to implement, which may cause the demand for power to increase faster than the amount of available power. This is the case for Fosen in Trøndelag, where end users want to increase their power consumption, but cannot do so due to capacity limits in the regional power grid. The deployment of stationary energy storage solutions, such as battery energy storage systems (BESSs), is often presented as a solution to challenges with power grid limitations and expensive reinforcements. Energy storage systems can reduce power peaks by shifting load in time, and thereby relieving the power grid. A BESS could also be a solution for the case in Fosen [2, 3].

1.1   Challenges in Distribution Grids and How Batteries Can Be a Solution

The Norwegian Water Resources and Energy Directorate (NVE) expects energy consumption to increase more than energy production until at least 2030, mainly due to electrification of the transport sector and the establishing of new industries. Approximately 50 % of the energy consumption of today originates from electrical power, and the share is assumed to grow. This development requires the need for importing power through power grid infrastructure with high capacity. However, there are several bottlenecks in the Norwegian power grid, where the power capability of grid infrastructure set limits on the power flow. These are mostly found in the distribution grids (voltage below 22 kV) and regional grids[1] (voltage ranging from 66 kV to 132 kV) [4].

The power capability of distribution grids depend on the amount of power that can be transferred without harming its components and causing bad voltage quality. The required quality of electricity supply, including voltage quality, is defined in laws and standards such as *the Norwegian regulation of quality of supply [5]*. When the power flow in the grid exceeds certain levels, depending on the grid

---

[1]The regional grid is a part of the transmission grid.

design, the voltage waveforms, frequency and magnitudes will be affected. This must be avoided, and has traditionally been solved by grid upgrades. However, as mentioned, grid upgrades may not be economical feasible or immediately possible in several cases [6].

The above-mentioned issues can be solved by installing batteries at strategical locations in the power grid. These solutions can also be economically feasible compared to grid upgrades [7, 8]. Battery installations located in the grid, providing services for the system operators (DSOs and TSOs), are known as front-of-the-meter (FTM) batteries as they are located on the grid side of an electric meter. Examples of use cases for such installations are frequency regulation, energy shifting / load leveling, voltage support, capacity reserves, phase balancing, reducing curtailment of renewable energy generation and backup power [9, 8].

The two first properties are illustrated in figure 1. The frequency of the grid is balanced by providing power when the grid frequency is found to be too low and by absorbing power when the grid frequency is too high (above 50 Hz). This is illustrated in figure 1a. In figure 1b, the load is covered within the power capability limits of the grid. The latter case can for instance be relevant if the power required by a low voltage load would cause too high voltage drop in the transfer system if provided directly by the grid.

(a) BESS for frequency regulation.　　　　(b) BESS for load leveling / Load shifting.
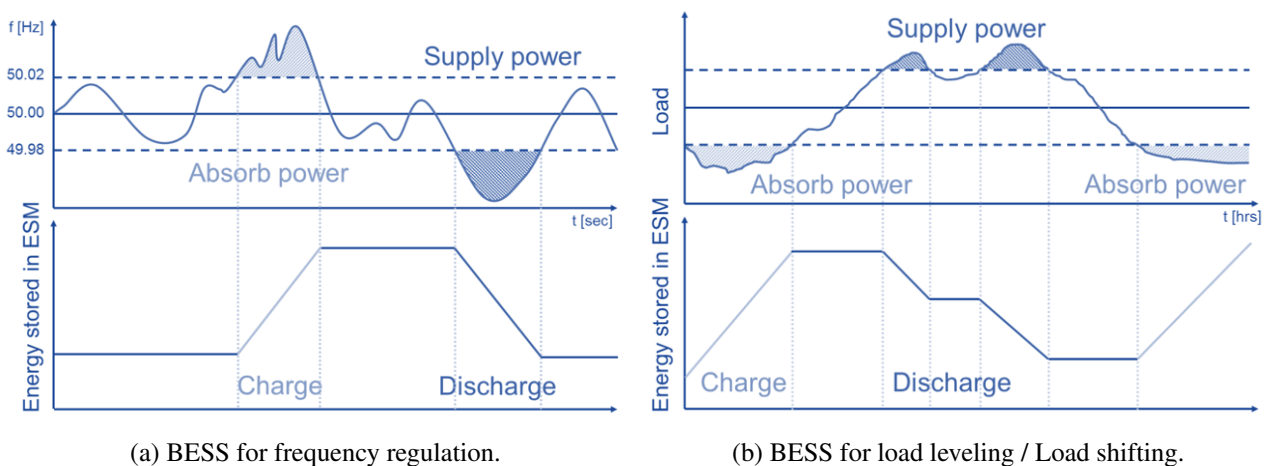
Figure 1: Example on BESS charging and discharging for grid support. Adapted from [10].

According to *the Norwegian regulation of quality of supply [5],* the Norwegian DSOs are obligated to ensure that the variations ins system voltages are minimized. Slow variations in the RMS value of the system voltage must be within ± 10 % of nominal value, measured as an average over one minute, at the point of connection between high voltage and low voltage. In addition, short-term and rapid overvoltages and undervoltages are not allowed to be higher than 3 % and 5 % of nominal system

voltage, for $dU_{s.s}$ and dU_{max}[2], respectively *[5]*. Referring to figure 1b again, the peaks in load could potentially result in voltage reductions that are too high according to the above-mentioned criteria. By rather providing the load with energy from a battery during these instances, the system voltage can stay within the required limits [8, 10].

It must be noted that distribution system operators (DSOs) have not been allowed to own, develop or operate own energy storage systems. This is stated in the EU directive on common rules for the internal market for electricity, article 36 ([11], 2019). However, energy storage systems like batteries can be allowed for some exceptions, where regulating authorities (NVE in Norway) give approval. Such circumstances can be if the batteries are necessary for the grid operation [8, 7]. The main reason for this regulation is that DSOs, being monopolists, can exploit own energy storage systems over other flexibility solutions, and thereby reduce the effectiveness of the electricity market. A proposed solution to this challenge is that a third party is involved. Some DSOs own and operate batteries in Norway today, with dispensation from NVE [6].

1.2   Batteries for Demand Side Management

As mentioned initially, the need for increased power transfer capabilities are to a large extent caused by an increased demand for electric power, due to electrification and new industry. Therefore, another approach to deal with this challenge, is to deploy battery storage systems at the load (demand) side. These are known as behind-the-meter (BTM) installations, where grid customers own the battery systems and pays for the electricity needed for charging [9]. A BTM battery facilitates for demand side management, which could be beneficial for both the DSO and the end user owning the battery. In short, load side management are measures to control energy usage, in order to postpone investment in new electrical installations, reduce operating costs and/or to ensure that energy usage stays within limits on available energy to avoid overload situations [12].

Figure 2 illustrates four categories of demand side management, that can be facilitated with a BESS. Peak shaving, also referred to as load clipping and load shedding, means reducing or cutting the load for periods. This can be a measure to avoid high peaks or operation that can cause overloading on the energy input source (being for instance the connection point of the power grid). If it is possible to rather cover the peak with local (own) energy production, this could be done in stead [12].

---

[2]$dU_{s.s}$: Stationary (steady state) change of voltage due to a characteristic of change in voltage [5]
dU_{max}: Maximum change of voltage during a characteristic of change in voltage [5]
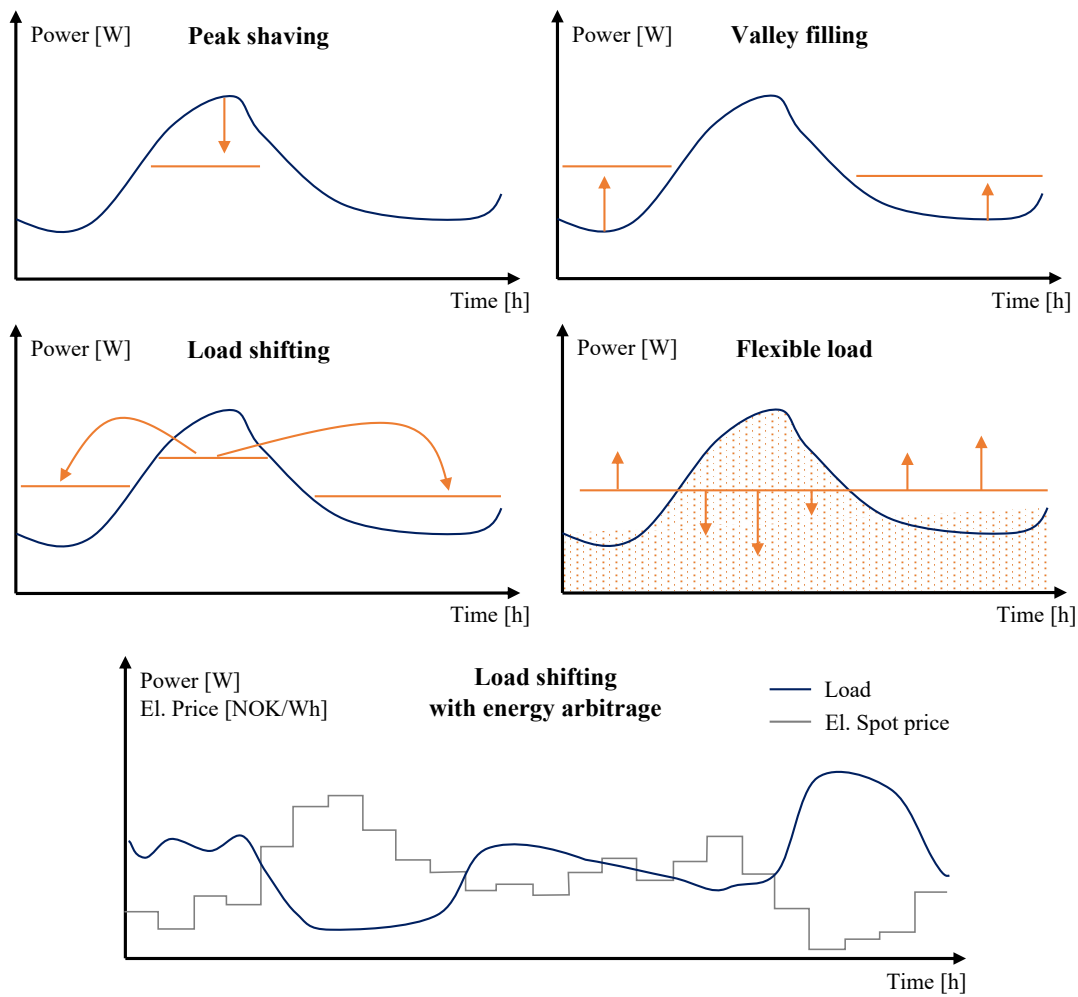
Figure 2: Examples on demand side management. Adapted from [12].

Having a BESS, it is possible to charge during periods of low demand, and discharge during periods of high demand. This is called load shifting, and makes the load profile more flat. The total energy consumption, and amount of energy imported from the grid, remains the same[3]. Many grid costumers pay for their peak power, as a part of the grid tariff, which means that there are also economical motivations for peak shaving and load shifting[6]. Valley filling is the case when the load is increased only in periods of low demand, without reducing the power peak. If the load can combine several of these demand side techniques over time, for instance in cooperation with a DSO, the load is said to be flexible [12].

Another advantage with BTM batteries is that the above-mentioned techniques can be combined with energy arbitrage. This is the process of buying energy when the price is low, and selling it or using it, when the price is high. By using a BESS with energy arbitrage, it is possible to cover the load at lowest possible energy costs, by charging when prices are low and discharging when prices are high.

---

[3]Except for some losses in energy storage and conversion.

The discharged power can then cover the load, and give savings in energy costs, and excess power can be sold to the grid and generate revenue. Customers who do the latter are referred to as prosumers. In Norway, NVE has set a maximum limit on the power that can be sold without having to pay for production, currently being 100 kW [13, 14].

1.3   BESS Deployments and Battery Costs

On a global scale, the use of battery energy storage systems for both FTM and BTM purposes is becoming significant. According to the International Energy Agency, IEA, the total capacity of stationary battery installations reached 16 GW by the end of 2021. Of these installations, batteries with Li-ion chemistries are dominant and constitute 71 % to 96 % of the capacity added each year from 2015 to 2021 [15]. An overview of the annual add-ons in installed capacity of battery installations, with country of location, is given in figure 3.
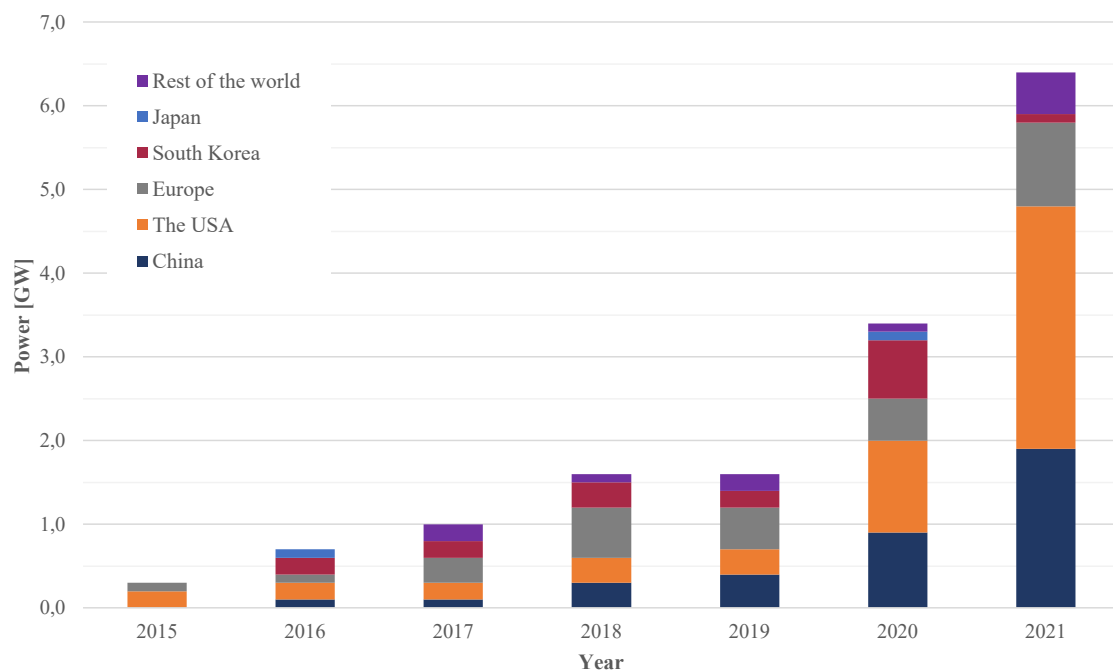
Figure 3: Annual add-ons of global stationary battery energy storage capacity from 2015 to 2021. Data from IEA [15].

As shown in the figure, the annual add-ons have increased at a significantly higher rate since 2019 than earlier. This is likely due to a combination of the need for battery services to cope with capacity challenges and a reduction in the prices of Li-ion batteries. According to BloombergNEF, the average prices of Li-ion battery packs, being used for both electric vehicles and stationary applications, have fallen with almost 80 % the last ten years. In 2021, the average price of Li-ion battery packs where

around 140 USD, and the price is expected to go below 100 USD before 2025 (2021-USD) [16, 17]. It must be noted that these prices are for battery packs, and exclude other required components for a BESS, that contribute significantly to the investment costs. However, the reduction in the prices of battery packs are making stationary batteries a more feasible investment for several projects.
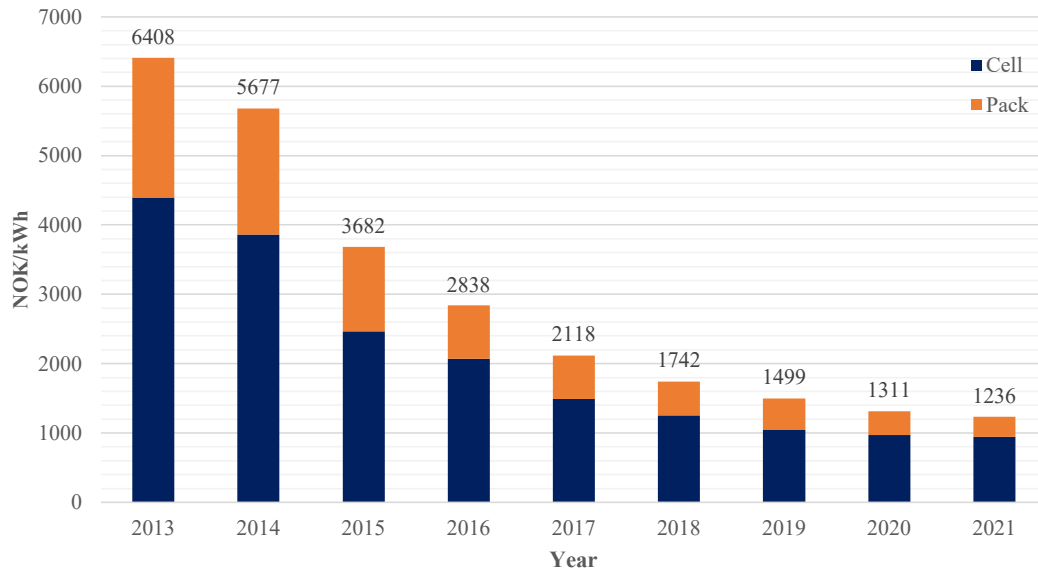
Figure 4: Volume-weighted average battery pack and cell prices, from 2013 to 2021 in 2021-NOK/kWh. Data from BloombergNEF [17].

1.4 Problem Statement and Research Question

The municipality of Ørland in the region of Fosen (in Trøndelag) got a notice in the spring of 2022, requiring grid customers to limit new power demand with a maximum of 0.5 MW. The reason is that the overlying power grid, connecting the distribution grid at Fosen with the transmission grid, is not able to meet higher power requirements until reinforcements are in place. Due to the process of licensing, procurements and construction, it will not be possible to let grid customers increase their load significantly until the end of 2027, the earliest. After this time, it is expected that the regional grid is upgraded from 66 kV, being the system voltage of today, to a new voltage level of 132 kV [3].

Several private and commercial customers want to increase their electricity consumption, in order to expand production processes and change energy supply from fossil fuels. In forecast scenarios, new aquaculture industry in the region is expected to require power of 8.5 MW within the next ten years. Including scenarios on high electrification, this can increase to 16.5 MW [3].

The case for this thesis is focused on a single end user (grid customer), being a business that wants to increase its power supply in order to increase production and sales. The peak load today is at

200 kW, but it is assumed that the peak of a new load would need to increase to 1.5 MW. As this change ($\Delta P \approx 1.3$ MW) is higher than the above-mentioned, possible, increase in power demand, this power cannot be taken directly from the grid continuously. One solution, that this thesis aims to investigate, is to use a battery energy storage system to charge when power is available from the grid, and discharge the energy in periods when the power grid faces capacity limitations. In other words, this means combining some of the demand management techniques presented in figure 2.

Figure 5 and 6 give an overview of the case investigated in this thesis. The first figure shows the overlying grid with the capacity limitations (bottleneck), the transformer connecting the regional grid to the distribution grid at Fosen (T2), some loads, some power generators and the end user of concern. The latter is assumed to install a BESS. The second figure shows the daily average of power imported through the distribution transformer (T2, with label "1") as well as the load of the end user (with label "2")[4]. The load profile of the end user is characterized by a continuous anf high power demand. The peak of power flow through T2 is around 23.95 MW, and the total installed capacity of local power producing units is around 25 MW. However, most of this power production is from wind power, generating intermittent electrical power, and the region is therefore dependent on power from other areas [18].
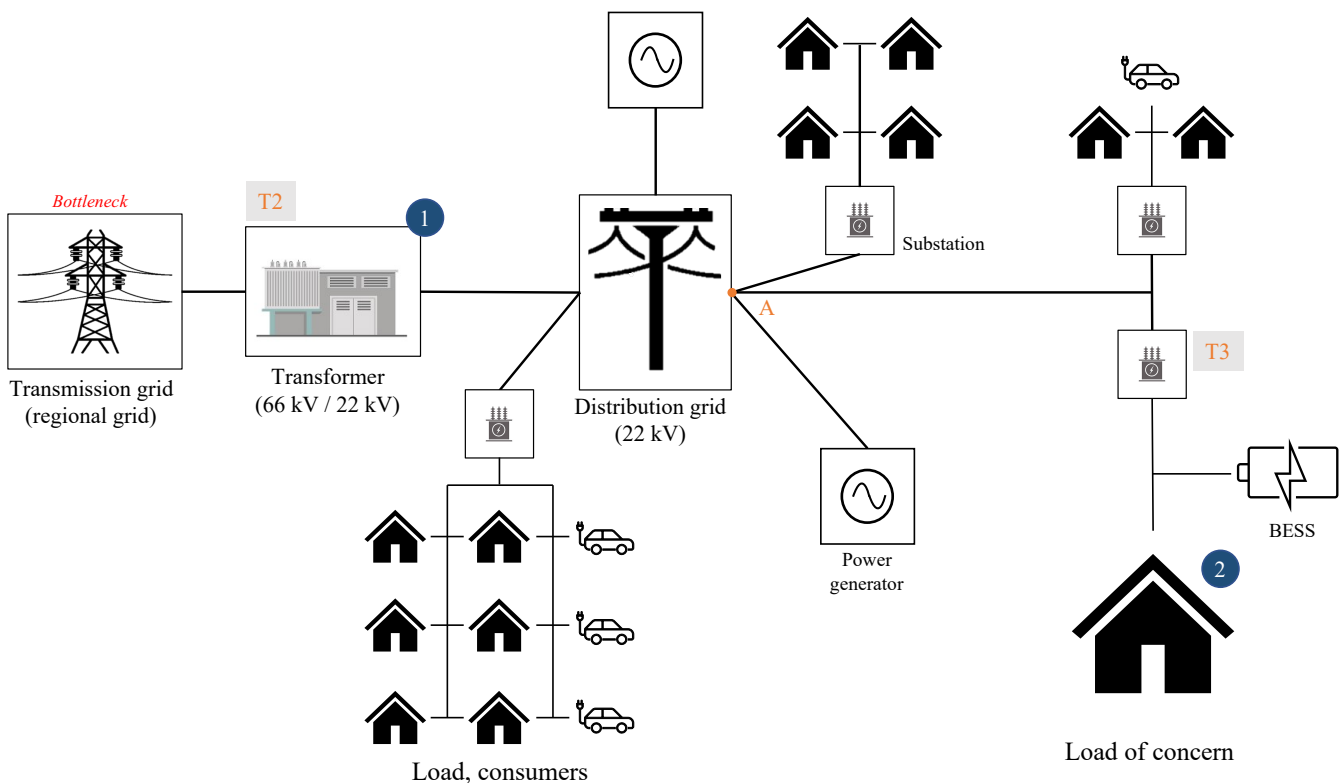
Figure 5: The case of the thesis.

---

[4]Note that the plots are made from daily averages. Actual peaks in power are higher, and the power variations are significantly higher in hourly resolution.
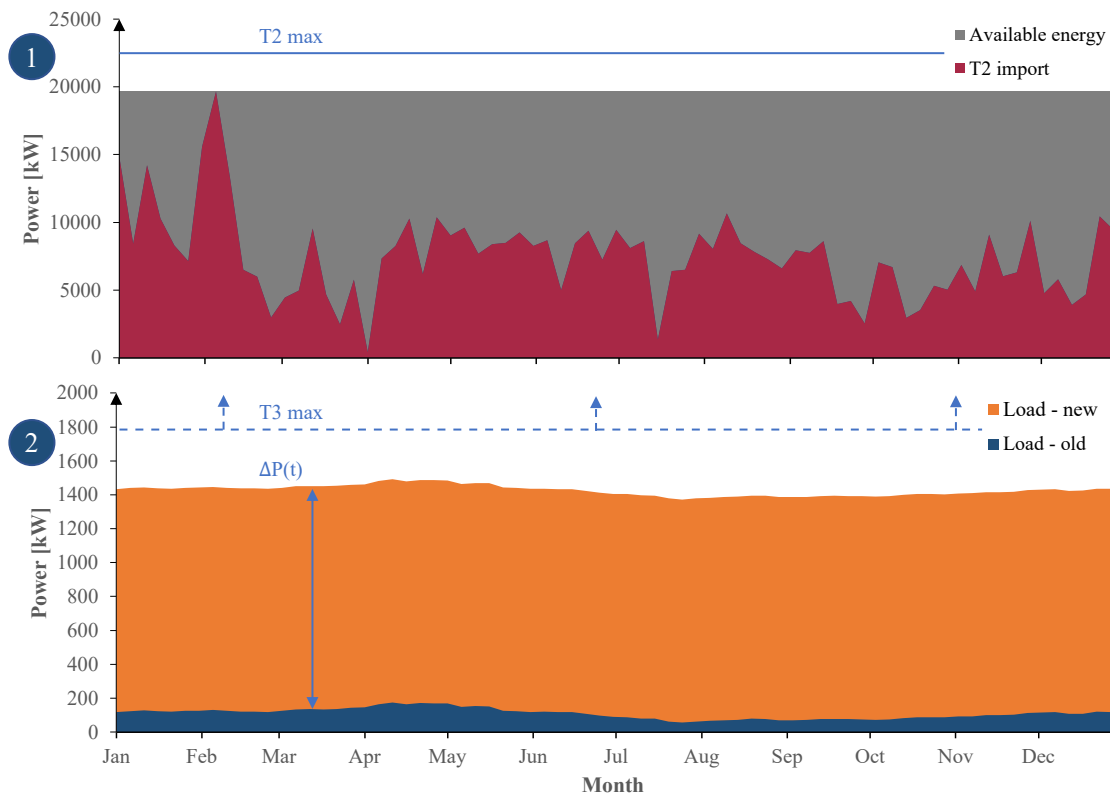
Figure 6: Plots illustrating required power (load) and available power in the case. Load data from 2021.

In short, the idea for this thesis is to let a BESS exploit the available energy, defined by the maximum power imported through T2 today (2021). It investigates whether this can be a possible way of providing the load with the wanted amount of energy, given the above-mentioned restrictions in available grid power. Referring to figure 6, this means that the BESS alone must provide the load with the increased power (ΔP) when there is no or little available power from the grid. Additionally, the thesis will investigate if the solution can be economically feasible, by letting the BESS exploit the techniques of demand side management and energy arbitrage. Based on this, the research question is formulated as follows:

Can a BESS be a technically and economically feasible solution for the capacity expansion of an end user in Fosen, given the restrictions on available grid power of today?

In order to answer this, optimization models are made as a part of the thesis, to find optimal sizing of the battery energy storage system and to simulate optimal operation.

1.4.1 Assumptions and Limitations

The solving of the case problem is based on several assumptions, some of them being introduced here. The BESS is set to consist of LMO-NMC[5] battery packs, a type of Li-ion batteries. This is due to the versatile characteristics, and that a degradation[6] model has been available, for this type of battery. Further, the case assumes that the BESS is owned and operated by the end user, who also takes the cost of transformer losses at the substation (T3) as operating costs of the battery system. The substation, T3, is also assumed replaced to fit the new power requirements. Only the power flow on the radial from point *A* to the end user, indicated in figure 5, is investigated. Both regional load and the load of the end user are assumed to follow the same load profiles as in 2021, for all years of BESS operation. The restrictions in available power are assumed to apply until 2028, meaning that the BESS would be required in this period.

1.5 Related Work and Literature

There exist many articles and reports that touch upon the topics of stationary battery systems. These include cases with power limitations of power grids, grid balancing, reducing power peaks and delaying grid investments or demand side management with the goal of reducing energy costs. Several articles, reports and previous master theses have given inspiration to the contents and approaches of this thesis.

Batteries to Help With Grid Challenges

Several articles and reports connected to the IntegER[7] project (with SINTEF, Skagerak Nett AS and several) are relevant for the problem case of this study [6]. The project aimed to evaluate the values of location, ownership, technical integration and business models for energy storage systems, for both DSOs and others. In a guide for batteries for the distribution grids ([13], 2020), a NVE project on the same topic ([8], 2019) and a cost-benefit analysis ([7], 2019), the benefits of stationary batteries are divided in market and grid categories. They all present cases where batteries can provide required grid services, and discuss possible scenarios where involvement in the electricity market can make them economically feasible.

One of the cases described in the first example is about an end user that wants to increase its load from 24 kW to 30 kW. The power grid is found to be to weak to allow for the increased power flow without

---

[5]Manganese Oxide/Nickle-Manganese-Cobalt blend
[6]A Li-ion battery experiences a loss in available capacity with time ans usage (known as degradation).
[7]IntegER - Integration of energy storage in the distribution grid (project period: 2017 - 2020).

facing too high voltage drops. Two alternative solutions are presented, being the installation of a BESS close to the end user or upgrading the power grid. It is found that the solution with BESS can be economically feasible for an investment cost below 3 500 NOK/kWh[8]. The report also investigates different cases for ownership and location, where the end user owns the battery installation or the DSO buys a battery service from a third party [13].

The second example describe similar scenarios, and concludes that investment costs below 6000 NOK/kWh could be economically beneficial if the radial to the customer is longer than 300 meters (due to voltage drops). This report also discusses challenges and possibilities with ownership. A possibility is to remove economical incentives for battery operation (by not allowing to exploit the variations in electricity prices). This significantly reduces the economical feasibility of the battery solution. Another way could be to involve third parties, similarly as for the first exampl. As this third party would be driven by profit maximization, this solution would require that the selling of grid services would generate enough revenue [8].

The last of the above-mentioned literature investigates the situations, and for which costs, that batteries are attractive solutions. It finds that batteries for grid support can be attractive for investment costs below 14 500 NOK/kWh (2019), if used for grid services such as frequency regulation[9]. For cutting power, load shifting and increasing self-consumption with photovoltaics (PV), batteries are only feasible for investment costs below 2 000 - 6 000 NOK/kWh (2019), depending on electricity costs and power tariffs [7].

Optimal Battery Operation

A techno-economic analysis of Skagerak EnergyLab ([19], 2020), investigates a case study where battery operation is simulated to cover some loads and increase self-consumption of a PV installation. It includes two types of Li-ion battery chemistries, being NCA and NMC[10]. The different cases involved maximizing self-consumption, covering flood lights, energy arbitrage and general minimization of energy and power costs. For investment costs between 4 000 and 10 000 NOK/kWh, none of the cases with NCA battery proved economically feasible. For the NMC type however, the battery investment could be feasible for investment costs below 4 000 NOK/kWh, when PV self-consumption and general minimization of energy and power costs are prioritized.

In a master's thesis from 2018 ([20]), an optimization model with the goal of minimizing total system operating costs for a combined PV and BESS installation was developed. For an optimal battery size

---

[8]Cost per nominal battery capacity

[9]This assumes a battery composition of 1 MW (power) and 400 - 500 kWh (capacity)

[10]Nickel cobalt aluminium and Nickel manganese cobalt oxide

of 150 kWh, with respect to operating costs, the BESS would provide yearly savings in energy costs for a BESS investment cost of 3 600 NOK/kWh. The case investigated a battery of the NMC type, and included a model of degradation. The optimization model of this thesis also aims to limit degradation, by setting a cost on the type of operation that provokes degradation.

Optimal Battery Sizing (and Operation)

The above-mentioned master's thesis found the optimal BESS size from an iterative process, running the optimization model for different battery capacities. The value resulting in the lowest operating costs was then chosen. In a similar work ([21]), a function including both operating and capital (investment) costs was formulated, and the optimal value of the variable representing BESS sizing was found for the case where the function was at minimum. The results showed that the sizing was very sensitive to the grid power constraints, being the most important factor for the sizing.

In a master's thesis from 2020 ([22]), a battery installation is evaluated against reinforcing the power grid, for a fast charging station in Trøndelag. The case assumed a NMC-LMO battery and an investment cost of 9 000 NOK/kWh. The investment cost was split in a power cost and a capacity costs, in order to find optimal ratio of power and energy (P/E). The method for sizing the BESS is similar to the one from the above-mentioned article ([21]), and resulted in a 300 kW/225 kWh battery system. Given the investment costs, it was concluded that reinforcing the grid would be better than to use the BESS solution, given an economical point of view. Another interesting finding was that degradation is significantly higher when simulating at minute resolution rather than hourly resolution. However, different degradation cases only contribute with about 1 % difference in operating costs.

As observed from the descriptions of previous works on the topic, there are many different cases that are relevant for a BESS. It is also shown that economical feasibility depends on many factors, and vary from case to case. It therefore seems that all cases require tailored solutions and cost-benefit studies that are case specific. This thesis includes several elements from, among others, the above-mentioned sources, but with the case being unique. One of the most significant differences is the fact that the restrictions on available power is not based on the point of connection between grid and load, but the available power from the regional grid.

1.6 Structure of the Report

The report consists of seven main chapters (sections), in addition to this introduction. The contents of these are as follows:

Section 2:

In this part, technical details on components, working principles and terminology that are relevant for understanding battery energy storage systems are introduced.

Section 3:

Important principles of energy pricing, the composition of energy costs and approaches for economical analysis, including optimization, are explained in this section.

Section 4:

In this section, the case is described in more detail, and the approaches (including mathematical formulations) are depicted thoroughly. Overviews of important assumptions and input data, as well as descriptions of the investigated scenarios, are also presented.

Section 5:

The results are presented, evaluated and discussed in this part. In addition, case assumptions and methodology are reviewed.

Section 6 and 7:

Conclusions and points on further work are presented in the last two sections.

2 Battery Energy Storage Systems and Battery Fundamentals

This chapter introduces and describes relevant theory and background material. Components and technical principles for battery energy storage systems, with Li-ion being in focus, is presented first. An important part of this is the aging mechanisms and the models that are used to account for degradation in battery operation. Furthermore, BESS investment and operating costs are presented and compared. Costs associated with energy and power are considered more in depth in section 3.

There are many different energy storage technologies, that fit for different purposes and scales. In general, these can be categorized as electrochemical technologies (e.g. batteries), electrical technologies (e.g. super capacitors), thermal technologies (e.g.sensible thermal), chemical technologies (e.g. hydrogen/fuel cells) and mechanical technologies (e.g. flywheel). An overview of these technologies are given in appendix A. One advantage with electrochemical technologies, such as batteries, is that this technology is mobile, easy to implement and is suitable for most locations [2].

2.1 BESS Components

A battery energy storage system (BESS) consist of several components and elements. The main components, illustrated in figure 7, are the battery packs (consisting of battery cells and organized in racks), power conversion systems and different control and management systems. It is common that most of these components and elements are gathered in a battery container that also equipped with HVAC[11] systems for thermal management. In addition to these main components, some supporting components are required. These are referred to as the balance of system (BOS) [13, 23]:

- Electrical BOS: Wiring (DC and AC), conduits, switchgear, transformer, controllers and monitors.

- Structural BOS: Foundation, container materials, inverter house and cable laying.

---

[11]HVAC = heating, ventilating, and air conditioning

Battery cell   Battery module   Battery racks   Battery container
(battery pack)
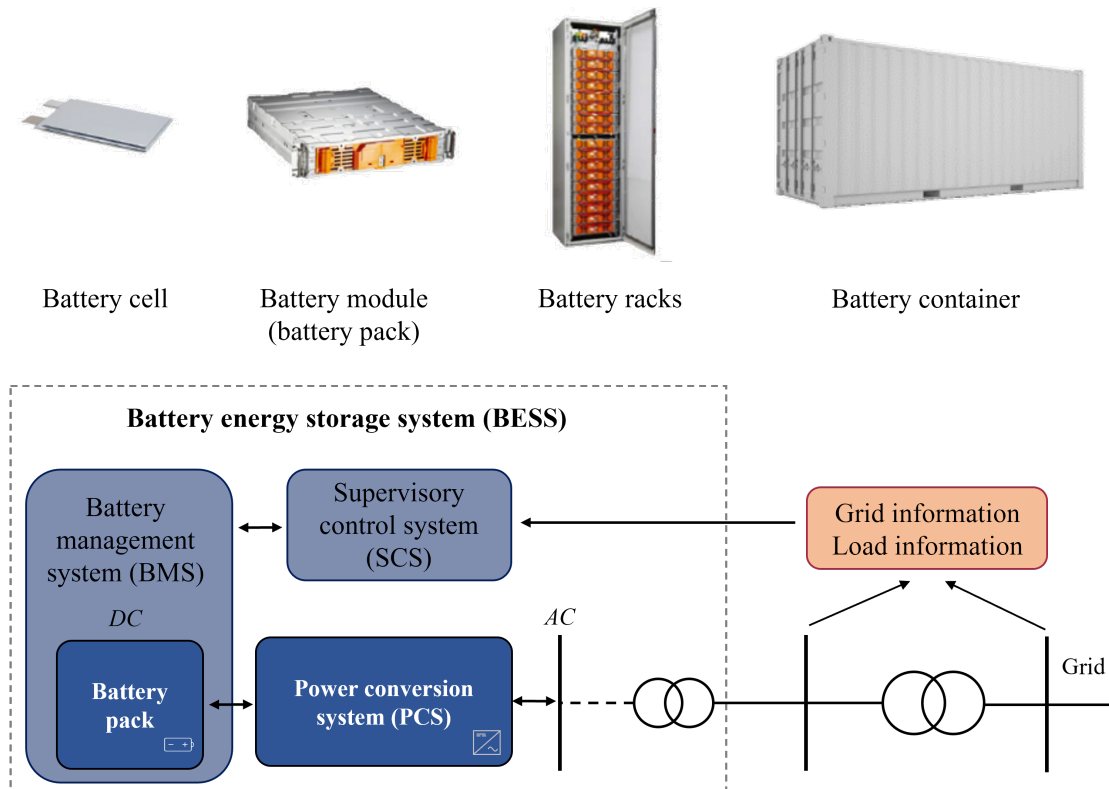
Figure 7: Key components and elements of a grid connected BESS. Adapted from [13, 23].

While the battery packs decide the energy storage capacity of a BESS, the amount of power that can be drawn from the system (the power capability) is mainly determined from the power conversion system. This is required as the grid power is in AC voltage, while the battery only works for DC voltage. The power conversion system must therefore convert AC to DC (rectifier operation) in order to charge the battery, and convert the DC to AC (inverter operation) in order for the battery to provide the AC side with power. When these processes are conducted in the same component, *inverter* and *converter* are often used interchangeable for the component name. Smaller battery energy storage systems can do with only one inverter, while it is more common to have several for larger installations. The efficiency of an inverter depends on the power, but is generally in the area of 95 % [13, 21].

The battery packs and battery cells are governed by the battery management system (BMS), which ensures safe operation by balancing the energy of the battery cells and monitor the state of the battery. The supervisory control system is the main controller, which decides when to charge and discharge and at what current and power. This system takes input from for instance the load, the power grid and the electricity market, depending on the purpose of the BESS. For the case in this thesis, relevant input data could be measurements of load and available grid power, electricity spot prices and forecasts on future load [13, 23].

2.2   Battery Fundamentals

Most of the above-mentioned components remain the same for different types of BESS. However, the battery can be of many different types, such as lead-acid, sodium-sulphur and Lithium-ion (Li-ion). In general, a battery cell is an electrolytic cell (electrochemical cell) which generate electrical energy. The most essential components are a positive and a negative electrode, an electrolyte and a separator. Battery cells that are "single use" are called primary batteries, while rechargeable batteries are called secondary batteries [24].

2.2.1   General Working Principles and Terminology

The main components and working principle of a secondary battery cell is presented in figure 8. In order to generate electrical energy (electricity), two half-cell reactions must happen at the two electrodes. These electrodes consist of active material, which generate ion movement, and the current-collector (also known as the grid). Positive ions are called cations, and negative ions are called anions. An electrolytic cell in which a current is produced is known as a galvanic cell (*a* in figure 8), while a charging cell, that receives current, is known as an electrolysis cell (*b* in figure 8).
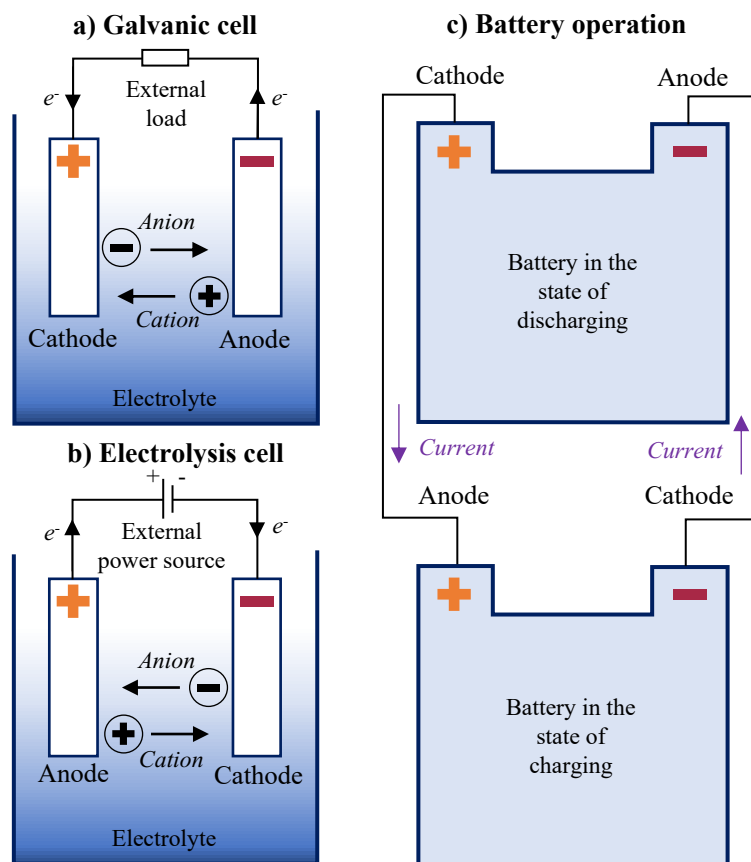
Figure 8: Components and operation principles of secondary battery cells. Adapted from [24].

The electrodes are called anodes and cathodes depending on whether the battery cell is charging or discharging. An oxidation reaction, liberating electrons, occur at the anode and a reduction reaction, taking up electrons, occur at the cathode. As it is most common to speak of to the discharge state of a battery the anode is often understood as the negative electrode while the the cathode is understood as the positive electrode [24].

The voltage of a battery cell is measured as the difference in the potentials of the two electrodes. At no current flow (no load connected to the terminals / electrodes), this is known as the reversible voltage (V_r) or the open-circuit voltage. Having a load connected to the battery cell, the actual voltage will be lower as a result of voltage drops due to irreversible losses, such as polarization losses and ohmic losses. These cause, among other things, an increased cell voltage when charging and a decreased cell voltage while discharging. The losses related to charging and discharging of a battery are expressed through the round-trip efficiency. [24].

Cell voltages for common battery cells are around 2 V, for lead-acid, and 3.5 - 4.2 V, for Li-ion types. To achieve common battery pack voltages, for instance 12/24 V for lead-acid and 14/36/48V for Li-ion, several of these cells must be connected in series[12]. The voltage and capacity of a battery are closely related to each other [24].

Terminology

Before moving on, it is important to be aware of the terminology that is used for describing different battery characteristics and properties. The most common terminology is presented in table 1.

---

[12]Battery cells are most commonly connected in series, but they can also be connected in a series-parallel array.

Table 1: Battery terminology [13, 24, 25].

Term	Unit	Description
Cut-off voltage	V	The voltage limit of a battery. A battery should not be operated under / over certain voltage.
Nominal capacity	Ah, Wh	The capacity of a new battery under specific conditions. Energy that is available for discharge until a specific cut-off voltage.
Useful capacity	Ah, Wh	The amount of energy that is available for charge/discharge, given restrictions in minimum and maximum levels.
Available capacity	Ah, Wh	The amount of energy that is available for charge/discharge, given the age and state of the battery or battery system.
Max power (max load)	W (A)	The maximum power (current $\times$ battery voltage) that can be drawn from the battery.
Response time	ms., sec.	The time needed for the battery to start charging and discharging when requested to do so by the control system.
Specific energy	Wh/kg	Energy storage potential per weight. Also known as gravimetric energy density.
Energy density	Wh/L, Wh/m^3	Energy storage potential per volume. Also known as volumetric energy density.
Round-trip efficiency	%	The combined efficiency of charging and discharging a battery. There are losses associated with both charging and discharging.
C-rate	-	The rate of charge and discharge. 1C means a power rate that corresponds to a full discharge / charge in one hour. 2C: a full discharge / charge in $1/2$ hour. 0.5C: a full discharge / charge in 2 hours...
SoC (State of charge)	%	The energy level of the battery, expressed as a fraction of the available capacity.
DoD (Depth of discharge)	%	The discharged capacity of a battery, being the opposite of the SoC.
SoH (State of health)	%	The amount of capacity of a battery, relative to the nominal capacity, at any given time. Expresses the loss in capacity with time and usage.
Cycle	#	Charging and discharging, starting and ending up at the same SoC.
Full Equivalent cycle	#	Energy throughput from charging and discharging equivalent to the scenario where the SoC at the beginning and end is 100 %.
Cycle life	#	The number of cycles a battery can go through before the capacity is below a certain limit.[*].
Shelf lifetime	years	The time (number of years) a battery can be stored without being used, at certain conditions, before the SoH is reduced to a certain limit due to self-discharge[*].

* The most common limit, being a SoH of 70 - 80 %, is mainly for applications requiring mobility, such as mobile devices and electric vehicles. For stationary applications, the battery can be useful for even lower states of health.

Indicated by the table, there are many factors to consider for a battery, both for instantaneous operation and conditions over longer time horizons. The discharge curves of figure 9 show how a Li-ion battery

cell is discharged for different operating conditions, and illustrates that voltage and capacity of a battery are closely related to each other. The characteristics are similar for other types of batteries. The discharge curves in figure 9a indicate that higher c-rates discharge the battery faster than c-rates being lower than one. The voltage drop is more significant, and the available capacity is less, the higher c-rate. Because of this characteristic of secondary batteries, it is important that the nominal capacity of a battery is presented together with corresponding c-rate, often being one (1C). Figure 9b shows that moderately high operating temperatures result in lower voltage drops than low temperatures. The latter also resulting in less available capacity [24].
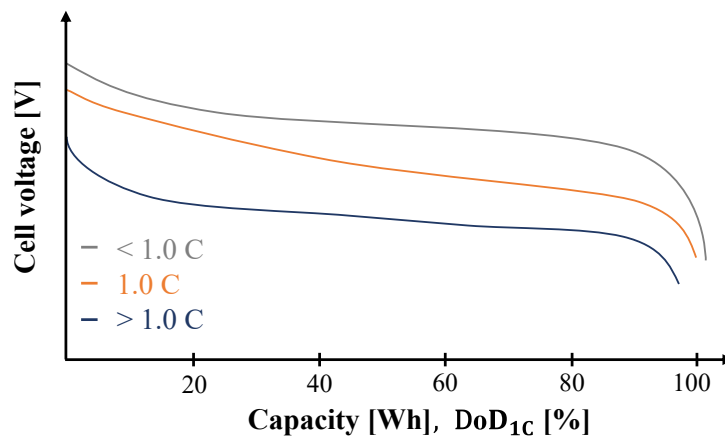
(a) Discharge curves of Li-ion battery cells for different c-rates.
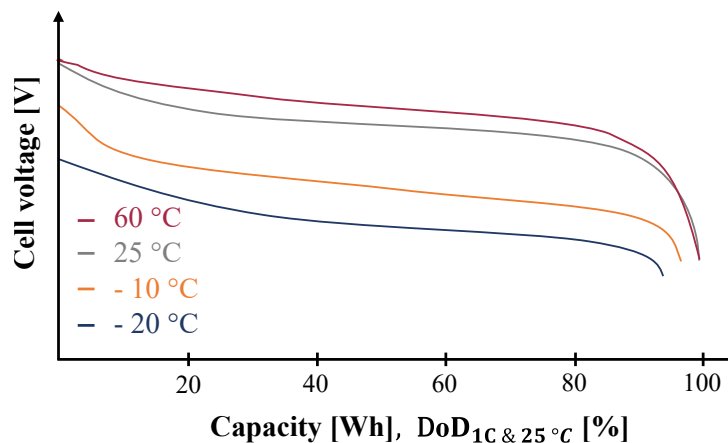
(b) Discharge curves of Li-ion battery cells for different temperatures.

Figure 9: General discharge curves of Li-ion battery cells for different c-rates and temperatures, based on the curves from a Sanyo Li-ion cell from [24].

The cut-off voltage is found in the area where the cell voltage starts falling at a higher rate, before 100 % DoD. It is common to operate the battery between a SoC of 20 to 90 %. The figures indicate that optimum, instantaneous, operation is achieved for low c-rates and moderately high temperatures.

However, as will be described in section 2.3, degradation over longer time intervals must also be considered [24].

2.2.2 Batteries for Stationary Storage

There exists many different types of batteries, that can be used for the same or different purposes. The components and chemical principles are mostly as described above, but the materials differ significantly. A comparison of technical details on the different types is presented in table A.2 in appendix A, while an overview of the most common types with key properties are introduced here.

Lead-acid (Pb-acid) is the most mature battery technology, and has existed for more than one hundred years. It has commonly been used in for instance starter batteries in cars and UPS (uninterruptible power supply) systems. Its positive electrode contains PbO_2 while the negative electrode is made from lead. These are both immersed in sulfuric acid electrolyte. An advantage with this battery chemistry for stationary storage is that it is relatively cheap (560 - 3 200 NOK/kWh). However, disadvantages such as low cycle life, bad performance at low temperatures, high weight, large volume and danger of environmental damages from highly toxic lead, may motivate for using different technologies [26].

Sodium-sulfur (NaS) is a different type, where the positive electrode consists of molten sulfur (S) and the negative electrode is molten sodium (Na). These are separated by solid ceramic, serving as electrolyte. Stationary storage systems of this types are more expensive than for lead-acid, but has higher cycle life and requires less volume and weight. However, it requires high operating temperatures, approximately 300 to 400 °C [26].

The flow batteries, also known as redox flow batteries, represent a quite different technology. These batteries consist of two liquid electrolytes (anolyte and catholyte) that are stored in different tanks. The electrolytes flow through an electrochemical cell, separated by a membrane, that converts chemical energy to electricity. About 80 % of all registered energy storage installations based on flow batteries are of the Vanadium redox flow (VRFB) type ([26], 2018). Advantages of VRFBs are long lifetime (up to 25 years), high cycle life, almost no degradation, very low self-discharge over time and medium investment costs. In addition, the available and useful capacity is very close to the nominal capacity, meaning that almost all of the energy stored in the system can be used[13]. Disadvantages are that the round-trip efficiency is lower than for the above-mentioned technologies, the systems become heavy and space-intensive, it uses battery acid (toxic) and have slow response time [26, 27].

Lithium-ion batteries requires little weight and space per unit of capacity, have the highest efficiency of the above-mentioned technologies, have long cycle life and can be operated at room temperatures.

---

[13]In order to stay within optimal efficiency, it is advantageous to not drain the electrolyte tanks entirely, as this will require more energy to the pumping system)

In other words, it represents a good mix of the advantages of the different technologies presented so far. However, the investment costs of stationary energy storage systems based on Li-ion are high, even though the battery prices are reducing. But the greatest advantage of Li-ion battery systems is the versatile characteristics. As illustrated in figure 10, this technology is suitable for many different purposes when connected to the grid and load side [26].
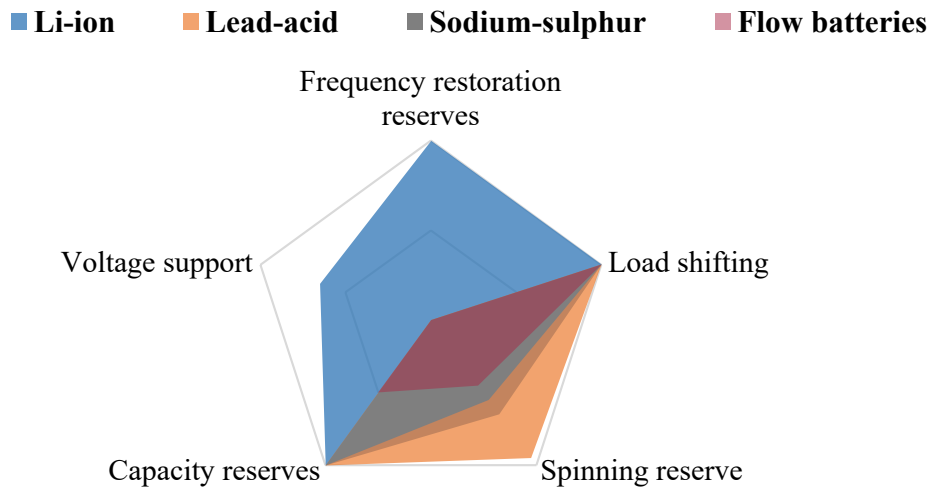
Figure 10: A comparison of common battery types for different purposes in grid and load support [26, 28].

As shown in the figure, most of the technologies are suitable for load shifting and capacity reserves. However, only Li-ion is clearly suitable for voltage support and frequency control. The other types are unsuitable due to for instance long response time. The Li-ion technology is able to cover all the illustrated needs. However, the technology covers a group of different variants that are better suited for the different purposes. These are described in the next section [26, 28].

2.2.3   Lithium-ion Battery Chemistries

Lithium-ion batteries were discovered by researchers at oxford University (UK) in the 1970s, and was later commercialized by Sony in the 1990s. Lithium as material has been very attractive as a component for the negative electrode due to high electrochemical potential in combination with low atomic mass. In the beginning, several anode and cathode materials were tested, but it was soon found that the preferred negative electrode material (anode material) was carbon in the form of graphite. The working principle of Li-ion batteries is based on the movement of Li-ions (Li^+) between the positive and negative electrodes, which are separated by a porous polymeric material (that allows for flow of ions). These are also immersed in an electrolyte consisting of Lithium salts [24, 26].

Graphite, serving as the negative electrode, has a high gravimetric energy potential of 372 mAh/g. However, the materials used for the positive electrodes (the cathode materials) have significantly lower energy potentials. For instance, metal oxides based on Cobalt, Nickel and Manganese have gravimetric energy potentials ranging from 120 to 130 (maximum 160) mAh/g. Therefore, the cathode material is the limiting part that contribute the most to the total weight of the battery. Different Li-ion chemistries, with different anode-cathode combinations, are compared in table 2, considering specific energy and cycle life. It shows that NMC and NCA are the best types with respect to specific energy, while NMC, LFP and LTO have the highest cycle life [29, 30, 31].

Table 2: Parameters for the most common Li-ion chemistries [29, 31].

Type of Li-ion	Anode material	Cathode material	Specific energy [Wh/kg]	Cycle life[14]
LCO (Lithium cobalt oxide)	Graphite (LiC_6)	$LiCoO_2$	150 - 200	500 - 1000
LNO (Lithium nickel oxide)	Graphite (LiC_6)	$LiNiO_2$	150 - 200	> 300
LMO (Lithium nickel manganese)	Graphite (LiC_6)	$LiMn_2O_4$	100 - 150	300 - 700
NMC (Lithium nickel manganese cobolt oxide)	Graphite (LiC_6)	$Li(NiMnCo)O_2$	150 - 220	1000 - 2000
LFP (Lithium iron phosphate)	Graphite (LiC_6)	$LiFePO_4$	90 - 150	1000 - 2000
NCA (Lithium nickel cobalt aluminium oxide)	Graphite (LiC_6)	$Li(NiCoAl)O_2$	200 - 260	~500
LTO (Lithium titanate)	Lithium titanate $Li_4Ti_5O_{12}$	$LiMn2O_4$, $Li(NiCoAl)O_2$	70 - 85	3000 - 7000

The development of other material combinations is an ongoing research, aiming to increase specific energy, efficiencies and safety of operation. New anode materials can be Silicon (Si), potentially having a capacity of 4 200 mAh/g, and Tin (Sn), potentially having a capacity of 980 mAh/g. However,

---

[14]Assumed full equivalent cycles (FECs). Actual cycle life is dependent on operating conditions. For shallow DoDs (below 30 %), moderate temperatures and moderate c-rates, several battery types (LMO, NMC and LFP) are expected to have a cycle life greater than 14 000 cycles. LFP is generally considered to have longer cycle lifes [32].

the cathode will still be the limiting part. LiFePo$_4$ (LFP) currently has one of the highest cathode capacities, being 170 mAh/g, but suffers from poor conductivity characteristics [30].

Characteristics for Stationary Applications

The characteristics for the most important of the above-mentioned Li-ion chemistries are illustrated in figure 11 for stationary applications. It shows, for instance, that NCA batteries have high specific power and energy, but a high investment cost. LFP batteries score high on safety and are not that expensive. NMC and LMO show quite balanced characteristics [31, 29].
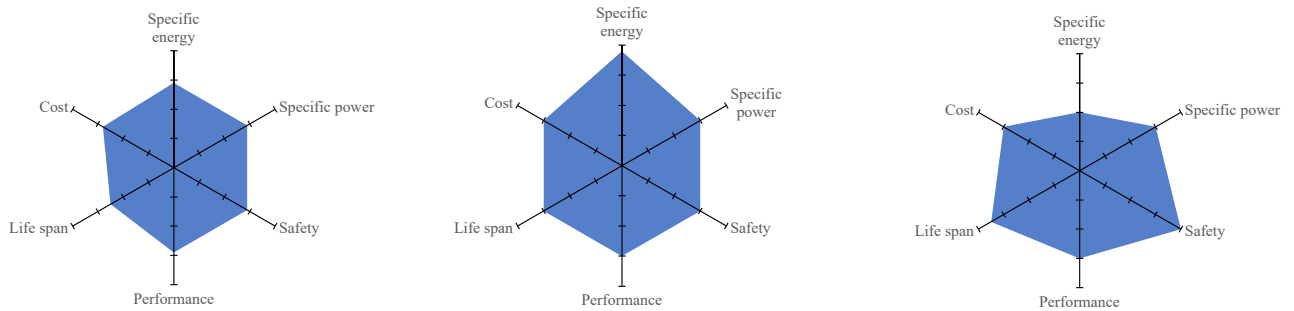
(a) Lithium-manganese spinel (LMO)

(b) Lithium-nickel-manganese-cobalt (NMC)

(c) Lithium-iron phosphate (LFP)
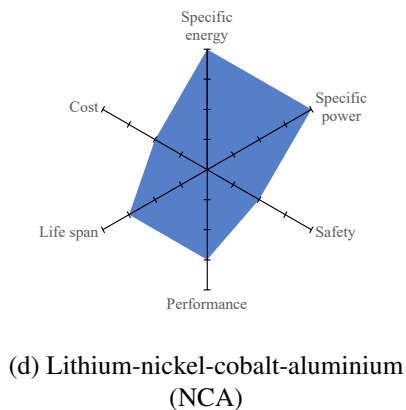
(d) Lithium-nickel-cobalt-aluminium (NCA)
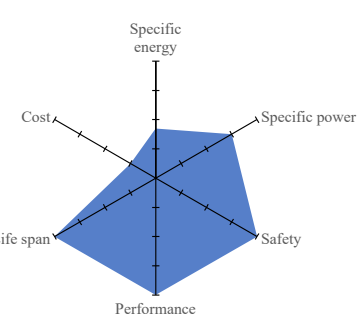
(e) Lithium titanate (LTO)

Figure 11: Comparison of properties, advantages and disadvantages of different Li-ion chemistries. Adapted from [29, 31].

2.3 Degradation Mechanisms in Li-ion Batteries

All secondary batteries, including those of Li-ion, have reversible processes with irreversible losses. This means that both the usable power and capacity reduces with time and use, which is referred to as power and capacity fade. Only the latter is the focus for this thesis. The mechanisms of capacity fade are further categorized as cyclic and calendric aging. The first type happens even though the battery is at rest, without any external load or power source connected to it. The second type only occurs when the battery is charging and discharging. The state of health (SoH) is used as a measurement on the degradation of batteries [29].

Degradation mechanisms for Li-ion batteries are complex, occur on different components and depend on many factors. An overview of many of the mechanisms can be found in appendix B, while the most important are presented below.

Calendric Aging

At the anode (negative electrode) of a Li-ion battery cell, a chemical reaction occurs which forms a passivating layer on the electrode surface. This layer is called solid electrolyte interface (SEI). Having a high amount of this, the internal resistance of the battery cell become unacceptable high, while too little SEI can cause corrosion because of electrolyte reaching the anode material. The growth of SEI is the most prominent contributor to degradation of Li-ion batteries, and is especially important for calendric degradation. Other important contributors is the loss of active material and the change of surface phase [29].

As the name suggests, calendric aging depends on time. Experiments show that an underlying dependency on time follow the function t^z, where z is close to 0.5 (making it equivalent to $\sqrt{t}$). In addition, it is found to be highly dependent on temperature and SoC through an *Arrhenius relationship*. A general equation for this relationship is presented in equation 1, where A is the pre-exponential factor, k is a rate constant, T_K is the temperature (in Kelvin), R is the gas constant and E_a is the activation energy[15] for the reaction [29].

$$k = A \cdot \frac{-E_a}{R T_K} \tag{1}$$

Figure 12 shows how SoC and temperature, at storage, contribute to the calendric degradation of a LMO battery. The tendencies are similar for other Li-ion chemistries. It is shown that higher storage

---

[15]Activation energy: The minimum amount of energy to cause the chemical reaction

temperatures and SoCs cause higher degradation, than lower temperatures and SoCs. At least down to 15 °C and 60 % SoC. By charging this battery to half capacity and keeping it at a temperature of 55 °C, the SoH ends up at 60 % after five years. In other words, 40 % of the original nominal capacity is lost [32].
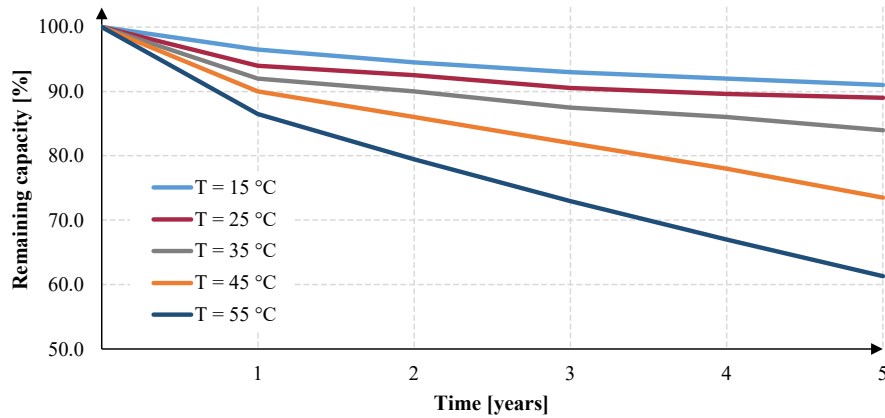
(a) Calendric aging for different storage temperatures and SoC at 50 %.
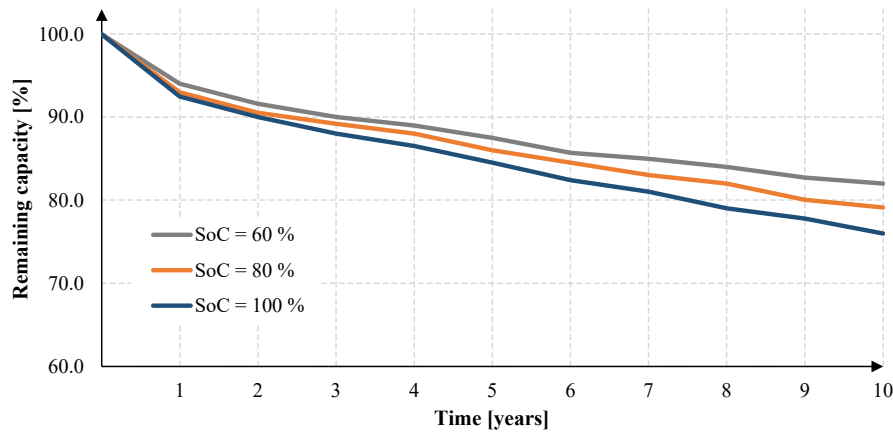
(b) Calendric aging for different SoCs while temperature is held at 25 °C.

Figure 12: The effects of temperature and SoC on calendric aging of storing Li-ion batteries. Based on data for a LMO battery [32].

Cyclic Aging

Cyclic aging is more complex than calendric aging, as it depends on more factors and conditions. The degradation mechanisms causing cyclic aging are mainly having to do with the lithium plating and general mechanical failure. In addition to temperature and storage SoC, the cyclic aging depends on DoD and c-rate. The latter case is already touched upon in figure 9a. In general, high c-rates cause the battery to degrade faster than low c-rates [29, 32].

The depth of discharge affects degradation in several ways. Firstly, large charge and discharge intervals should be avoided, as this result in capacity fade. Secondly, the average SoC between starting and ending DoD is contributing as well. From figure 13 it is shown that operation between 25 and 85 % SoC (marked in green) is better than operation between 40 % and 100 % SoC (marked in red), even though both cases use 60 % of the energetic battery capacity (i.e. the same amount of energy throughput). In the first case, the battery degrades to 84 % of SoH while the second case ends up at a SoH being 79 %, for a lower amount of DST cycles [16] [29, 32].
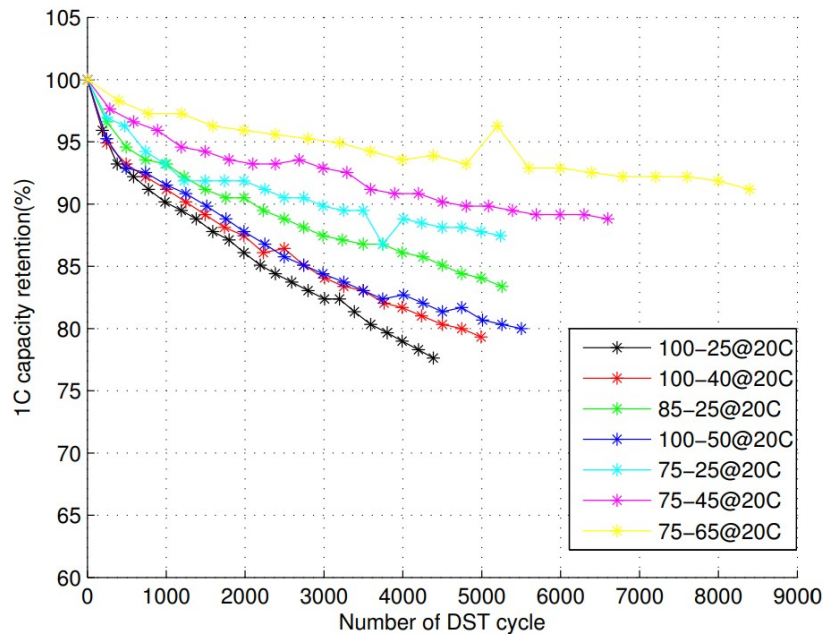
Figure 13: Degradation of a Li-ion (LMO) battery for different cycling conditions (starting and ending SoC), at 20 °C [32].

Obviously, shallow discharges (as for the yellow data) can allow for many more cycles, with the same depth of discharge, than a deep discharge (as for the black data). Therefore, a cycle in this sense is not adequate to measure life time when varying the length and profiles of charge and discharge. In order to correctly compare degradation effects and show the true effects on storage capability, the term energetic throughput is introduced. This can for instance be obtained by measuring the energy flowing in and out of the battery, by considering ampere-hours (Ah) or watt-hours. A common way is to define 1 Ah charge and 1 Ah discharge, as a charge throughput of 1 Ah [29].

In equation 2 from [33], the charge throughput (Q) is based on the charge or discharge current during a certain time. This can further be generalized by relating the energetic throughput to the useful battery

---

[16]DST cycle: Dynamic stress test. Starting from a specific SoC, a DST profile (with certain charging and discharging pattern) is applied until wanted SoC is reached, before the battery is recharged at a c-rate equal to one (1C) back to starting SoC to finish one test cycle [32].

capacity, E_B^{cap}, based on the nominal battery capacity, E_B^{nom}, and limits on state of charge. In a PhD report by Maik Naumann ([34]), the term "full equivalent cycle" (FEC) is defined as the energetic throughput during a certain time period related to the twice of the battery capacity, according to equation 3. $E_B^{cum}(t)$ is the cumulative energetic throughput from charging and discharging the battery with a power of $P_B(t)$ and an efficiency of η_B. This occurs during a time interval from t_{start} to t_{end}. For a single time step of Δt, the equation is simplified from being an integral. The half ($1/2$) represents that an interval of charging or discharging only constitute a half cycle.

$$Q = 0.5 \cdot \int_{t_{start}}^{t_{end}} |I| dt \tag{2}$$

$$FEC(t) = \frac{1}{2} \cdot \frac{E_B^{cum}(t)}{E_B^{cap}} = \frac{1}{2} \cdot \frac{\int_{t_{start}}^{t_{end}} |P_B(t)| \eta_B dt}{E_B^{nom} \cdot (SoC_{max} - SoC_{min})} \approx \frac{1}{2} \cdot \frac{|P_B(t)| \eta_B}{E_B^{nom} \cdot (SoC_{max} - SoC_{min})} \cdot \Delta t \tag{3}$$

In the literature, many terms are used to describe this concept. In this thesis, a full equivalent cycle (FEC) is defined as a factor describing the energetic throughput relative to the nominal battery capacity at a certain time, according to equation 3. These factors are accumulated to express the total number of equivalent cycles, N_{eq}, for a period of operation (T) as in equation 4. The concept is also illustrated in figure 14, showing the charging and discharging of a battery from 80 % SoC down to 20 % SoC and back again to 80 % SoC in several time steps, at a constant c-rate. From *t1* to *t2,* there is a discharge corresponding to a FEC of 0.1, and from *t1* to *t11*, ten such partial charges and discharges accumulates to one equivalent cycle ($N_{eq} = 1$).

$$N_{eq}(T) = \sum_{t=1}^{T} FEC(t) \tag{4}$$
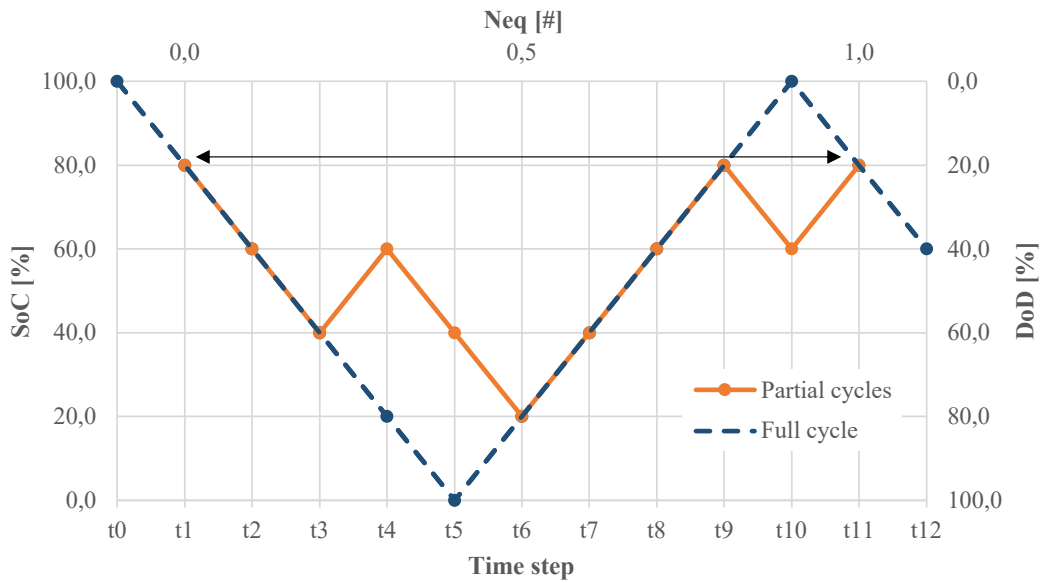
Figure 14: The concept of equivalent cycle counting.

Chemistry Dependency on Degradation

Capacity fade, as well as power fade, happens for all Li-ion chemistries. However, the degree of dependency to the different conditions vary, for both calendric and cyclic aging. In [29], the chemistries presented in section 2.2.3 are compared with respect to sensitivities for degradation mechanisms. The best chemistry in terms of calendric aging is reported to be for the NCA chemistry, being least sensitive to both temperature and storage SoC. LFP and NMC both have a high temperature sensitivity, and a variable sensitivity on SoC. The LMO-NMC blend is found to have the poorest calendric life time, and the most capacity fade in total, having both a high dependency on SoC and temperature.

Optimal Operation of Li-ion

Due to the degradation mechanisms of Li-ion batteries, optimal operation and storage is important in order to prolong the life time and usefulness of the battery. According to [35], optimal operation (for minimizing degradation), can give 130 to 260 % longer life time of the battery, compared to operation without concerning the effects of degradation. This can be achieved by operating within a certain operating window [29]:

- To minimize calendric aging: maintain a low SoC (< 50 %) and a low temperature.

- To minimize cyclic aging: keep a moderate temperature, a moderate/low c-rate (around or below 1C) and shallow discharging (DoD) around an optimal SoC (commonly around 50 %). For example: discharge from a SoC of 60 % to 40 % and en charging back to 60 % SoC, at a c-rate of one (1C)

Figure 15 shows a suggested, general, operating window for Li-ion batteries.
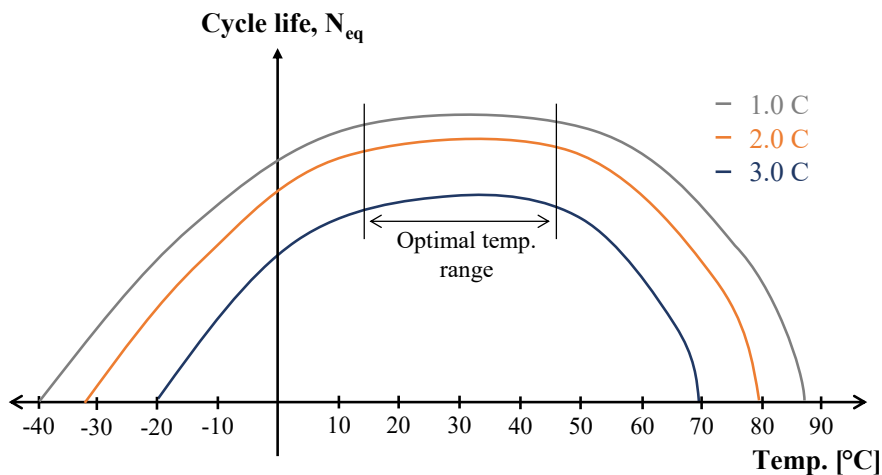
Figure 15: Generalized relationship between cycle life and operating temperature for Li-ion batteries, for different c-rates. Adapted from [36].

2.3.1 Different Degradation Models

In order to correctly simulate and analyze battery operation, a model of battery degradation is required. There exists many different approaches for this, that can be found in literature, in which a few of them are presented here.

Model with Focus on DoD and Calendric/Cyclic Aging Split

In [37], a battery degradation model is developed to account for capacity fade and related costs during operation and cycling. The model assumes NMC type, and split the degradation in calendric and cyclic aging, where either part is set to define the reduction of capacity for a certain time step. The variations in DoD, causing reactions with deposited lithium, is the basis for cyclic degradation in this work.

The calendric aging, or shelf degradation as stated in the report, is set as a linear function of time, according to equation 5. Here, L_{shelf}, is the assumed life time (shelf life) of the battery when stored

at certain conditions and *DP* is the degradation percentage. If the shelf life is 20 years, and the time resolution is in hours, the calendric degradation at any time step is assumed to be 0.00057 %. The cyclic aging of time step t is found based on the total amount of cycles that the battery is assumed to go through, if the battery is operated similarly for the rest of its life, according to equation 6. For each time step, the greatest of these two degradation estimations are used to set the actual degradation percentage (DP) of time t, as in equation 7 [37].

$$DP^{cal}(t) = \frac{100\%}{L_{shelf}} \tag{5}$$

$$DP^{cyc}(t) = \frac{100\%}{N_{cy}(t)} = \sum_t deg_t^{cyc} \tag{6}$$

$$deg_t^{cyc} = 0.5 \cdot |deg_t - deg_{t-1}|$$

$$DP(t) = max\left\{DP^{cal}(t), DP^{cyc}(t)\right\} \tag{7}$$

The cyclic degradation is based on $N_{cy}(t)$, which is a predefined function for the number of cycles the battery can have before end of life (EOL) or failure. The function, obtained from [38], is presented in equation 8. $N_{100\%}^{fail}$ is the number of cycles to EOL with operation at 100 % DoD and k_p is a type specific constant ranging from 0.8 to 2.1 depending on battery chemistry. The graphical illustration of this function, for the case from [37], is given in figure 16.

$$N_{cy}(t) = N_{100\%}^{fail} \cdot DoD^{-k_p} \tag{8}$$
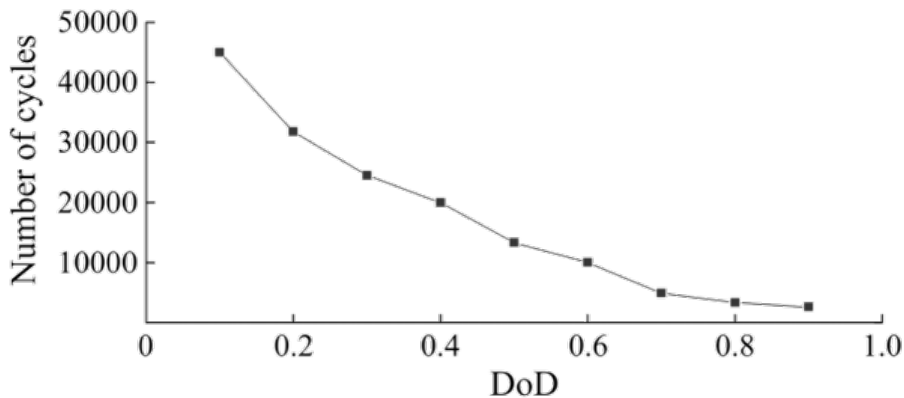
Figure 16: Cycle life for different DoD [37].

The degradation percentage for the cyclic degradation, DP^{cyc}, is found by calculating a loss percent-

age for several points in this graph, using equation 6. From this, figure 17 is created, expressing degradation for different intervals in SoC. To illustrate the principle, an example is given where the battery discharges from a SoC of 80 % to 20 % at time t. The cyclic degradation percentage for this period is found to be 0.014 %, based on the number of cycles from figure 16:

$$0.5 \cdot |\tfrac{1}{34957} - \tfrac{1}{3221}| = 0.014\%$$
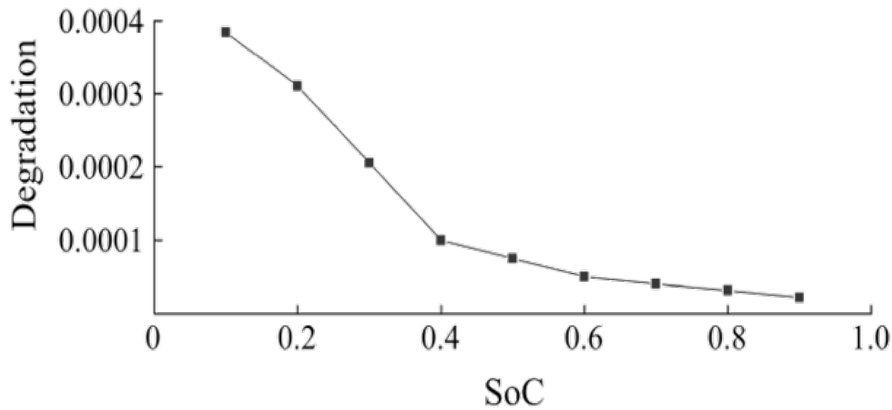
Figure 17: Degradation for different levels of SoC [37].

In [20] and [37], the degradation percentages are found for all possible SoC values, using the above figure and mixed integer linear programming (MILP), in order to include the values between the data points that are known.

Models Assuming Addable Calendric and Cyclic Aging

In contrast to the above-mentioned model, several degradation models assuming that degradation effects from calendric and cyclic aging are additive are presented in [29]. The author presents these models with the names of their origin, being the NREL Model ([39]), the MOBICUS Model ([40]) and the Wang Model ([40, 41]). These are briefly described in the following parts.

The NREL Model

The NREL Model ([39]), was originally made for the NCA chemistry, but has been updated to include other chemistries such as the LFP. It includes losses in battery capacity, due to the loss of active lithium (Q_{Li}), the loss of active sites in the electrolyte (Q_{Sites}) and internal resistance. The minimum of the two first contributors are set to define the capacity loss, according to equation 9. The internal

resistance is defined in equation 10. The coefficients (a, b, c) are chemistry specific and can be tuned [29].

$$Q = min(Q_{Li}, Q_{Sites}) \tag{9}$$

$$where:$$
$$Q_{Li} = b_0 + b_1 t^z + (...)$$
$$Q_{Sites} = c_0 + c_1 N + (...)$$

$$R = a_0 + a_1 t^{1/2} + a_2 N \tag{10}$$

The model incorporates temperature, SoC and DoD. However, it does not include any direct dependency on c-rate. To summarize the model, it predicts incremental aging for a certain period, over a standard aging profile. It includes cyclic and calendric aging terms together, as these two effects in reality cannot be separated from each other [29].

The MOBICUS Model

The MOBICUS[17] Model ([40]) is the product of a french national collaborative project from 2013 to 2017. It builds upon earlier research on the separate effects of cyclic and calendric aging [42]. The new approach of this work was about linking calendric and cyclic aging with a nonlinear and strong coupling. The model should work for both first and second life batteries [29].

For the cyclic aging, the temperature was found to have the most significant effect. This was for a LMO-NMC chemistry. Furthermore, the effect of energetic throughput was found to be more important than the effect of current (c-rate). For storage and calendric aging, the temperature was chosen to have a stronger effect than storage SoC, in line with earlier observations and documentation from others work. The model descriptions are to little extent available in the literature at present time.

The Wang Model

The Wang Model ([40, 41]) has been built using accelerated life testing of many different battery operating conditions. It is developed based on the 1.5 Ah 18650 LMO-NMC Sanyo battery technology, including a combined relationship between calendric and cyclic aging. It is based on a large set of data, that is used to make a theoretical-empirical model [29].

The calendric aging part of the model is established from fitting parameters to a relationship following the Arrhenius dependence on temperature, as introduced with equation 1. As the available data from

---

[17]Modeling of Batteries Including the coupling between Calendar and Usage aging

testing did not include battery cells at storage, cycling data for low c-rate (0.5C) and shallow DoD (10 %) was used to simulate approximate storage conditions. The resulting model, for calendric degradation only, is expressed in equation 11.

$$Q_{loss,\%}^{cal} = 14876 \cdot e^{-24.5kJ/(RT)} \cdot days^{1/2} \tag{11}$$

In order to find a model for the cyclic aging, the above-mentioned calendric degradation was calculated and subtracted from the total capacity loss, which was measured for the different test conditions. Equation 12 shows the fundamental form of the function used to fit the obtained results. B_1 and B_2 are both fitting factors.

$$Q_{loss,\%}^{cyc} = B_1 \cdot e^{B_2 \cdot c_{rate}} \cdot Ah_{throughput} \tag{12}$$

By combining the expressions for calendric and cyclic degradation, the overall degradation model becomes equation 13[18]. The coefficients and parameters, with values and units, are presented in table 3. Note that this relationship is highly nonlinear, involving both exponential terms, the square root of time and several variables (temperature and c-rate).

$$Q_{loss,\%}^{tot}(t) = |aT_K^2 + bT_K + c| \cdot e^{[(dT_K+e)\cdot c_{rate}]} \cdot Ah_{throughput} + f \cdot t_{day}^{1/2} \cdot e^{\frac{-E_a}{RT_K}} \tag{13}$$

The equation can be further adapted by replacing the energetic throughput with the number of equivalent cycles, from equation 4, and gather some of the parameters into the equivalent constants k_1 and k_2. The latter can only be done when assuming constant temperature. This, in addition to expressing the time on an hourly resolution in stead of a daily resolution, is done in equation 14.

$$Q_{loss,\%}^{tot}(t) = k_1 \cdot e^{[(dT_K+e)\cdot c_{rate}]} \cdot N_{eq}(t) + \sqrt{\frac{t}{24}} \cdot k_2 \tag{14}$$

Table 3: Coefficients and constants for the Wang model (degradation) [29].

Coeff.	Value	Unit	Coeff.	Value	Unit
a	$8.61 \cdot 10^{-6}$	$1/(Ah \cdot K^2), 1/(N_{eq} \cdot K^2)$	T_K	(...)	K
b	$-5.13 \cdot 10^{-3}$	$1/(Ah \cdot K), 1/(N_{eq} \cdot K)$	E_a	24.5	kJ/mol
c	$7.63 \cdot 10^{-1}$	$1/Ah, 1/N_{eq}$	R	8.314	$J/(mol \cdot K)$
d	$-6.7 \cdot 10^{-3}$	$1/(K \cdot c_{rate})$	t	(...)	$day, (hour)$
e	2.35	$1/c_{rate}$	$k_1(@ 15 °C)$	$3.176 \cdot 10^{-4}$	$1/N_{eq}$
f	14 876	$1/day^{1/2}$	$k_2 (@ 15 °C)$	0.5384	$1/\sqrt{hour}$

The battery degradation during five years (1825 days) is plotted in figure 18 for different tempera-

---

[18]The equation from the source ([29]) does not include the absolute value of the first term. This is added to avoid negative degradation for some conditions.

tures and an energy throughput of 0.8 full equivalent cycles per day ($N_{eq} = 0.8/day$). It includes temperatures of 5, 15 and 35 degrees Celsius.
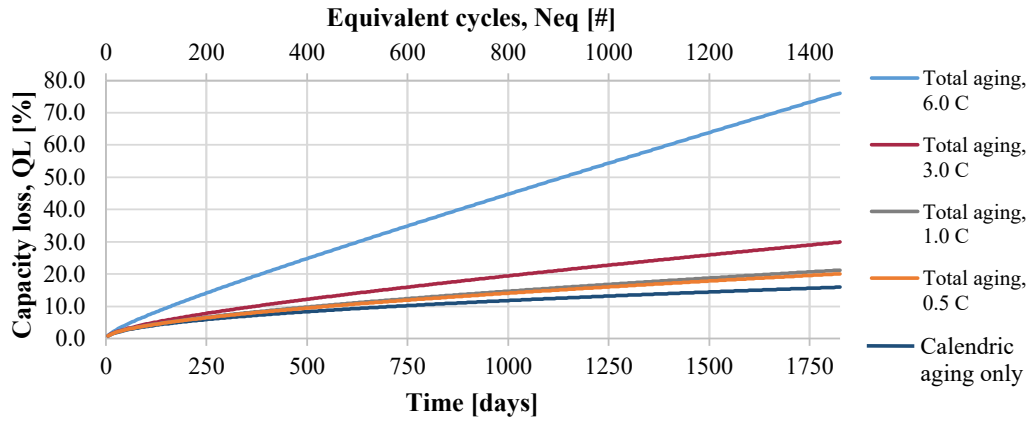
(a) Temperature: 5 °C.
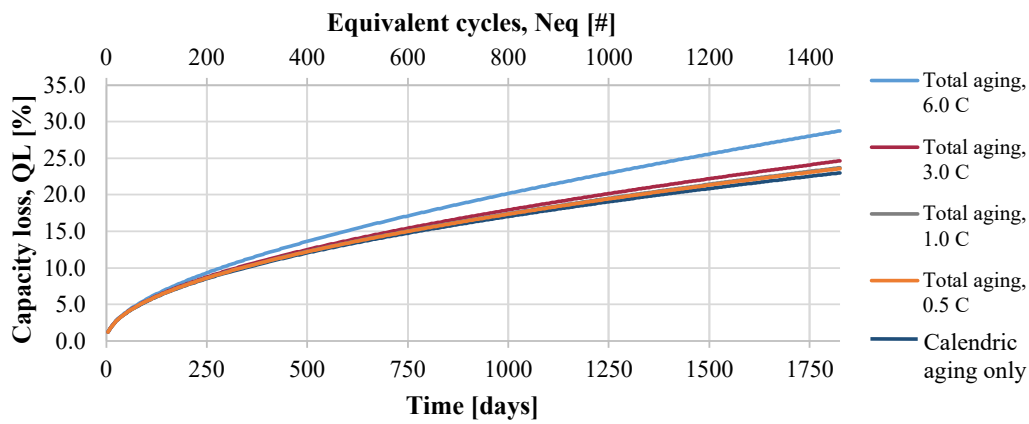
(b) Temperature: 15 °C.
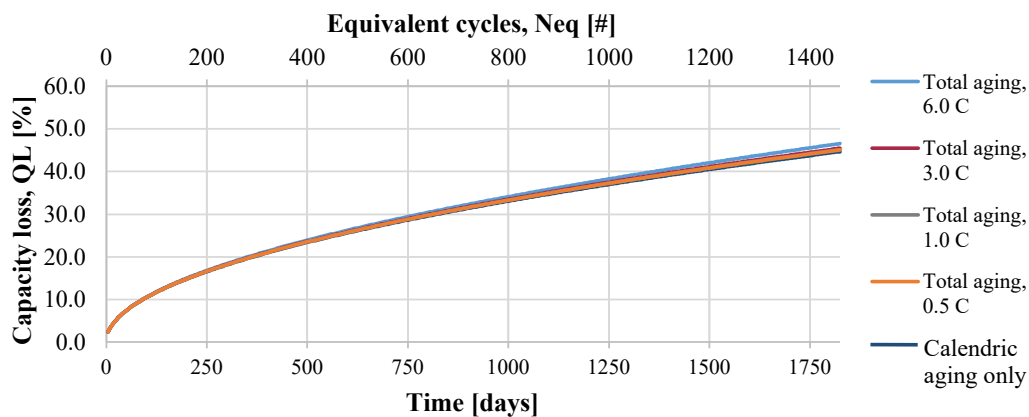
(c) Temperature: 35 °C.

Figure 18: Degradation of a LMO-NMC battery during 5 years, according to the Wang model. For different temperatures and 0.8 FECs per day.

Observations from the model indicate that the total degradation follows an almost linear relationship at lower temperatures (e.g. 5 °C). Cyclic aging is dominant at this operating temperature, which is especially notable for large c-rates as in figure 18a. At higher temperatures, for instance 35 °C, the square root relationship with time is more evident as the calendric aging is dominant. This is also observed in figure 18b and 18c [29].

Limitations of Battery Degradation Models

The battery degradation models are useful, because they allow for extrapolation of future conditions that would be too time and cost-intensive too find empirically. In addition, it can help making good estimations on optimal, future, operation. However, it is difficult to catch all dependencies as the degradation mechanisms are very complex. Therefore, and to limit computational effort, different models weights some factors higher than others [29].

The models described in this section have different focus. The first model (used by [20] and [37]) emphasizes the importance of DoD and SoC, and splits calendric an cyclic degradation. It excludes temperature dependencies. The other three models all combine calendric and cyclic aging, and states that temperature dependencies are the most important. They include several of the factors mentioned in section 2.3, to some extent. However, the Wang Model does not capture the effects of variations in DoD and SoC [29].

2.4 BESS Investment and Operation Costs

The economical benefit of a battery energy storage system is to a large extent a question of investment costs. The other, very important, factor is the operating costs concerned with buying energy and power from the grid, and the amount of savings a BESS can provide by for instance exploiting energy arbitrage and peak shaving. The latter case is described more in depth in section 3, while the investment costs of Li-ion batteries are presented here. The cost data provided in this section is gathered from various literature and reports on real projects, accounting for currency differences, inflation and assumed price development[19].

The investment costs of battery energy storage systems depend on several factors, such as type of technology, battery chemistry, power electronics, power capabilities and storage capacity. In addition, the investment costs also include designing, planning (engineering) and labor, summarized as installation costs. These cost items depend on factors such as geographical location, wage levels and

---

[19]Currency rates from June 1, 2022 (average): 10.06 NOK/EUR, 9.368 NOK/USD.
Inflation: 2.3 % per year until 2022 (see figure E.3 in appendix E).
Assuming a linear cost decrease of 5 %/year from 2020 to 2025. Taxes excluded unless otherwise mentioned.

the sizing (scaling). In other words, it is difficult to give precise estimates on investment costs and the cost data found in literature also varies significantly [43].

When looking at the investment cost of a BESS, it is especially important to note the type of technology and size of the system that the cost data covers. The investment costs are especially sensitive to the ratio between power and capacity capability, and it is therefore useful to know the costs per unit of power and per unit of energy (capacity). This is especially an advantage when scalable costs are required, which is the case when costs are to be compared or when the system sizing, during the planning phase of a BESS investment, depends on the costs.

For cost analyzes in this thesis, the investment costs are provided per unit of power (NOK/kW) and per unit of nominal capacity (NOK/kWh). These are addable, meaning that the total cost is the sum of the two elements, as described in [43]. The two parts cover the following:

- Energy (capacity) part [NOK/kWh]: Contains the costs associated with the battery packs, BMS and some wiring for the battery packs.

- Power part [NOK/kW]: Contains the costs associated with the power parts and materials that are dimensioned based on power, such as the power electronic devices (inverter/converter), transformer, electrical BOS and structural BOS.

Equation 15 and figure 19 show the principles of splitting the costs of power and energy, and how this affects the system price. It is common to inform about the capacity of a BESS by providing the power capability and the maximum time of operation. For instance, a BESS can be characterized by 1.0 MW and 4 hour of operation, which makes it a *4 hours system*. From figure 19, it is evident that a one hour system, with higher power capability, is more expensive than a four hours system per unit of capacity. This split of costs is even more important considering that the costs of battery packs are assumed to decrease faster than the cost of power equipment [43].

$$C_{BESS} = C_{BESS}^{kWh} \left[\frac{NOK}{kWh} \right] + \frac{\text{costs of other components}}{kW} [NOK] \cdot \frac{1}{T} \left[\frac{1}{h} \right] \qquad (15)$$
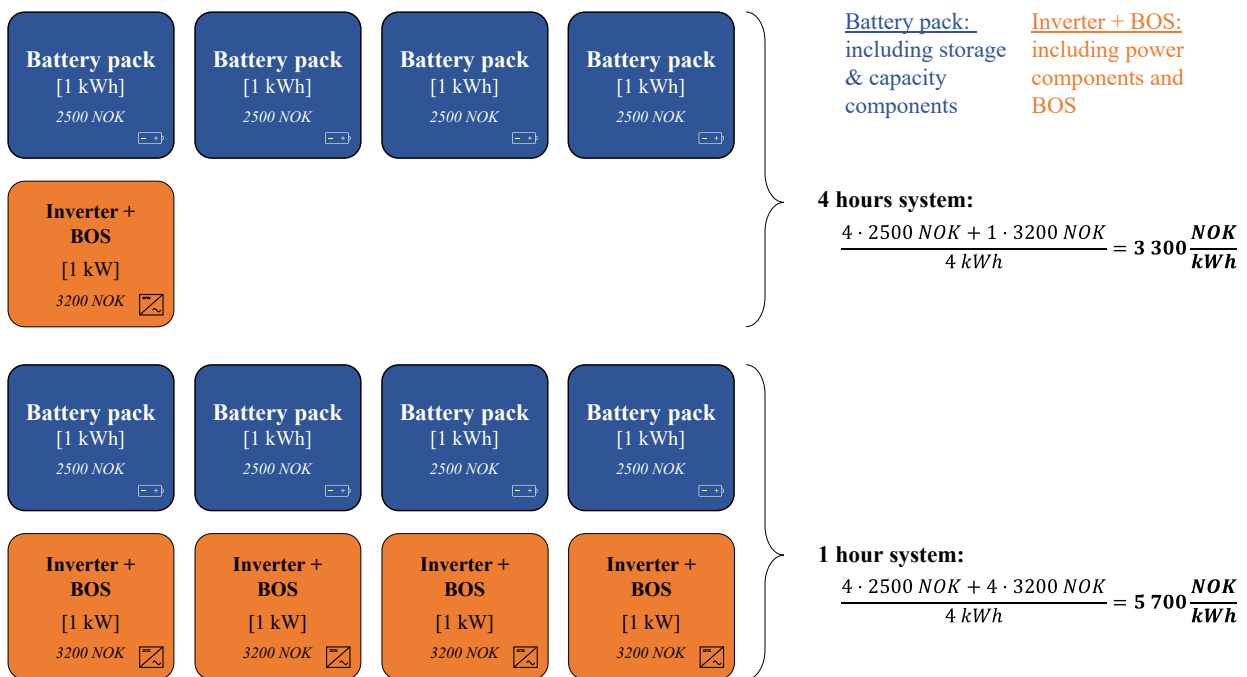
Figure 19: How power capability and capacity affects BESS investment costs.

Figure 20 shows the cost compositions for a medium and large scale BESS, based on Li-ion, with data adapted from NREL ([23], 2020). Figure 20a shows the breakdown of costs for a 600 kW BESS for 0.5 to 4 hour operation (300 kWh - 2.4 MWh). The same is shown for a 60 MW, utility scale, BESS in figure 20b (30 MWh - 240 MWh). The costs of the battery packs and central inverter is the same per kWh and per kW, respectively, while the costs of BOS-equipment are lower for the case of a utility-scale BESS. The same relationship is observed for engineering, design and installation labor[20] (summarized as installation costs).

The installation costs, expressed as a fraction of the material costs, differ significantly for the different cases. For the commercial BESS of 600 kW, these ranges from 0.608 for the 4 hours system to 1.22 for the 0.5 hour system. For the utility scale BESS, the fraction varies from 0.274 to 0.538 for the same compositions. This shows that installation costs constitute a large share of the investment costs, especially for the commercial scale [23].

---

[20]Note that all costs associated with engineering and labor are for US cost levels. Costs related to wages varies for different countries
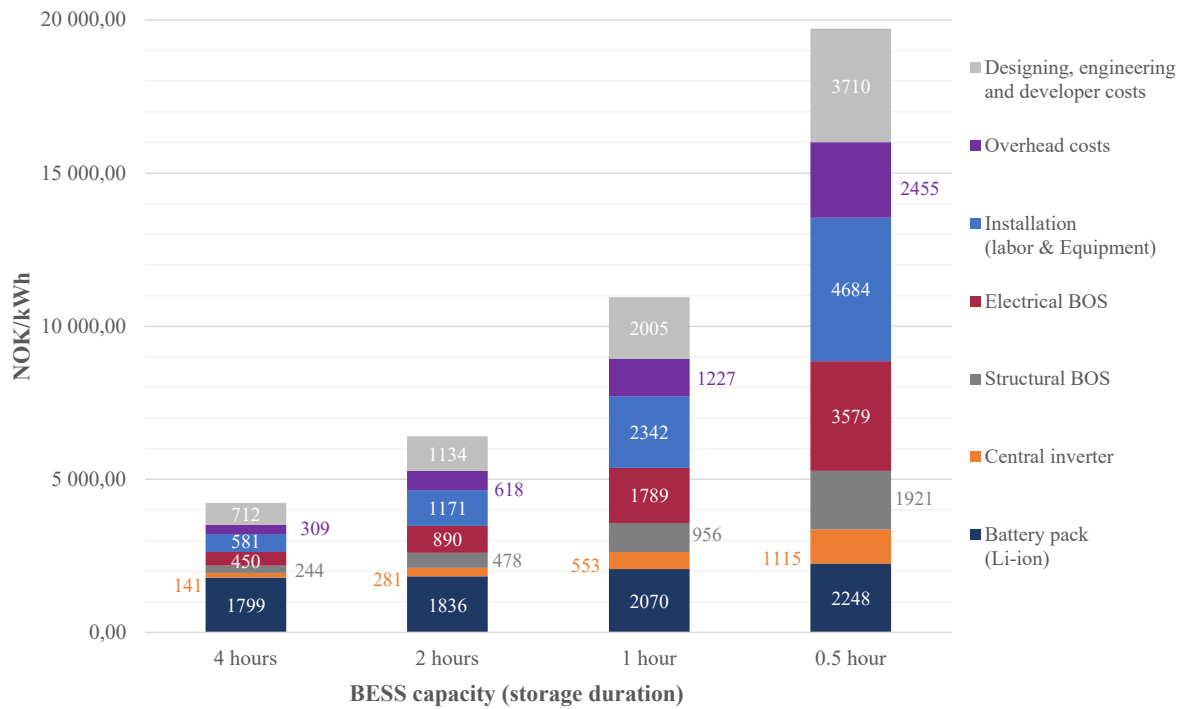
(a) Commercial Li-ion BESS with power capability of 600 kW and capacities for 0.5 to 4 hours.
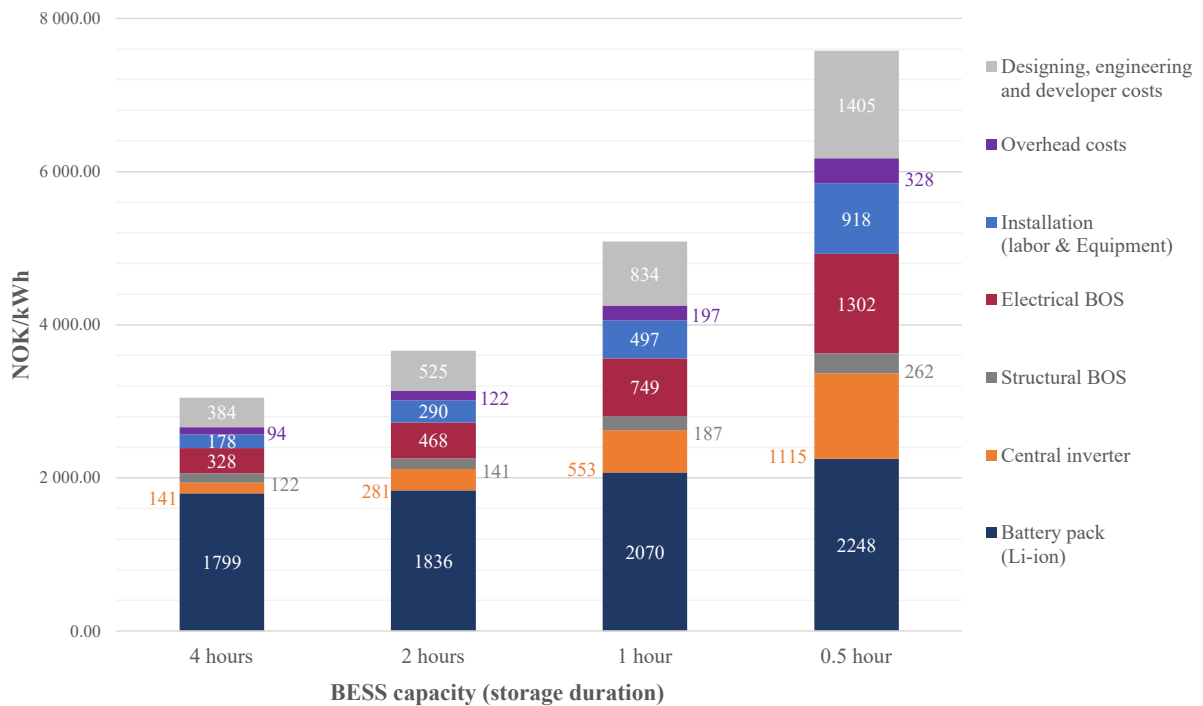
(b) Utility-scale Li-ion BESS with power capability of 60.0 MW and capacities for 0.5 to 4 hours.

Figure 20: Cost components, per nameplate kWh, of Li-ion BESS for different capacities. Costs in 2019-NOK. [23].

The inverters (converters) contribute with a big part to the total investment costs. For small and

residential systems of 3.0 to 5.0 kW, prices can be found in the range of 3 000 to 6 000 NOK/kW. For the larger systems, as the 600 kW and 60 MW depicted above, the costs of power converters are assumed to be in the range of 500 - 600 NOK/kW. In addition, the costs of both structural and electrical BOS add to the total investment costs [23].

Figure 21 shows estimates on future investment costs, until 2050, for both energy (capacity) components and power components that are addable. The data, obtained from a NREL report [43] analyzing current and future BESS costs, includes three scenarios on future developments. These are high, medium and low price reductions It is shown that the prices of energy components, mostly for battery packs, are assumed to fall for most of the scenarios. However, the costs of power components are shown to fall less.

(a) Energy components (capacity). (b) Power components.
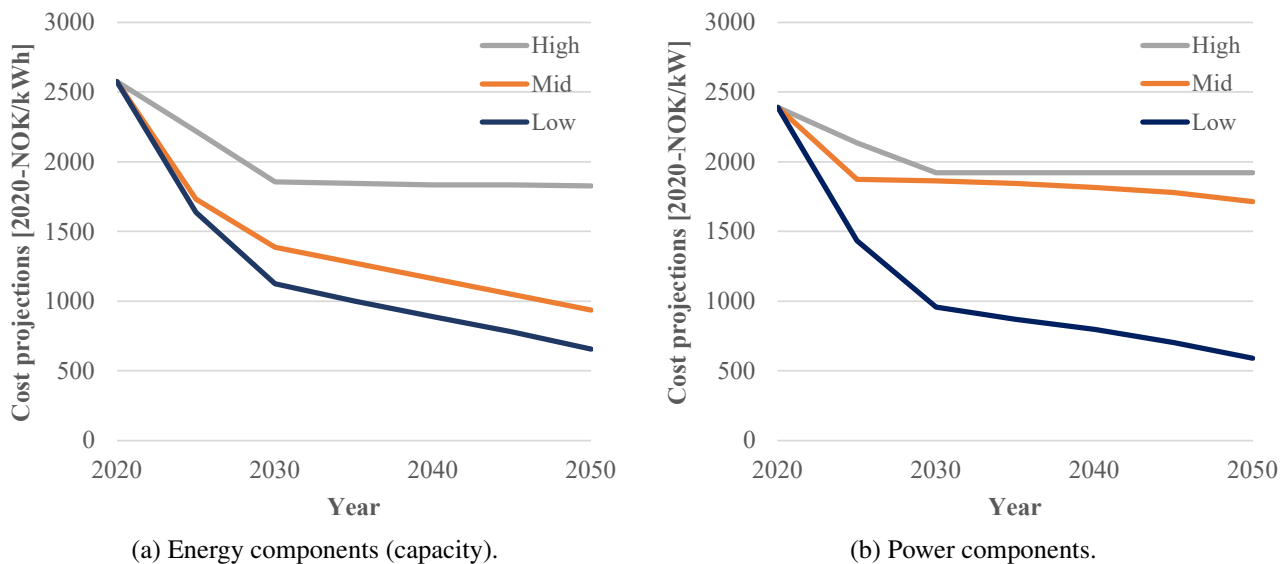
Figure 21: Cost projections in 2020-NOK for the energy (storage / capacity) components and the power components for a Li-ion BESS. Adapted from [43].

A different source ([44]), with data presented in table 4 for both LFP and NMC chemistry, show similar costs as the figure with NREL data. The tabulated data is however even more conservative with respect to changes in the costs of power components. It also shows that the NMC chemistry is often more expensive than for instance LFP. Both these figures and the data from the illustration above are assumed to exclude installation costs.

Table 4: Ranges of BESS addable cost elements, for capacity (energy) and power (LFP and NMC). For 2021 and estimates for 2030 [44].

21,22	2021				2030			
	Capacity part [NOK/kWh]		Power part [NOK/kW]		Capacity part [NOK/kWh]		Power part [NOK/kW]	
	Low	High	Low	High	Low	High	Low	High
LFP	1 500	1 900	2 400	2 600	900	1 200	2 300	2 500
NMC	1 800	2 200	2 400	2 600	1 100	1 500	2 300	2 500

A summary and comparison of cost data from the literature can be found in appendix C. The average costs from this comparison is found to be 3 100 - 5 600 NOK/kWh (2022-NOK), for battery sizes that are relevant for the case of this thesis. This includes materials and installation costs, but excludes taxes.

2.4.1   Operation and Maintenance Costs

Operation and maintenance costs are also important to consider. These cover the costs for small material replacements and the need for trained crew to enter the BESS installation for cleaning, inspection and replacement work. Table 5 summarizes some cost levels, presented per unit of installed power capability, that are obtained from different sources. In general, smaller facilities and systems with high power capabilities will have higher operational costs per unit of installed power than a larger facility with moderate power capabilities [43].

Table 5: A comparison of O&M costs (OPEX) for stationary Li-ion BESS, obtained from literature (2021).

Source name / citation	Annual costs [NOK/kW/year]	Comment
PNNL [44]	25 - 33	LFP type
PNNL [44]	30 - 36	NMC type
Abraham A. Kebede et al. [2]	50 - 110	-
Cole Wesley et al. (NREL) [43]	45 - 230	Ranges from several sources (2019 and later)

---

[21]All data for a 4 MWh, 1 MW BESS, excluding taxes, design work and installation.
[22]Capacity part only includes storage elements. Power part includes power equipment and all BOS

2.5 Introduction to Regulations and Environmental Considerations

So far, the technical and economical aspects of a battery energy storage system has been described. However, other factors, such as regulations, HSE precautions and environmental considerations need to be evaluated before choosing to install a BESS. This is out of scope to evaluate in this thesis, as the topics are complex, but a brief introduction is given for the sake of overview.

HSE, Standards and Regulations

There is certain risk involved with the use and storage of Li-ion batteries. Overcharging, large currents and short circuit currents can cause fire and explosions, if the BESS is not designed and operated correctly. One very important process that must be avoided is thermal runaway, when the battery cell enters a self-heating, unstable, state. Good ventilation and heating management (HVAC), with for instance water cooling, is an important safety measure to avoid this from happening, and reduce the danger of fire and explosions [13].

Battery energy storage systems are often bought, transported and installed with container systems, as illustrated in figure 7. The location of the BESS must be such that the risk of fire spreading to other components, buildings and infrastructure is minimized. The systems should therefore be installed with certain distance from other elements, and such that personnel from fire departments have easy access. Safety distances and other measures for precaution are listed in relevant regulations, guides and standards. NEK, The Norwegian Electrotechnical Committee, has for instance published several standards on BESS installations. These, and other relevant examples on documentation, can be found in appendix D.

Area Footprint of BESS Installations

Another consideration for the planning and installation of a BESS system is the area footprint. This must be considered, due to the above-mentioned safety requirements and the fact that a larger installation will require more construction work and higher installation costs. Table 6 gives an overview of the space requirements for different types of battery energy storage systems, that are based on real projects [45]. It shows that Li-ion systems require less area than for instance systems based on sodium-sulfur (NaS). Flow batteries, represented by VRFB, require the largest footprints, which can be more than ten times larger than those of Li-ion. Based on the specific energy and energy density of lead-acid batteries, systems based on this technology are assumed to have space requirements between the ones of NaS and VRFB.

Table 6: Space (area footprint) requirements for some BESS types [45].

BESS type	Space requirements [m^2/MWh]	Footprint of example installations	
Li-ion, NMC	5.00 - 7.50	2 MWh: 20 ft. container ($\sim$14 m^2)	4 MWh: 40 ft. container ($\sim$30 m^2)
NaS	17.5 - 77.0	1.5 MWh: 6.10m $\times$ 2.40m ($\sim$15 m^2)	6 MWh: 6.10m $\times$ 5.60m ($\sim$34 m^2)
VRFB (flow)	75.0 - 100	1.5 MWh: 12.9m $\times$ 4.90m ($\sim$60 m^2)	6 MWh: 27.0m $\times$ 17.0m ($\sim$459 m^2)

Environmental Impacts and Considerations

The manufacturing, transportation, operation and end-of-life (EOL) management of a battery energy storage system all have environmental impacts that should be considered. Life cycle assessments (LCAs) investigate these impacts, from "cradle-to-grave". According to [46], a LCA comparing lithium-ion and lead-acid batteries for grid energy storage, the operation phase and battery cell manufacturing constitute the largest impacts on the environment. Lead-acid is found to have the biggest, overall, impact and is used as benchmark. The NCA chemistry is found to be the best performer for climate change and use of resources (especially fossil fuels), while NMC performs better considering the acidification potential, both constituting around 50 % of the impacts from lead-acid batteries. An important reason for the environmental benefit of Li-ion, is the life time. In the report, the life time of lead-acid is 8.5 years while the life time of Li-ion batteries ranges from 15 to 20 years, depending on chemistry [46].

A large share of the manufacturing processes for Li-ion batteries are located in China and America (e.g. the USA and Mexico). Because of the large share of fossil fuels in the energy mix of these countries, the production of batteries causes emission of greenhouse gases (mostly CO_2), that must be accounted for [46]. The making of a battery pack with capacity of 1.0 kWh requires approximately 400 kWh of energy [2]. In order to calculate the environmental footprint of this production, the emissions related to the energy supply must be known. If the power source is natural gas, having an emission factor[23] of approximately 500 $g_{CO_{2-eqv}}$/kg, a 1.0 kWh battery pack would cause the emission of around 200 kg CO_2, before being used [47].

---

[23]Emissions related to production of electricity, including life time estimates on emissions for the production technology.

3 Energy Costs and Economical Analysis

There are several economical aspects that are relevant to introduce when speaking of grid connected energy storage systems. The investment and maintenance costs have already been introduced in section 2.4, but there are also significant costs associated with the usage of such systems. Being connected to the power grid, a BESS would be a part of the electricity market where electrical energy is sold and purchased. The operating costs associated with energy and power affects the feasibility of a BESS installation, and the BESS should be operated in a way that minimizes these costs.

On the other hand, the electricity market that a grid connected BESS would be involved in, needs to be efficient and economically attractive for all parts that are included. To ensure this, and to ensure best possible operation of a BESS, the mathematical technique of optimization is important. In this section, the general principles of optimization, the power market, pricing for energy and power and tools for economical analysis are introduced.

3.1 The Optimization Technique

Mathematical optimization is, as the name suggest, a method for finding the best possible solution to a problem, where several solutions are possible. Having a mathematical function that describe something, the goal is to assign the best possible values for the variables of this function while considering some criteria. The goal can for instance be to maximize or minimize this function. In these cases, the optimization problem is called a maximization problem and minimization problem, respectively.

Equation 16 shows a simple example of a minimization problem. The same general setup also applies for maximization problems, the only difference being the goal (represented by "*min*" or *"max"*). The function that is to be minimized, *f(x)*, is called the objective function. It is followed by a number of constraints, being a list of functions and statements (four in this example). The constraints can for instance be formulated such that some variables must be within certain limits, or that a function of one or more variables must equal, be greater than or be equal to, certain value. In this example, there are three function of variables that are required to be less than, equal to or larger than some constants (a, b and c). Optimization problems usually contains several functions and variables [48].

$$\min_{x} \quad f(x) \tag{16}$$

$$\begin{aligned}
s.t. \quad & g(x) \leq a \\
& h(x) = b \\
& i(x) \geq c \\
& x \geq 0
\end{aligned} \tag{17a}$$

If all of the mathematical functions are linear, the problem is said to be a linear programming problem[24]. There are several ways of solving such problems, by for instance graphical and algebraic methods. One technique that is widely known is the simplex algorithm. In short, this method is based on finding the most optimal value of all variables, by defining a feasibility region and checking the objective value for possible variable values, within this region. The feasibility region is formed based on the restrictions (constrains). The combination resulting in the best objective value, depending on whether the goal is minimization or maximization, is the output and the optimal solution [48].

Simple problems can be solved manually with this method. However, as many optimization problems are complex, a computer program such as Excel and MATLAB, or programming languages like Python or Julia, are often required. Furthermore, complex problems usually have several solutions, which are called local optimums. The best of these solutions are referred to as the global optimum. A local solution may, or may not, be the global optimum.

3.2 The Electricity Market and Costs of Energy and Power

Norway is a part of the Nordic and European electricity market. In this market, electrical energy is sold and purchased between producers, consumers, prosumers, grid companies, system operators (SO) and retailers. In Norway, the grid companies are also the system operators (DSOs for distribution grids). As electricity cannot be stored in large quantities for long time periods, it must be consumed once it is produced. A goal of the electricity market is to ensure that the energy resources are exploited in an effective manner, to cover the energy requirements of the societies [49].

Nord Pool AS is the largest trading platform of power, having a futures market, a day-ahead (also known as elspot) market and an intra-day market. In addition, the balancing market is important and

---

[24]"Programming" in this case can be understood as a synonym of "planning"

interesting concerning BESS installations. From 2023, the minimum power that is possible to bid in the balancing market is 1.0 MW [50]. In Norway, it is Statnett that is responsible for, and the only trader in, this market [49].

The day-ahead market, also known as the elspot market, is the central instrument where all producers and consumers submit their bids on power production and consumption, including prices and volumes (amount of energy). Based on the above-mentioned optimization techniques, a market clearing price is found from solving an optimization problem with the goal of maximizing the benefits for both producers and consumers. In short, it is about finding the optimal electricity price for both parts, given restrictions on power production, available resources, power transfer and other limitations of the power systems. The optimal electricity price is found for every hour, every day, and is known as the electricity spot price [49].

The above-mentioned process of market clearing is done for all regions that are involved in the market. Each country has one or more such zones, which are known as price zones. In Norway, there are currently five different price zones, which are illustrated in figure 22. Trøndelag is located in NO3, which borders to NO5 and NO1. In figure 23, it is shown that there are different prices for different areas, at the same time. This is mainly caused by the regions having surplus or deficit of power, and that there are capacity limits on the power transfer between neighboring zones [49].

Figure 22: Price zones in Norway [51].
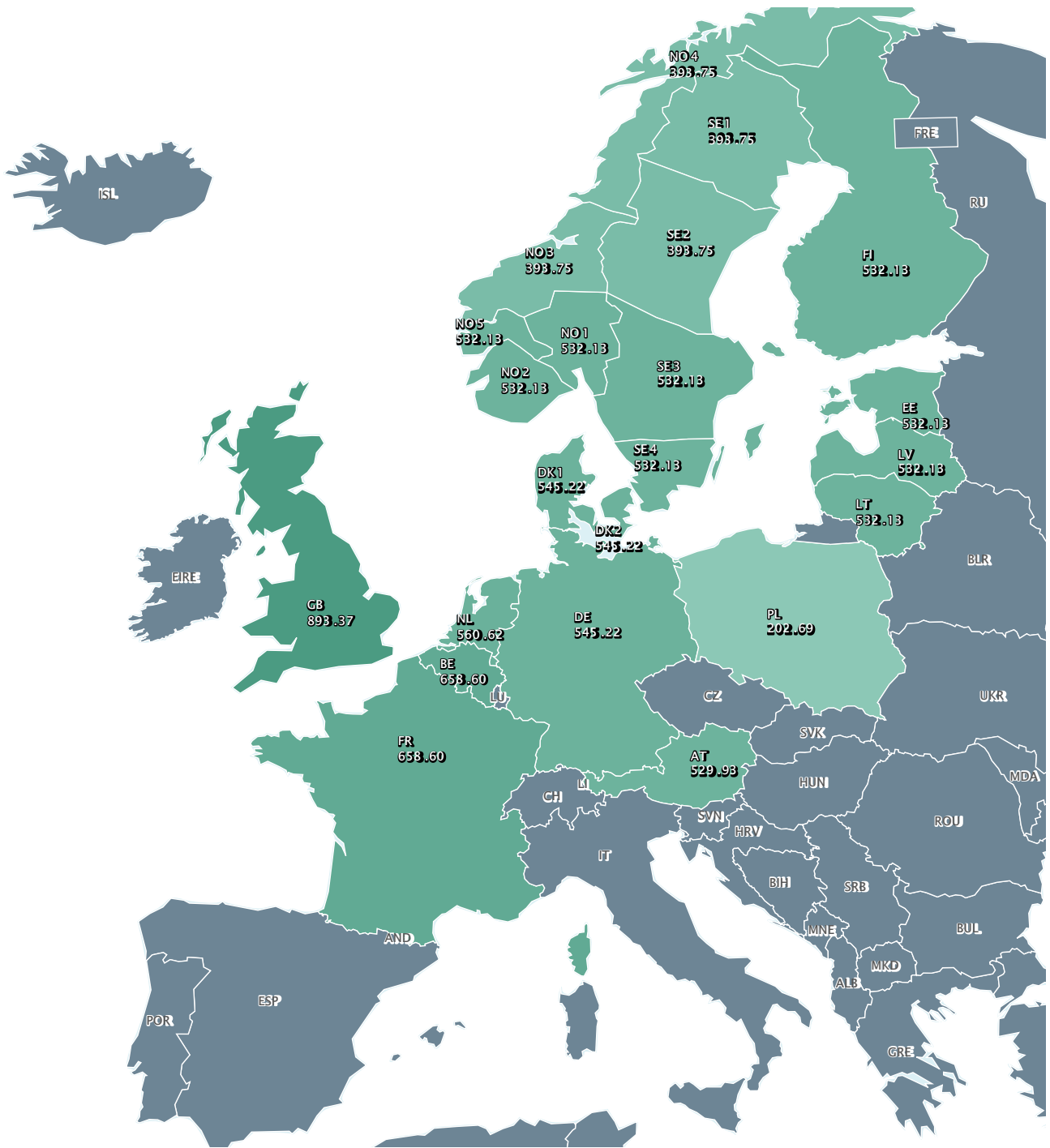
Figure 23: Day-ahead prices for Europe, [EUR/MWh]. Dec 12, 2022 (08:00) [51].

3.2.1 Pricing of Power and Energy

All of the above-mentioned market segments are a part of the wholesale market. In the end-user market, individual end users (being private households or businesses) buy their power from a power supplier of their choice. These power suppliers are the retailers in the wholesale market, and can make contracts of different types with their customers. These contracts often include a fixed, monthly price, the spot price or a fixed electricity price, and a surcharge. The electricity spot price, varying for every hour in a day according to the clearing in the day-ahead market, is the most common contract type and is used as basis in this thesis [49].

Figure 24, with data from Nord Pool AS [51], shows how the electricity spot price (NOK/kWh) varies throughout the year. The daily average for NO3 in 2020 and 2021, as well as for NO5 in 2022 are plotted. It shows significant variations for the three different years and the two different price zones. The spot price is much higher in 2022 compared to 2020 and 2021 due to several reasons[25], such as high prices on gas and coal which is used for power generation in several European countries [52]. In addition, the prices of 2021 and 2022 are volatile compared to the prices of 2020. The year of 2020 had the lowest electricity prices of its preceding decade, which can be observed from appendix E.
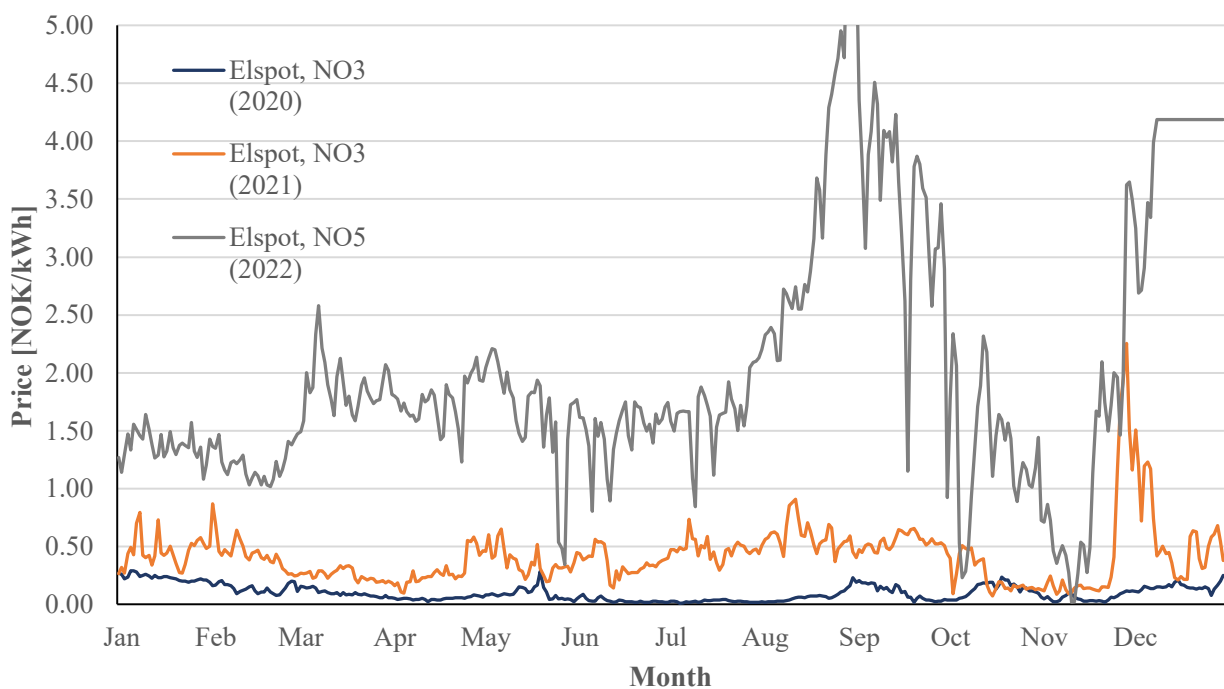
Figure 24: Comparison of the electricity spot prices (daily average), for 2020-2022 and NO3/NO5 [51].

---

[25]The energy prices can be seen in conjunction to the geopolitical situation in Europe from 2020 to 2022. The outbreak of Covid in 2020 resulted in less activity and the escalation of the Russo-Ukrainian War in 2022 resulted in high gas prices.

The electricity spot price, $c_{E,spot}$, constitutes one part of the energy costs of a power consumer. The other part is the grid tariff that must be paid to the local grid owner (DSO). This is a cost for everyone who imports energy from the power grid, and the pricing is set to cover the expenses of the grid-owner such as losses in the grid, maintenance, fees and some margin to account for price variability[26]. As the grid owners (DSOs) are monopolists, these companies are regulated by NVE-RME[27]. The grid tariff usually consist of the following [49, 53]:

- A Fixed part [NOK/month]

- A fixed energy part, related to actual consumption, $c_{E,tar}$ [NOK/kWh]

- A power part: A customer has to pay for their peak consumption, usually measured as the average of the three highest power peaks (registered at three different days): $c_{P,tar}$ [NOK/kW$_p$/month]

- Taxes, such as VAT[28]. Business/industry also pays tax on electric power, $c_{E,tax}$.

The power part of the grid tariff is organized in two different ways, depending on the consumption and type of customer. If the customer is a household or small business with consumption below 100 000 kWh/year, the power part is a fixed cost for different intervals of peak power. For large businesses/industries with consumption above 100 000 kWh/year, the power part is a variable cost depending on the actual peak power [53].

To summarize, a Norwegian electricity customer must pay for the energy to a retailer of own choice, most commonly based on the spot price, and a grid tariff to the local DSO.

Costs of Losses (Grid Components)

The above-mentioned pricing model captures the costs of energy consumption behind-the-meter. However, it does not capture the cost of operation of power and grid components that are located in front of the electricity meter. In order to give a more holistic overview, the costs of energy losses in relevant grid components can be calculated. In Norway, statistics indicate that the losses of electrical energy constitute 5 % of yearly power generation in average, and 11 % in max load situations [54].

In a planning guide [54], created by SINTEF and REN, a method is suggested for estimating costs of losses in components such as transformers, substations and power cables/lines. The model, with clarifications, is presented in equation 18. The advantage of this model, is that costs of power and

---

[26]The power cost of the grid tariff is also included to motivate for reductions in power peaks.

[27]*The Norwegian Energy Regulatory Authority*

[28]Value added tax: Tax that is paid when buying goods and services. General level: 25.0 %

energy losses can be calculated based on a few equivalent costs and a time factor, T_{loss}. The equivalent costs are tabular data, obtained from the planning guide. The utilization time of losses is a standard way of expressing the equivalent duration of maximum load (and maximum losses) that would give the actual, annual energy losses[29]. The equivalent costs of interest for this thesis is provided in appendix E.

$$
\begin{aligned}
C_{losses} &= k_p \cdot \Delta P_{max} + \int_t k_w(t) \cdot \Delta P(t) \\
&= k_p \cdot \Delta P_{max} + \Delta P_{max} \cdot k_{weqv} \int_t \frac{\Delta P(t)}{\Delta P_{max}} dt \\
&= k_p \cdot \Delta P_{max} + \Delta P_{max} \cdot k_{weqv} \cdot T_{loss} \\
&= \Delta P_{max} \cdot (k_p + k_{weqv} \cdot T_{loss})
\end{aligned}
\tag{18}
$$

Where:

C_{losses} : Annual costs of losses [NOK/year]

k_p : Cost of maximum power losses (during max load) [NOK/kW/year]

ΔP_{max} : Maximum power loss [kW]

$k_w(t)$: Energy cost at time t [NOK/kWh]

$\Delta P(t)$: Power loss at time t [kW]

k_{weqv} : Equivalent yearly cost of losses [NOK/kWh]

T_{loss} : Utilization time of losses [h/year]

For a transformer or substation (and similarly for other power grid components), the instantaneous power loss can be calculated according to equation 19. To calculate this, the nominal power/capacity (S_n) must be known, in addition to the transformer load losses at maximum load (P_k), the transformer no-load losses (P_0) and the active power flow at time t ($S(t) = P(t)$). By taking the integral of this expression, the total energy losses for the whole period (for example one year), can be calculated using equation 20. The latter can further be used to define the utilization time of losses, T_{loss}, with equation 21. The maximum power loss of a transformer is the sum of the load and no-load losses [54].

$$
\Delta P(t) = P_k \cdot \left(\frac{S(t)}{S_n} \right)^2 + P_0
\tag{19}
$$

---

[29]Values of T_{loss} depend on consumer category, but are most often between 2000 - 2400 hours/year

$$\Delta E_{loss} = \int_t \left[P_k \cdot \left(\frac{S(t)}{S_n} \right)^2 + P_0 \right] \tag{20}$$

$$T_{loss} = \frac{\Delta E_{loss}}{P_k + P_0} = \frac{\Delta E_{loss}}{\Delta P_{max}} \tag{21}$$

3.2.2 Economical Analysis Using Net Present Value (NPV/NPC)

There are many mathematical tools that can be used to evaluate the economical befts of an investment. The net present value (NPV) is perhaps the most known measures on economical feasibility. The general procedure for the method is to refer the values of all future cash flows to the value of money at a certain time, most commonly to the time of investment. All future costs and benefits are discounted back to this time, such that the time value of money is accounted for. The method is meant to account for the fact that a certain amount of money is worth more today than the same amount of money in the future, because of inflation and missed financial returns [54].

The general formulation for net present value is presented in equation 22, where I_0 represents the initial investment, C_t is the cash flow at time t, RV is the residual value of the investment after the period of interest ($t = N$) and r is the discount rate, also known as the rate of return or the calculation interest. The term $1/(1+r)^t$ can be substituted by a discount factor, $\alpha_r(t)$. It is most common to use years as the time resolution, and an investment resulting in a positive NPV (when $t = N$) is regarded as feasible [54].

$$NPV = -I_0 + \sum_{t=1}^{N} \frac{C_t}{(1+r)^t} + \frac{RV}{(1+r)^N} = -I_0 + \sum_{t=1}^{N} \alpha_r(t) \cdot C_t + \alpha_r(N) \cdot RV \tag{22}$$

The cash flows are defined such that benefits (e.g. revenue) are positive and costs are negative. In the cases when only the costs are of concern, the term "Net present costs" (NPC) can be used. The equation remains the same, with the exception that the signs are switched. The net present cost favors income, or cost savings, that occur in the beginning, and costs that occur at a later time.

The discount rate is an important element of the NPV, and reflects the time value of money. It usually accounts for inflation and required yields, that for instance could be the result of other, alternative, investments. NVE recommends a discount rate of 4.0 % for socioeconomic analyzes, which is also used as basis for this thesis [55].

4 The Case Study: Approaches and Methodology

In this chapter, the case that was introduced in section 1.4 is described in more detail. It includes an explanation on the approaches, assumptions and methods that are used. The mathematical formulations that are established in order to propose a solution to the case are presented, step-by-step.

The flow chart in figure 25 summarizes the methodology of this thesis, where optimization is a key element. The approach involves the making and simulation of two different optimization models. The first one aims to find the optimal sizing of the BESS (kWh and kW rating), and includes a model of the distribution grid connected to it. This model is simulated for one year of operation. The second model takes the optimal BESS sizing as input, and aims to find the most optimal operation of the BESS system for a period of four years. The case assumes operation of the BESS until the grid reinforcements of the regional grid are finished in 2028 (as explained in section 1.4).
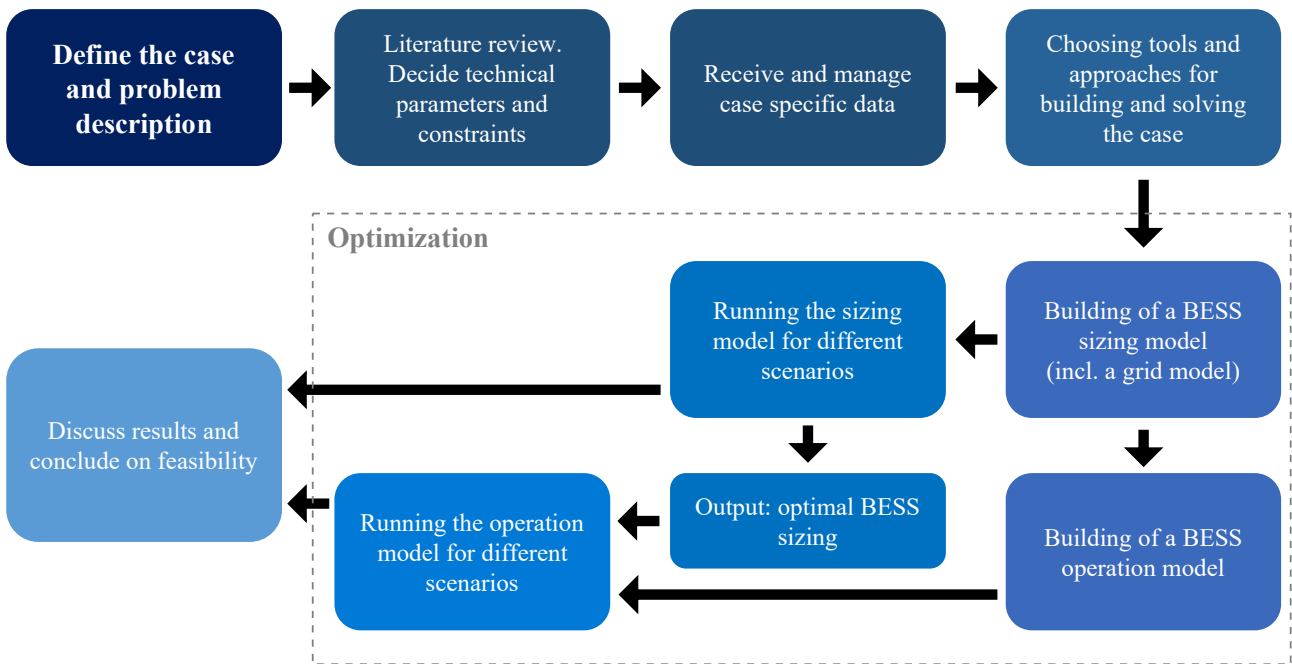
Figure 25: A flow chart describing the approaches and the methodology of the thesis.

4.1 Notations and Sketching of the Case

The initial drawing of the case from figure 5 is redrawn in the single line diagram of figure 26, representing a three-phase power system. The area of focus is on the radial going from transformer T2, through pint *A* to the end user located after substation T3. The single line diagram is made to approximately locate power production and regional loads. The goal is to achieve realistic power flows and system states in the simulation of a new load situation that includes a BESS. The sizing

model includes the whole grid model, while the operation model only considers the load side, which is indicated in the figure.
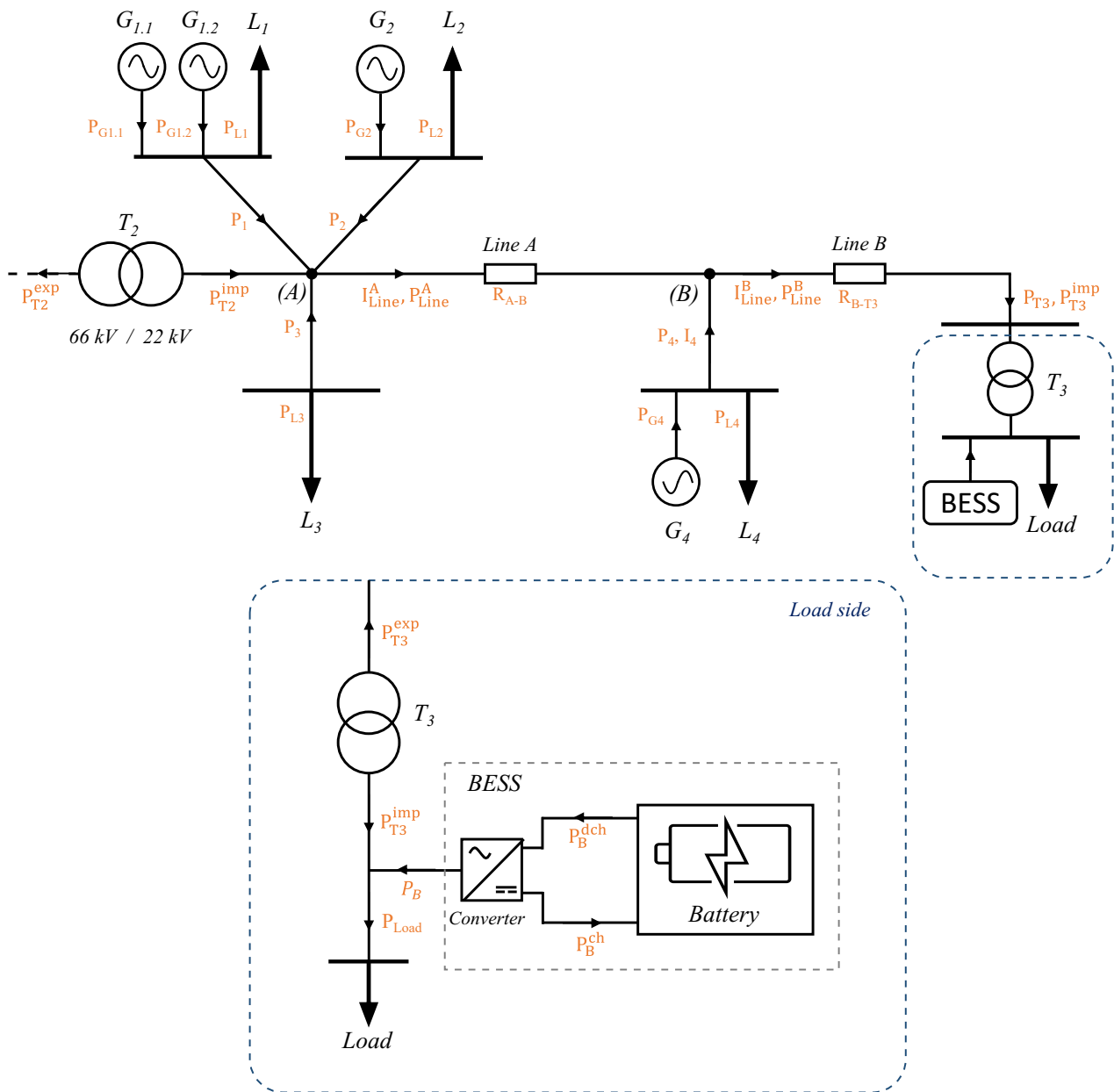
Figure 26: A single line diagram of the case.

Inputs and Outputs In the Model

Several elements and characteristics are indicated in the figure. These are both constants that are known, such as line resistances and nominal voltages, hourly time series on production and power flows, and unknown variables. For instance, the power flow through T2 and the power production from the four generators are known for 2021, while the battery power (P_B) and line currents (I_{Line}^A

and I_{Line}^B) are unknown variables. The optimization models aim to assign the optimal values for these unknown variables. Relevant data on load, power production and characteristics of the distribution grid is provided by Nettselskapet AS, the local grid owner at Fosen [18].

Assumptions and Clarifications

The models, as well as the approach for solving, involves several assumptions that are elaborated further in the following list:

- The models are made and run for hourly resolution. Power flows, voltages and currents are assumed to be fixed for each hour.

- The models are solved for 8760 hours per year. All input data and variables that are time dependent are adapted for this.

- Transformer T2 has a capacity of 25 MVA, and the maximum available, active, power that can flow through T2 is set to be 23.9 MW.

- Only active power flows are considered, but a margin obtained by a power factor, $cos(\phi)$, of 0.9 is used.

- The overlying regional grid is assumed to be capable of delivering up to 23.9 MW at all times.

- The total load of the region is calculated as the sum of the power imported through T2 and the power generated by the four generators, subtracting the exported power through T2, for every time step. (Excluding losses).

- Both the total load of the region and the power generation is assumed to follow the same load profile as of 2021, unless otherwise stated.

- The load of concern is assumed to follow the same load profile as of 2021, and the new load equals the consumption of 2021 (with a peak of $\sim$200 kW) scaled up with 1306 kW for every hour (giving a peak of $\sim$1500 kW). See figure 6.

- The substation, T3, is assumed replaced to fit the new power requirements. A 3150 kVA (22 kV/415 V) substation from Møre Trafo AS [56] is assumed in the case.

- The maximum limits on import and export through T3 are set to 3.0 MW and 100 kW, respectively, according to the capacity of the transformer and the restriction concerning the feed-in tariff of power export [14].

- The battery is assumed to consist of LMO-NMC battery packs, having aging that is described according to the Wang degradation model [41]. Degradation is only included in the operation model.

4.2 Mathematical Formulation of The Case

Based on historical data on loads, power generation and electricity prices, as well as a new load for the end user and the restriction in available power, the goal is to find optimal sizing and operation of a BESS. The approach is to build an optimization model that minimizes the net present costs (NPC) of investment and operation, and compare different scenarios in order to say something about the feasibility of a BESS. Two minimization models are created, based on the principles introduced in section 3.1, for sizing and operation. The objectives are split in two models in order to reduce the complexity of solving. In the following subsections, the mathematical formulations of these models are described, which include the constraints and objective functions.

4.2.1 Model Constraints

The sizing model includes several constraints that describe the physics of the distribution grid depicted in figure 26. In general, these are formulated such that power flows are balanced, and that voltages and currents are related according to the laws of physics. In addition, the technical limits and working principles of the BESS are incorporated in the load side of the models. The equations and notations are presented in accordance with the sketch of figure 26.

The Grid Side

The first set of constraints define the power flows through transformer (T2) and power injections at point *A*. The power flow through T2 can either flow out of the distribution grid, referred to as export, or into the distribution grid, referred to as import (into point *A*). The power flow is defined to be positive when imported. In addition, the power flow through the transformer cannot exceed the power rating of the transformer. All of these relationships are formulated in equation 23, and must be valid for all time steps (*t*) in the simulations. The latter fact also applies to all other constraints.

$$P_{T2}(t) = P_{T2}^{imp}(t) - P_{T2}^{exp}(t)$$
$$P_{T2}^{imp}(t) \leq P_{T2}^{max} \tag{23}$$
$$P_{T2}^{exp}(t) \leq P_{T2}^{max}$$

Furthermore, the power balance at each node (*1, 2, 3* and *4*) must be defined. All of these nodes have both producing units (generators) and consuming units (loads), except for node *3* which only has consumption. Power into the distribution grid (Power injections at point *A* or point *B*) is defined

to be positive, such that equation 24 is valid.

$$P_1(t) = P_{G1.1,t} + P_{G1.2,t} - P_{L1}(t)$$
$$P_2(t) = P_{G2,t} - P_{L2}(t)$$
$$P_3(t) = -P_{L3}(t) \tag{24}$$
$$P_4(t) = P_{G4,t} - P_{L4}(t)$$

While the power production is known for every hour, based on data from 2021, the loads and the load distribution must be calculated and assumed. The total amount of electricity consumption, on the 22 kV side of T2, can be found by adding the power production to the imported power through T2, and subtracting the exported power through T2 from this sum. This is formulated in equation 25 for all time steps. The t in the subscripts indicate that these are fixed values for corresponding time steps. The formulation assumes no losses and that all of the power production and power throughput through T2 is registered.

$$P_{Load,reg,t}^{tot} = \left(P_{G1.1,t} + P_{G1.2,t} + P_{G2,t} + P_{G4,t}\right) + P_{T2,t}^{imp} - P_{T2,t}^{exp} \tag{25}$$

As the load distribution is not known in detail, the four different loads are located based on assumptions on power demand. For instance, areas with large industries and/or many households are assumed to have a higher electricity consumption than areas that are sparsely populated. Therefore, the four nodes are set to have loads within the ranges presented in table 7. The ranges also allow for some flexibility, which ease the solving of the sizing model. The biggest loads are assumed to be in node *3*.

Table 7: Possible ranges of the loads at the different nodes.

Node (i)	Minimum fraction ($P_{L,i}^{min}$),	Maximum fraction ($P_{L,i}^{max}$),
1	0.2	0.4
2	0.1	0.3
3	0.4	0.6
4	0.05	0.3

In order to ensure that the load follows the correct load profile, the sum of all loads are required to equal the total load at corresponding time step, $P_{Load,reg,t}^{tot}$. This, as well as the mathematical formula-

tions for the possible ranges of loads, are defined in equation 26.

$$
\begin{aligned}
P_{L1}^{min} \cdot P_{Load,reg,t}^{tot} &\leq P_{L1}(t) \leq P_{L1}^{max} \cdot P_{Load,reg,t}^{tot} \\
P_{L2}^{min} \cdot P_{Load,reg,t}^{tot} &\leq P_{L2}(t) \leq P_{L2}^{max} \cdot P_{Load,reg,t}^{tot} \\
P_{L3}^{min} \cdot P_{Load,reg,t}^{tot} &\leq P_{L3}(t) \leq P_{L3}^{max} \cdot P_{Load,reg,t}^{tot} \\
P_{L4}^{min} \cdot P_{Load,reg,t}^{tot} &\leq P_{L4}(t) \leq P_{L4}^{max} \cdot P_{Load,reg,t}^{tot} \\
P_{Load,reg,t}^{tot} &= P_{L1}(t) + P_{L2}(t) + P_{L3}(t) + P_{L4}(t)
\end{aligned}
\tag{26}
$$

The power flowing from point A into the radial of interest (P_{Line}^{A}), is the sum of the power from nodes *1, 2* and *3* and the power flowing into the distribution grid through T2. This is described by equation 27. Further, the line currents and voltage of point A are related to this power flow according to equation 28. The latter is the expression for three-phase power, where V_A is the line RMS voltage of point A and $cos(\phi)$ is the power factor.

$$
P_{Line}^{A}(t) = P_{T2}(t) + P_1(t) + P_2(t) + P_3(t)
\tag{27}
$$

$$
P_{Line}^{A}(t) = \sqrt{3} \cdot V_A(t) \cdot I_{Line}^{A}(t) \cdot cos(\phi)
\tag{28}
$$

The same approach is used to define the power flow on the lines from point B, P_{Line}^{B}. The positive direction is defined for power flowing from B to $T3$. The three-phase power injection at this node, flowing either to point A or T_3, is defined in equation 29, similarly as for point A. However, in this case it is not related to the sum of powers, but rather to the sum of currents (I_{Line}^{A} and $I_{4,@22kV}$) because of ohmic losses on *line A*. The currents are defined according to equation 30 and 31, based on Kirchhoff's current law[30]. As both the power at node *4* and the voltage at point B are unknown, the currents are approximated by assuming 22.0 kV.

$$
P_{Line}^{B}(t) = \sqrt{3} \cdot V_B(t) \cdot I_{Line}^{B}(t) \cdot cos(\phi)
\tag{29}
$$

$$
I_{Line}^{B}(t) = I_{line}^{A}(t) + I_{4,@22kV}(t)
\tag{30}
$$

$$
I_{4,@22kV}(t) = \frac{P_4(t)}{\sqrt{3} \cdot 22kV \cdot cos(\phi)}
\tag{31}
$$

---

[30]Also called Kirchhoff's first law: The sum of currents flowing into one point equals the sum of currents flowing out of that same point.

Having defined all voltages and currents until T3, the connection point of the end user of interest, the power flowing into or out of this substation can be defined with equation 32. This also requires V_{T3} to be decided.

$$P_{T3}(t) = \sqrt{3} \cdot V_{T3}(t) \cdot I^B_{Line}(t) \cdot cos(\phi) \tag{32}$$

Voltages, currents and line impedances are related through Ohm's law. By using this, the voltages at each point as well as the voltage drops on the power lines are formulated using equation 33 and 34. The resistance of the two line segments are found from datasheets [54]. Only the resistive part of the impedance is included, and only active power flow is considered.

$$V_A(t) = \sqrt{3} \cdot I^A_{line}(t) \cdot R_{A-B} \cdot cos(\phi) + V_B(t) \tag{33}$$
$$V_B(t) = \sqrt{3} \cdot I^B_{line}(t) \cdot R_{B-T3} \cdot cos(\phi) + V_{T3}(t) \tag{34}$$

Lastly, all voltages and currents are restricted to stay within some boundaries, in order for the grid to be operated safely. The currents cannot exceed the ratings of the power lines, which are decided based on the *current carrying capacity*[31] [54]. The voltages cannot deviate more than a certain percentage from nominal system voltage, as mentioned in the introduction (section 1.1). These constraints are mathematically formulated in equation 35.

$$
\begin{aligned}
I^A_{Line}(t) &\leq I^{A,limit}_{Line} \\
I^B_{Line}(t) &\leq I^{B,limit}_{Line} \\
V^{min}_A &\leq V_A(t) \leq V^{max}_A \\
V^{min}_B &\leq V_B(t) \leq V^{max}_B \\
V^{min}_{T3} &\leq V_{T3}(t) \leq V^{max}_{T3}
\end{aligned}
\tag{35}
$$

The Load Side

The battery installation is located on the load side in figure 26, which is the low voltage side of substation T3. Power balances and limitations in possible variable values are also important in this part of the model. In addition, the constraints on the load side are also used to register and control the power and energy that is imported from and exported to the power grid.

Similarly as for T2, the power flowing through T3 is split into imported and exported power. Equation 36 is established such that power imported from the grid is defined as positive. Furthermore, the power

---

[31] Also known as the thermal loading limit: the maximum stationary current that gives a certain increase of temperature in the conductor.

that can be imported and exported is restricted due to limitations of the substation and regulations.

$$P_{T3}(t) = P_{T3}^{imp}(t) - P_{T3}^{exp}(t)$$
$$P_{T3}^{imp}(t) \leq P_{T3}^{imp,max}(t) \qquad (36)$$
$$P_{T3}^{exp}(t) \leq P_{T3}^{exp,max}(t)$$

In order to estimate the operating costs of energy and power, the power flow through T3 must be known for all time steps. The monthly power peak of the imported power, being the basis for the power cost in the grid tariff, is registered in P_{grid}^{max}, according to equation 37. This variable is assigned with a value for every month of the simulation period. By setting it to be greater or equal to the imported power of all time steps within the given month, the variable will be assigned with the maximum value. The model assumes that the grid tariff is based on the absolute peak power of a month, while a true grid tariff uses an average of the three highest peaks.

$$P_{grid}^{max}(m) \geq P_{T3}^{imp}(t) \qquad (37)$$

For the main case of this thesis, the new load has to be covered by power from the battery in periods when the power grid is not able to meet the demand alone. In the sizing model, the use of battery will be required when P_{T2}^{imp} is at its boundary. However, the operation model does not include the grid side of this model. Therefore, an extra limit on the imported power through T3 is introduced, only for the operation model, being $P_{T3,t}^{avail.}$. Equation 38 expresses this constraint.

$$P_{T3}^{imp}(t) \leq P_{T3,t}^{avail.} \qquad (38)$$

The notation represents a fixed value for every time step. It is set based on the imported power through T2, subtracted from the yearly maximum of T2 (23.9 MW) and assuming 5.0 % losses between T2 and the end user. The power through T2 is estimated according to equation 25, knowing $P_{Load,reg,t}^{tot}$ and the local power generation.

The case of using battery is mathematically summarized with equation 39, which allows the load to be covered by grid power (P_{T3}), power from the battery (P_B) or a combination of these. It also allows for exporting power to the grid, when the battery power is higher than the load.

$$P_{load,t} = P_{T3}(t) + P_B(t) \qquad (39)$$

The battery power is further divided between charging power (P_B^{ch}) and discharging power (P_B^{dch}), according to equation 40. Discharging gives a positive power flow. Further, the battery level with the

energetic capacity that is available for discharge or recharge, is defined in equation 41. The change of available battery energy is expressed as the battery power of time step t, added or subtracted from the battery level of the previous time step, $E_B(t-1)$, depending on whether the battery is charged or discharged. The losses of charging and discharging, including the losses in power conversion, are incorporated here.

$$P_B(t) = P_B^{dch}(t) - P_B^{ch}(t) \tag{40}$$

$$E_B(t) = E_B(t-1) + \left(\eta_{ch} \cdot P_B^{ch}(t) - \frac{1}{\eta_{dch}} \cdot P_B^{dch}(t) \right) \cdot \Delta t \tag{41}$$

Note that in figure 26, the battery power, P_B is indicated on the AC side of the converter, but it is set equal to the charge or discharge power in the equations. That is, the efficiency of the battery and the converter is already accounted for when P_B is given a value, even though the label is always put on the AC side of the converter.

The goal of the sizing model is to decide the optimal value of nominal battery capacity and the power capability of the power converter (inverter) of the system. In order to manage the first, E_B^{nom} is defined as a variable. In equation 42, this is linked to the state of charge of the battery, which again is restricted to stay within some limits. The limits, included in equation 43, are set to ensure safe operation of the battery, and improve life time. As it appears from the first equation, the available battery capacity depends on the state of health (SoH) of the battery at the given time. When disregarding the degradation, which is the case for the sizing model, the SoH is always fixed to 1.0.

$$SoC(t) = \frac{E_B(t)}{E_B^{avail.}(t)}$$
$$SoC(t) = \frac{E_B(t)}{E_B^{nom} \cdot SoH(t)} \tag{42}$$

$$SoC(t) \geq SoC_{min}$$
$$SoC(t) \leq SoC_{max} \tag{43}$$

The sizing of the power capability is also managed by defining a new variable. P_{max}^{inv} is defined according to equation 44, and ensures that the power of the converter is set based on the battery power, accounting for losses.

$$P_{inv}^{max} \geq P_B^{dch}(t) + P_B^{ch}(t) \tag{44}$$

Battery Degradation

The degradation of the Li-ion battery is only accounted for in the operation model, when the BESS sizing is fixed. The key variable for the degradation is the *SoH*, which adjusts the available capacity of the battery depending on the time and use of the BESS. As mentioned, this is done according to equation 42. The battery degradation (γ_{deg}), measured by the reduction in SoH, depends on calendric and cyclic aging. The Wang Model from equation 14 is used to include these mechanisms, and is reformulated to include the SoH in equation 45. The different coefficients can be found in table 3.

$$SoH(t) = SoH_{initial} - \gamma_{deg}(t)$$

$$SoH(t) = SoH_{initial} - \frac{1}{100} \left(k_1 \cdot e^{[(dT_K+e) \cdot c_{rate}(t)]} \cdot N_{eq}(t) + \sqrt{\frac{t}{24}} \cdot k_2 \right) \tag{45}$$

The degradation depends on time, some temperature dependent coefficients, the c-rate and the number of equivalent cycles (N_{eq}). The c-rate, being the rate of charge and discharge, is defined in equation 46. Equation 47 gives the number of equivalent cycles, which is the cumulative number of full equivalent cycles for every time step, defined by equation 48.

$$c_{rate}(t) = \frac{P_B}{E_B^{nom}} \tag{46}$$

$$N_{eq}(t) = N_{eq}(t-1) + FEC(t) \tag{47}$$

$$FEC(t) = \frac{1}{2} \cdot \frac{P_B^{ch}(t) + P_B^{dch}(t)}{E_B^{nom} \cdot (SoC_{max} - SoC_{min})} \tag{48}$$

4.2.2 Objective Functions

The two optimization models have two different goals, and thereby two different objective functions. However, they both include the operating costs of energy and power based on electricity spot prices and grid tariff.

The part having to do with costs of power and energy are equal for the two models, and is presented in equation 49. The equation is split in two sums, where the first sum includes all terms that are factors of time in hours. These are the elspot price $c_{E,spot,t}$, the fixed energy part of the grid tariff, $c_{E,tar}$ and taxes on electric power, $c_{E,tax}$, all being in the units of NOK/kWh. The last term in the first sum accounts for the selling of power back to the grid, which is expressed as a reduction of the

energy costs. The other sum includes the power part of the grid tariff, $c_{P,tar}$, which is a factor of time in months with the unit of NOK/kW/month.

$$\sum_{t=1}^{T} \left(P_{T3}^{imp}(t)\Delta t \cdot (c_{E,spot,t} + c_{E,tar} + c_{E,tax}) - P_{T3}^{exp}(t)\Delta t \cdot c_{E,spot,t} \right)$$
$$\sum_{m=1}^{M} c_{P,tar}(m) \cdot P_{grid}^{max}(m) \tag{49}$$

Furthermore, the sizing model includes a part for the investment costs for the BESS system. This is shown in equation 50, where C_{BESS}^{cap} contains the costs of capacity components in NOK/kWh and C_{BESS}^{pow} represents the costs of power components in NOK/kW. The designing, engineering and installation costs are expressed by the factor c_{inst}.

$$I_0 = (C_{BESS}^{cap} \cdot E_B^{nom} + C_{BESS}^{pow} \cdot P_{inv}^{max}) \cdot c_{inst} \tag{50}$$

In total, the objective function for the sizing model is given in equation 51

$$\sum_{t=1}^{T} \left(P_{T3}^{imp}(t)\Delta t \cdot (c_{E,spot,t} + c_{E,tar} + c_{E,tax}) - P_{T3}^{exp}(t)\Delta t \cdot c_{E,spot,t} \right)$$
$$+ \sum_{m=1}^{M} c_{P,tar}(m) \cdot P_{grid}^{max}(m) + \left(C_{BESS}^{cap} \cdot E_B^{nom} + C_{BESS}^{pow} \cdot P_{inv}^{max} \right) \cdot c_{inst} \tag{51}$$

The objective function of the operation model has some different elements. Firstly, it expresses the net present cost of operation for the period of interest. While the sizing model only considers one year, with T time steps, the operation model considers Y years, all consisting of T time steps (hours). As it aims to estimate the net present cost, a discount factor is set for all of the years in line with the theory from section 3.2.2. It also includes the residual value (RV) of the BESS, being the economical value it is assumed to have after Y years, and a degradation cost, C_{deg}^{tot}. The objective function of the operation model is presented in equation 52.

$$\sum_{y=1}^{Y} \alpha_r(y) \cdot \left(\sum_{t=1}^{T} \left(P_{T3}^{imp}(t)\Delta t \cdot (c_{E,spot,t} + c_{E,tar} + c_{E,tax}) - P_{T3}^{exp}(t)\Delta t \cdot c_{E,spot,t} \right) \right.$$
$$\left. + \sum_{m=1}^{M} c_{P,tar}(m) \cdot P_{grid}^{max}(m) + c_{O\&M} \cdot P_{inv}^{max} \right) - RV \cdot \alpha_r(Y) + C_{deg}^{tot} \tag{52}$$

The degradation cost, C_{deg}^{tot}, is included in the objective function to penalize the type of operation that causes degradation. Thereby, the type of operation that prolongs the life time of the battery system

can be simulated. It is defined in equations 53a to 53c such that when the degradation (γ_{deg}) reaches a certain *EOL-fraction*[32] (e.g. 30 % reduction in SoH, from 1.0 to 0.7), the total BESS cost is accounted for. As the case is formulated as a minimization problem, the solving will imply the minimization of this cost, which is done by limiting degradation. It must be noted that this term of the objective function is an optional part in the model, only being used for some scenarios.

$$C_{deg}^{tot} = C_{deg}(t = T_{tot}) \tag{53a}$$

$$C_{deg}(t) = \frac{\gamma_{deg}(t)}{EOL} \cdot C_{BESS}^{tot} \quad , \quad t \in T_{tot} \tag{53b}$$

$$\gamma_{deg}(t) = \Delta SoH(t) = SoH_{initial} - SoH(t) \quad , \quad t \in T_{tot} \tag{53c}$$

Both of the models include several sets of time steps, being hours per year, months per year, number of years, the number of hours in total and the number of months in total. In the case of the operation model, the sets of total amount of hours and total amount of months are as follows:

$$T_{tot} = Y \cdot T, \quad T = 8760h$$

$$M_{tot} = Y \cdot M, \quad M = 12$$

4.2.3 The Optimization Models, Summarized

In the following part, all of the above-mentioned constraints and the objective functions are summarized in the standard form of an optimization problem. The sizing model is presented in equations 55 to 57q and the operation model is given by equations 58 to 59o.

---

[32]EOL: End of life. The reduction in SoH a battery can have before it is defined to be at its end of life.

The Sizing Model

$$\min_{\substack{\forall t \in T \\ \forall m \in M}} \quad \sum_{t=1}^{T} \left(P_{T3}^{imp}(t)\Delta t \cdot (c_{E,spot,t} + c_{E,tar} + c_{E,tax}) - P_{T3}^{exp}(t)\Delta t \cdot c_{E,spot,t} \right)$$

$$+ \sum_{m=1}^{M} c_{P,tar}(m) \cdot P_{grid}^{max}(m) + \left(C_{BESS}^{cap} \cdot E_{B}^{nom} + C_{BESS}^{pow} \cdot P_{inv}^{max} \right) \cdot c_{inst} \qquad (55)$$

$s.t$

$$P_{T2}(t) = P_{T2}^{imp}(t) - P_{T2}^{exp}(t) \qquad \forall t \in T \qquad (56a)$$

$$P_{T2}^{imp}(t) \leq P_{T2}^{max} \qquad \forall t \in T \qquad (56b)$$

$$P_{T2}^{exp}(t) \leq P_{T2}^{max} \qquad \forall t \in T \qquad (56c)$$

$$P_{1}(t) = P_{G1.1,t} + P_{G1.2,t} - P_{L1}(t) \qquad \forall t \in T \qquad (56d)$$

$$P_{2}(t) = P_{G2,t} - P_{L2}(t) \qquad \forall t \in T \qquad (56e)$$

$$P_{3}(t) = -P_{L3}(t) \qquad \forall t \in T \qquad (56f)$$

$$P_{4}(t) = P_{G4,t} - P_{L4}(t) \qquad \forall t \in T \qquad (56g)$$

$$P_{L1}^{min} \cdot P_{Load,reg,t}^{tot} \leq P_{L1}(t) \leq P_{L1}^{max} \cdot P_{Load,reg,t}^{tot} \qquad \forall t \in T \qquad (56h)$$

$$P_{L2}^{min} \cdot P_{Load,reg,t}^{tot} \leq P_{L2}(t) \leq P_{L2}^{max} \cdot P_{Load,reg,t}^{tot} \qquad \forall t \in T \qquad (56i)$$

$$P_{L3}^{min} \cdot P_{Load,reg,t}^{tot} \leq P_{L3}(t) \leq P_{L3}^{max} \cdot P_{Load,reg,t}^{tot} \qquad \forall t \in T \qquad (56j)$$

$$P_{L4}^{min} \cdot P_{Load,reg,t}^{tot} \leq P_{L4}(t) \leq P_{L4}^{max} \cdot P_{Load,reg,t}^{tot} \qquad \forall t \in T \qquad (56k)$$

$$P_{Load,reg,t}^{tot} = P_{L1}(t) + P_{L2}(t) + P_{L3}(t) + P_{L4}(t) \qquad \forall t \in T \qquad (56l)$$

$$P_{Line}^{A}(t) = P_{T2}(t) + P_{1}(t) + P_{2}(t) + P_{3}(t) \qquad \forall t \in T \qquad (56m)$$

$$P_{Line}^{A}(t) = \sqrt{3} \cdot V_{A}(t) \cdot I_{Line}^{A}(t) \cdot cos(\phi) \qquad \forall t \in T \qquad (56n)$$

$$P_{Line}^{B}(t) = \sqrt{3} \cdot V_{B}(t) \cdot I_{Line}^{B}(t) \cdot cos(\phi) \qquad \forall t \in T \qquad (56o)$$

$$I_{Line}^{B}(t) = I_{line}^{A}(t) + I_{4,@22kV}(t) \qquad \forall t \in T \qquad (56p)$$

$$I_{4,@22kV}(t) = \frac{P_{4}(t)}{\sqrt{3} \cdot 22kV \cdot cos(\phi)} \qquad \forall t \in T \qquad (56q)$$

$$V_{A}(t) = \sqrt{3} \cdot I_{line}^{A}(t) \cdot R_{A-B} \cdot cos(\phi) + V_{B}(t) \qquad \forall t \in T \qquad (56r)$$

$$V_{B}(t) = \sqrt{3} \cdot I_{line}^{B}(t) \cdot R_{B-T3} \cdot cos(\phi) + V_{T3}(t) \qquad \forall t \in T \qquad (56s)$$

...

$$I_{Line}^A(t) \leq I_{Line}^{A,limit} \qquad \qquad \forall t \in T \qquad (57a)$$

$$I_{Line}^B(t) \leq I_{Line}^{B,limit} \qquad \qquad \forall t \in T \qquad (57b)$$

$$V_A^{min} \leq V_A(t) \leq V_A^{max} \qquad \qquad \forall t \in T \qquad (57c)$$

$$V_B^{min} \leq V_B(t) \leq V_B^{max} \qquad \qquad \forall t \in T \qquad (57d)$$

$$V_{T3}^{min} \leq V_{T3}(t) \leq V_{T3}^{max} \qquad \qquad \forall t \in T \qquad (57e)$$

$$P_{T3}(t) = \sqrt{3} \cdot V_{T3}(t) \cdot I_{Line}^B(t) \cdot cos(\phi) \qquad \forall t \in T \qquad (57f)$$

$$P_{T3}(t) = P_{T3}^{imp}(t) - P_{T3}^{exp}(t) \qquad \qquad \forall t \in T \qquad (57g)$$

$$P_{load,t} = P_{T3}(t) + P_B(t) \qquad \qquad \forall t \in T \qquad (57h)$$

$$P_B(t) = P_B^{dch}(t) - P_B^{ch}(t) \qquad \qquad \forall t \in T \qquad (57i)$$

$$E_B(t) = E_B(t-1) + \left(\eta_{ch} \cdot P_B^{ch}(t) - \frac{1}{\eta_{dch}} \cdot P_B^{dch}(t) \right) \cdot \Delta t \quad \forall t \in T \qquad (57j)$$

$$P_{T3}^{imp}(t) \leq P_{T3}^{imp,max} \qquad \qquad \forall t \in T \qquad (57k)$$

$$P_{T3}^{exp}(t) \leq P_{T3}^{exp,max} \qquad \qquad \forall t \in T \qquad (57l)$$

$$P_{grid}^{max}(m) \geq P_{T3}^{imp}(t) \qquad \qquad \forall t \in T \qquad (57m)$$

$$SoC(t) \geq SoC_{min} \qquad \qquad \forall m \in M \qquad (57n)$$

$$SoC(t) \leq SoC_{max} \qquad \qquad \forall t \in T \qquad (57o)$$

$$SoC(t) = \frac{E_B(t)}{E_B^{nom}} \qquad \qquad \forall t \in T \qquad (57p)$$

$$P_{inv}^{max} \geq P_B^{ch}(t) + P_B^{dch}(t) \qquad \qquad \forall t \in T \qquad (57q)$$

$$P_{T2}^{imp}(t), P_{T2}^{exp}(t), P_{L1}(t), P_{L2}(t), P_{L3}(t), P_{L4}(t),$$

$$V_A(t), V_B(t), V_{T3}(t), P_{T3}^{imp}(t), P_{T3}^{exp}(t), E_B(t),$$

$$SoC(t), P_B^{ch}(t), P_B^{dch}(t), P_{grid}^{max}(m), P_{inv}^{max}, E_B^{nom} \geq 0 \qquad \forall t \in T, \forall m \in M$$

The Operation Model

$$\min_{\substack{\forall t \in T \\ \forall m \in M \\ \forall y \in Y}} \quad \sum_{y=1}^{Y} \alpha_r(y) \cdot \left(\sum_{t=1}^{T} \left(P_{T3}^{imp}(t) \Delta t \cdot (c_{E,spot,t} + c_{E,tar} + c_{E,tax}) - P_{T3}^{exp}(t) \Delta t \cdot c_{E,spot,t} \right) \right.$$

$$\left. + \sum_{m=1}^{M} c_{P,tar}(m) \cdot P_{grid}^{max}(m) + c_{O\&M} \cdot P_{inv}^{max} \right) - RV \cdot \alpha_r(Y) + \underset{..........}{C_{deg}^{tot}} \qquad (58)$$

$s.t$

$$P_{T3}(t) = P_{T3}^{imp}(t) - P_{T3}^{exp}(t) \qquad\qquad \forall t \in T_{tot} \qquad (59a)$$

$$P_{load,t} = P_{T3}(t) + P_B(t) \qquad\qquad \forall t \in T_{tot} \qquad (59b)$$

$$P_B(t) = P_B^{dch}(t) - P_B^{ch}(t) \qquad\qquad \forall t \in T_{tot} \qquad (59c)$$

$$E_B(t) = E_B(t-1) + \left(\eta_{ch} \cdot P_B^{ch}(t) - \frac{1}{\eta_{dch}} \cdot P_B^{dch}(t) \right) \cdot \Delta t \qquad \forall t \in T_{tot} \qquad (59d)$$

$$P_{inv}^{max} \geq P_B^{dch}(t) + P_B^{ch}(t) \qquad\qquad \forall t \in T_{tot} \qquad (59e)$$

$$P_{T3}^{imp}(t) \leq P_{T3,t}^{avail.} \qquad\qquad \forall t \in T_{tot} \qquad (59f)$$

$$P_{T3}^{imp}(t) \leq P_{T3}^{imp,max}(t) \qquad\qquad \forall t \in T_{tot} \qquad (59g)$$

$$P_{T3}^{exp}(t) \leq P_{T3}^{exp,max}(t) \qquad\qquad \forall t \in T_{tot} \qquad (59h)$$

$$P_{grid}^{max}(m) \geq P_{T3}^{imp}(t) \qquad\qquad \forall m \in M_{tot} \qquad (59i)$$

$$SoC(t) \geq SoC_{min} \qquad\qquad \forall t \in T_{tot} \qquad (59j)$$

$$SoC(t) \leq SoC_{max} \qquad\qquad \forall t \in T_{tot} \qquad (59k)$$

$$SoC(t) = \frac{E_B(t)}{E_B^{nom} \cdot SoH(t)} \qquad\qquad \forall t \in T_{tot} \qquad (59l)$$

$$SoH(t) = SoH_{initial} - \frac{1}{100} \left(k_1 \cdot e^{[(dT_K + e) \cdot c_{rate}]} \cdot N_{eq}(t) + \sqrt{\frac{t}{24}} \cdot k_2 \right) \quad \forall t \in T_{tot} \qquad (59m)$$

$$N_{eq}(t) = N_{eq}(t-1) + FEC(t) \qquad\qquad \forall t \in T_{tot} \qquad (59n)$$

$$FEC(t) = \frac{1}{2} \cdot \frac{P_B^{ch}(t) + P_B^{dch}(t)}{E_B^{nom} \cdot (SoC_{max} - SoC_{min})} \qquad\qquad \forall t \in T_{tot} \qquad (59o)$$

$$P_{T3}^{imp}(t), P_{T3}^{exp}(t), E_B(t), SoC(t),$$

$$P_B^{ch}(t), P_B^{dch}(t), SoH(t), \qquad\qquad \forall t \in T_{tot},$$

$$P_{grid}^{max}(m), N_{eq}(t), FEC(t) \geq 0 \qquad\qquad \forall m \in M_{tot}$$

4.2.4 Overview of Parameters, Variables and Input Data

Parameters and Constants

All of the parameters and constants are set based on information provided by Nettselskapet AS and observations from literature that is presented in chapter 2. All relevant parameters and constants are provided in table 8 and 9 for the grid side and load side, respectively.

The voltage limitations are set to be 5.0 % of the nominal voltage, in accordance with the regulations presented in section 1.1. The limits on SoC are set to 0.2 and 0.9, being minimum and maximum values. This is set in accordance with information presented in section 2.2. The efficiency of charging and discharging, including the step of power conversion, is set to be fixed and equal to 0.9 for both cases. Efficiency will in a real case vary depending on several factors, such as instantaneous power, but an average of 0.9 is assumed to be realistic [21]. The temperature is set as a constant value for every time step, being equal to 15 °C, unless otherwise mentioned.

BESS Investment and Operating Costs

Based on cost data from literature, described in section 2.4, the material and installation costs are set as follows:

- Cost of capacity components, C_{BESS}^{cap}: 2 500 NOK/kWh

- Cost of power components, C_{BESS}^{pow}: 3 200 NOK/kW

- Factor to account for the costs associated with designing, engineering and installation, c_{inst}[33]: 1.5

The operation and maintenance cost, that comes in addition to the energy costs, is set to be 50.0 NOK/kW/year, based on figures from table 5.

---

[33]The additional installation costs, which is used as a collective term, is set to be 50 % of the material costs

Table 8: Constants and parameters for the optimization models, grid side.

Parameter / Constant	Value	Description
P_{T2}^{max}	23.9	Active power limit of transformer T2 (25 MVA), [MW].
P_{L1}^{min}	0.2	Minimum factor of load 1.
P_{L1}^{max}	0.4	Maximum factor of load 1.
P_{L2}^{min}	0.1	Minimum factor of load 2.
P_{L2}^{max}	0.3	Maximum factor of load 2.
P_{L3}^{min}	0.4	Minimum factor of load 3.
P_{L3}^{max}	0.6	Maximum factor of load 3.
P_{L4}^{min}	0.05	Minimum factor of load 4.
P_{L4}^{max}	0.3	Maximum factor of load 4.
R_{A-B}	3.056	Resistance of line segment between A and B $[\Omega]$.[(*)][54]
R_{B-T3}	2.888	Resistance of line segment between B and T3 $[\Omega]$.[(**)][54]
$I_{Line}^{A,limit}$	629	Current carrying capacity of line segment between A and B [A].[(*)][54]
$I_{Line}^{B,limit}$	266	Current carrying capacity of line segment between B and T3 [A].[(**)][54]
$V_A^{min}, V_B^{min}, V_{T3}^{min}$	20.9	Minimum voltage for the nodes [kV].
$V_A^{max}, V_B^{max}, V_{T3}^{max}$	23.1	Maximum voltage for the nodes [kV].
$cos(\phi)$	0.9	Power factor.

(*)Line segment between A and B:
16 km with line of type 151-AL1/25-ST1A
$x_R : 0.192\Omega$/km, $x_L : 0.351\Omega$/km

(**)Line segment between B and T3:
1) 3.0 km with line of type 80-AL1/13-ST1A and 2) 2.5 km with line of type 40-AL1/7-ST1A
1) $x_R : 0.360\Omega$/km, $x_L : 0.373\Omega$/km and 2)$x_R : 0.723\Omega$/km, $x_L : 0.394\Omega$/km

Both assumed to be overhead lines with earthing (grounding) line, mounted on H-masts with 1.5 meters of phase distance.

Conditions that are assumed in the calculation of current carrying capacity:
Wind crossing the conductor: 1 m/s; Solar irradiance: 900 W/m^2; $Coefficient of absorption : \gamma = 0.5$;
Emissitivity: $K_e = 0.6$; $Ambient temperature : 20°C$; $Aluminium temperature : 80°C$

Table 9: Constants and parameters for the optimization models, load side and general.

Parameter / Constant	Value	Description
T	8 760	Set of hours.
M	12	Set of months.
Y	4	Set of years.
Δt	1.0	Time step of model simulation, [hour].
$P_{T3}^{imp,max}$	3 000	Power limit of the point of feed-in from the power grid (T3) [kW].
E_B^{nom}	-	Nominal battery storage capacity [kWh]. Output from the sizing model.
P_{inv}^{max}	-	Maximum inverter power [kW]. Output from the sizing model.
η_{ch}, η_{dch}	0.9	Efficiency of battery charging and discharging. Also including inverter losses.
SoC_{min}	0.2	Minimum state of charge.
SoC_{max}	0.9	Maximum state of charge.
$SoH_{initial}$	1.0	Initial state of health.
EOL	0.3	Degradation fraction corresponding to end of life.
k_1	-	Temperature dependent constant. See equation 13 [$1/N_{eq}$].
k_2	-	Temperature dependent constant. See equation 13 [$1/\sqrt{t}$].
T_K	288.15	Temperature (15 °C for the base case), [K].
d	$-6.7 \cdot 10^{-3}$	Coefficient (degradation), [$1/(K \cdot c_{rate})$].
e	2.35	Coefficient (degradation), [$1/c_{rate}$].
C_{BESS}^{cap}	2 000	Battery investment cost for the capacity part [NOK/kWh].
C_{BESS}^{pow}	3 200	Battery investment cost for power components (inverter, BOS), [NOK/kW].
C_{BESS}^{tot}	-	Total BESS investment cost [NOK]. Based on output from the sizing model.
$c_{E,tax}$	0.00546	Tax on electric power, [NOK/kWh].
$c_{E,tar}$	0.0375	Energy part of the grid tariff, [NOK/kWh].
$c_{P,tar}$	21.25 (S) 60.00 (W)	Power part of the grid tariff, for summer (S) and winter (W), [NOK/kW/month].
$c_{O\&M}$	50.0	Operation and maintenance cost for the BESS, in addition to energy/power costs [NOK/kW/year].
c_{inst}	1.5	Factor to include installation/engineering and labor costs.
RV	$0.15 \cdot C_{BESS}^{tot}$	Residual value of BESS investment after end of operation period.
r (in α_r)	0.04	Discount rate.

Transformer Data

In order to calculate the costs of losses through substation T3, some technical data is required. Relevant data, including the no-load and load losses, of a substation used as basis in this thesis is provided in table 10. The data is obtained from a datasheet from Møre Trafo AS [56].

Table 10: Technical data on substation T3 [56].

Parameter / specification	Value	Description
Capacity, power	3 150 kVa	The power capability of the transformer.
Voltage levels	22 000/415 V	The voltage levels of the HV and LV side.
Load losses, P_k	29 093 W	Losses at peak power.
No-load losses, P_0	1 920 W	Losses at no load.

Investment costs for transformers can be found in appendix E.

Input Data

Table 11 gives an overview of the input data, with values for every time step during a year (8760 hours). The data is based on figures from 2021, but is adapted for some scenarios.

Table 11: Overview of input data (time series with hourly resolution).

Symbol / name	Unit	Description
$c_{E,spot,t}$	NOK/kWh	Electricity spot prices, including VAT. Provided by Nord Pool AS.
$P_{G1.1,t}$	kWh/h	Power production from power generator 1.1.
$P_{G1.2,t}$	kWh/h	Power production from power generator 1.2.
$P_{G2,t}$	kWh/h	Power production from power generator 2.
$P_{G3,t}$	kWh/h	Power production from power generator 3.
$P_{Load,reg,t}^{tot}$	kWh/h	Total power demand in the region (22 kV side of T2).
$P_{Load,t}$	kWh/h	Load of the end user (adapted from 2021 data).
$P_{T3,t}^{avail.}$	kWh/h	(Only input data for the operation model): Available power for import from the grid, through T3. (Based on available power at T2 and 5 % losses from T2 to T3).

All other elements from the model summary, that are not described in the above tables, are variables. It must be noted that a few symbols represent a variable in the sizing model, but becomes a fixed parameter in the operation model. This includes E_B^{nom} and P_{inv}^{max}. Once the sizing model outputs the optimal values for these variables, the operation model takes these as constants.

The Inclusion of Costs of Losses

In addition to the operation costs, which is an output of the operation model, costs of losses in substation T3 are estimated. This is done after the running of the optimization model, when the total energy throughput of transformer T3 is known. The costs are calculated using equations 18 to 21, and tabular data from table 10 and appendix E. Costs of losses are included in the total operating costs that are reported in the results chapter.

4.3 Solution Method and Solvers

The models are written in the Julia programming language, using Visual Studio Code, which is free and open source (MIT licensed) [57]. It is a high-level and high-performance programming language, designed for scientific computations. It is similar to the Python programming language, but is known to have better performance and more simple syntax, which is why it is chosen for the work of this thesis. Furthermore, the modeling language JuMP is used in order to formulate the problem [58]. JuMP is a Julia based package, that allows for mathematical optimization of a variety of problem types and classes. Its syntax and output formulation is intuitive, and requires fewer formulations than similar tools based on, for instance, Python. The Julia language, as well as the relevant packages used for this thesis, are freely available.

Several of the constraints in the models are nonlinear, such as constraint 57p and 59m. These contain fractions with several variables and a term with an exponent. In order to be able to solve such models, a nonlinear solver is required. Having formulated the problem using Julia with JuMP, the nonlinear solver of Ipopt (Interior Point Optimizer) [59] is used. The software package is open source and distributed by the COIN-OR initiative for large-scale nonlinear optimization, based on the interior point method which is described in [60]. As the models are solved numerically, not analytically, the obtained solutions are not exact. However, they are good estimates [59].

The input data with hourly values, from table 11, are managed using Excel. The data of interest for the specific cases are saved in column vectors and taken as input by the Julia program. The optimization program is then run until a solution is found. The solution, being the objective value and the values of the variables at every time step, is then output to a new excel file. Both Julia and Excel are used for data analysis and graphical presentation of the solutions.

4.4 Simulation Scenarios: Cases of Analysis

In order to conclude on the feasibility of a BESS system as a solution for the case of this thesis, several scenarios must be analyzed as there are many variables. These are for instance the electricity

spot prices, the load situation and available power in the future. Data from 2021 is used as basis for all of the above-mentioned elements, while some data is adapted to investigate different scenarios. Electricity spot prices of NO3 from 2021, and the end user load adapted from 2021 data, are the basis for most of the scenarios, and are illustrated in detail in appendix F. Scenarios with this combination is referred to as the main cases of this thesis.

A few scenarios on the load situation of the region is considered for both the sizing and operation models. This is mainly included to see how possible future loads affect the sizing of the BESS and the state of the grid. The scenarios can be relevant if for instance other end users in the region implement similar solutions as the one presented in this thesis, or if the demand increases due to more electrification or new industry. In practice, the cases are adapted by increasing the total, regional, load ($P_{Load,reg,t}^{tot}$) for every time step t, according to the following definitions:

Region load case 1

This is the regional load registered in 2021, $P_{Load-21,t}^{reg}$, which is defined according to equation 25. This is the basis for most of the sizing and operation cases.

Regional load case 2

This load situation is adapted by adding a fixed power demand to the original load of 2021 (regional load case 1: $P_{Load-21}^{reg}$), for every time step, according to the following rules:

- If $P_{Load-21,t}^{reg} \in \langle 18\,MW, 21\,MW] \Rightarrow P_{Load,reg,t}^{tot} = P_{Load-21,t}^{reg} + \underline{1.5\,MW}$

- If $P_{Load-21,t}^{reg} \in \langle 15\,MW, 18\,MW] \Rightarrow P_{Load,reg,t}^{tot} = P_{Load-21,t}^{reg} + \underline{4.5\,MW}$

- If $P_{Load-21,t}^{reg} \leq 15\,MW \Rightarrow P_{Load,reg,t}^{tot} = P_{Load-21,t}^{reg} + \underline{5.0\,MW}$

Regional load case 3

This load situation is also adapted in the same way as for regional load case 2, according to the following set of rules:

- If $P_{Load-21,t}^{reg} \in \langle 20\,MW, 21\,MW] \Rightarrow P_{Load,reg,t}^{tot} = P_{Load-21,t}^{reg} + \underline{2.0\,MW}$

- If $P_{Load-21,t}^{reg} \in \langle 18\,MW, 20\,MW] \Rightarrow P_{Load,reg,t}^{tot} = P_{Load-21,t}^{reg} + \underline{3.0\,MW}$

- If $P_{Load-21,t}^{reg} \in \langle 15\,MW, 18\,MW] \Rightarrow P_{Load,reg,t}^{tot} = P_{Load-21,t}^{reg} + \underline{5.0\,MW}$

- If $P_{Load-21,t}^{reg} \in \langle 10\,MW, 15\,MW] \Rightarrow P_{Load,reg,t}^{tot} = P_{Load-21,t}^{reg} + \underline{7.0\,MW}$

- If $P_{Load-21,t}^{reg} \leq 10\,MW \Rightarrow P_{Load,reg,t}^{tot} = P_{Load-21,t}^{reg} + \underline{10\,MW}$

As the load situations are adapted without adapting the regional power production, the new power demand must be met by power imported through T2. Therefore, these cases may affect the amount of power that is available for charging the BESS. The regional load, $P_{Load,reg,t}^{tot}$, is illustrated for one year for the different load cases in figure 27. Note that the plots are for the daily average, and that the actual peaks are higher.
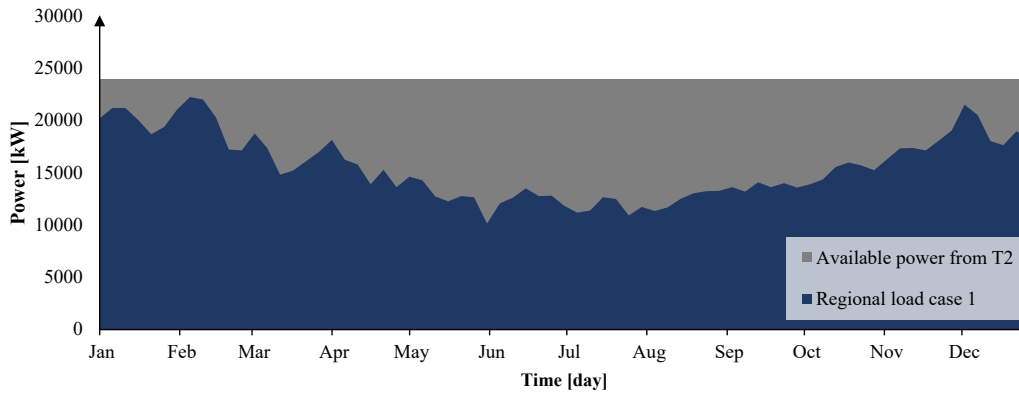
(a) Regional power demand, regional load case 1.
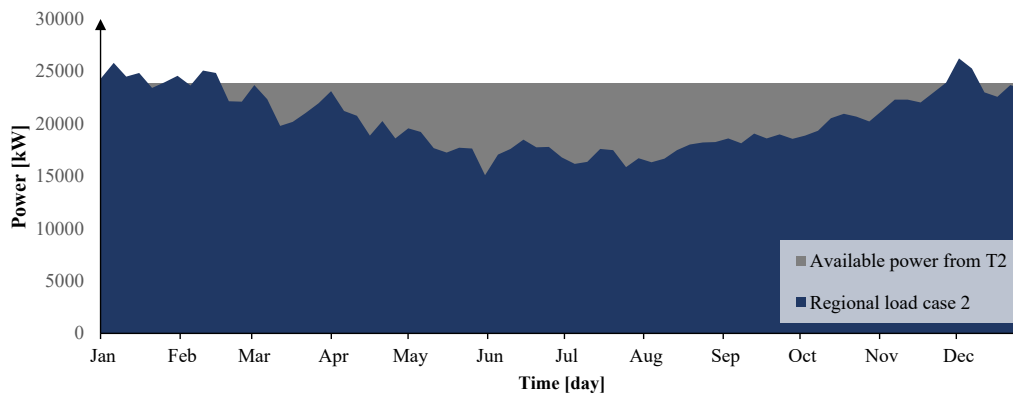
(b) Regional power demand, region load case 2.
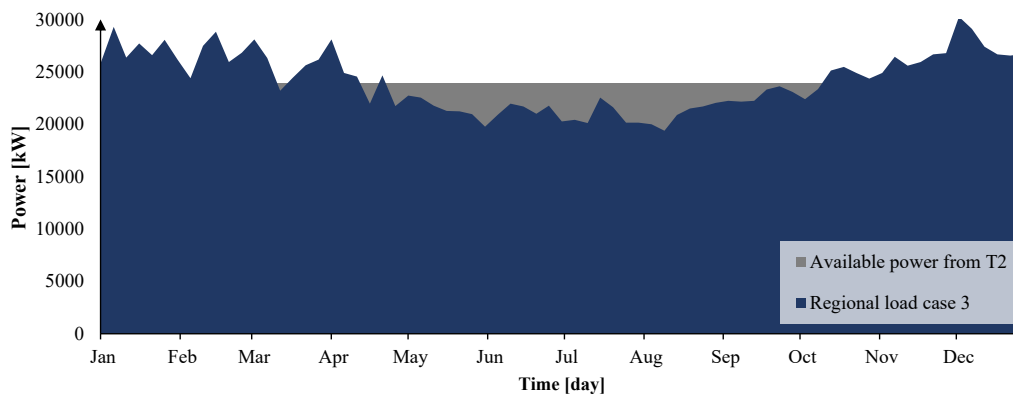
(c) Regional power demand, region load case 3.

Figure 27: Regional power demand, for the different load cases (daily average).

When the regional load exceeds the limit of the T2 transformer, being 23.9 MW, the demand must be covered by the local energy generators or stored energy. The transformer faces capacity limitations during the winter months, and especially in February for region load case 1.

Possible Load Shedding by the End User

A scenario where the end user reduces its power consumption, in stead of having it supplied from the battery, is also considered. This is done for some periods where the power grid is assumed to be operating at maximum load, meaning that the demand would have to be covered by the BESS otherwise. The scenario is established by adapting the input data on the load, such that it is reduced to its original power demand (measured for 2021) when the power imported through T2 exceeds 22.5 MW. In other words, the load is reduced significantly during these hours, referred to as load shedding. The updated load data, which is an input for the optimization model, is found to have 32 hours with load shedding within a period of two weeks in February. For this scenario, regional load case 1 is used.

Base Cases (no BESS)

Several base cases, where the load is directly connected to the grid without having a BESS installation, are investigated to establish benchmarks. These scenarios are hypothetical, as they assume that the grid is always capable of covering the new peak load of the end user, being 1.5 MW. This is not realistic. However, these cases are meant to give an impression of the levels on the energy cost that the end user would have to pay when not having a BESS. The base cases assume the installation of the same substation (T3) as for the cases with BESS, with the corresponding data on losses. The scenarios that are investigated are described in table 12, and are analyzed using Excel.

Table 12: Descriptions of the base cases (scenarios without BESS).

Case / scenario	Description
Base case 0	A fixed electricity spot price corresponding to the average elspot price of NO3 in 2021: 0.524 NOK/kWh.
Base case 1	Electricity spot price of NO3 from 2021 (medium high price level).
Base case 2	Electricity spot price of NO3 from 2020 (low price level).
Base case 3	Electricity spot price of NO5 from 2022 (low price level).
Base case 4	Electricity spot price of NO3 from 2021, 1.5x power cost (increased grid tariff).
Base case w/PV 1	Including PV production with irradiance data from 2019, and electricity spot price of NO3 from 2021. [Only included in appendix G]
Base case w/PV 2	Including PV production with irradiance data from 2019, and electricity spot price of NO5 from 2022. [Only included in appendix G]

The electricity spot price in NO5 from 2022 is only recorded until December 10th, 2022. The data for the remaining days are added manually by repeating the daily variations of the last day of record. The scenario is included to observe the effects of high electricity spot prices, that can occur if for instance the transfer capacity between the price zones increases significantly in the future.

Scenarios for Sizing

The scenarios for the sizing model includes variations in elspot prices, battery investment costs and regional power demand. These are summarized in table 13. The goal is to investigate how the different conditions and costs affect the sizing of the system.

Table 13: Descriptions of the BESS sizing scenarios.

Case / scenario	Description
Sizing case 0	A fixed electricity spot price corresponding to the average spot price of NO3 in 2021: 0.524 NOK/kWh.
Sizing case 1	Electricity spot price of NO3 from 2021 (medium high price level). Regional load case 1.
Sizing case 2	Electricity spot price of NO3 from 2021 (medium high price level). Regional load case 2.
Sizing case 3	Electricity spot price of NO3 from 2021 (medium high price level). Regional load case 3.
Sizing case 4	Electricity spot price of NO3 from 2021 (medium high price level). Load shedding of the end user.
Sizing case 5	Electricity spot price of NO5 from 2022 (high price level).
Sizing case 6	Electricity spot price of NO3 from 2020 (low price level).
Sizing case 7	Electricity spot price of NO3 from 2021 (medium high price level). Cheap BESS: 1000 NOK/kWh; 1200 NOK/kWh.
Sizing case 8	Electricity spot price of NO3 from 2021 (medium high price level). Expensive BESS: 4000 NOK/kWh; 5000 NOK/kWh.

Scenarios for Operation

The same type of scenarios are investigated for the operation model. These are found in table 14. However, as this model does not include the grid side, the available grid power is expressed by an updated input data for $P_{T3}^{avail.}$, as stated in equation 38. Also, the battery sizing is set as a fixed value, based on the output of the corresponding sizing model. All of the scenarios for the operation model is run for four years, except from the scenario of *BESS OPR 2.3* (load shedding of end user), which is only simulated for one year. The operation model also includes some extra scenarios, having to do with degradation. All cases, except from *BESS OPR 4.3,* include both cyclic and calendric degradation and assumes a constant temperature of 15 °C, unless otherwise mentioned. Degradation cost is only included in the objective value for *BESS OPR 1.2*, and *BESS OPR 4.3* excludes degradation entirely.

Table 14: Descriptions of the BESS operation scenarios.

Case / scenario	Description
BESS OPR 0	A fixed electricity spot price corresponding to the average spot price of NO3 in 2021: 0.524 NOK/kWh.
BESS OPR 1.1	Electricity spot price of NO3 from 2021 (medium high price level). $P_{T3}^{avail.}$ based on regional load case 1.
BESS OPR 1.2	Electricity spot price of NO3 from 2021 (medium high price level). $P_{T3}^{avail.}$ based on regional load case 1. Degradation cost included in the objective function.
BESS OPR 2.1	Electricity spot price of NO3 from 2021 (medium high price level). $P_{T3}^{avail.}$ based on regional load case 2.
BESS OPR 2.2	Electricity spot price of NO3 from 2021 (medium high price level). $P_{T3}^{avail.}$ based on regional load case 3. (Increased battery size).
BESS OPR 2.3	Electricity spot price of NO3 from 2021 (medium high price level). $P_{load,t}$ adapted for load shedding. Simulated for one year. Different BESS sizes.
BESS OPR 3.1	Electricity spot price of NO3 from 2020 (low price level).
BESS OPR 3.2	Electricity spot price of NO5 from 2022 (high price level).
BESS OPR 3.3	Electricity spot price of NO3 from 2021, high power cost (1.5x power cost).
BESS OPR 4.1	Electricity spot price of NO3 from 2021 (medium high price level). Low operating temperature: 5 °C
BESS OPR 4.2	Electricity spot price of NO3 from 2021 (medium high price level). High operating temperature: 35 °C. (Increased battery size).
BESS OPR 4.3	Electricity spot price of NO3 from 2021 (medium high price level). No degradation.
BESS OPR PV-1	Including PV production with irradiance data from 2019, and electricity spot price of NO3 from 2021. [Only included in appendix G]
BESS OPR PV-2	Including PV production with irradiance data from 2019, and electricity spot price of NO5 from 2022. [Only included in appendix G]

Two scenarios that also includes local energy production with a PV installation is also investigated to some extent. Information on this can be found in appendix G.

5 Results and Discussion

In this part, the results from the different models and scenarios are presented, analyzed and discussed. The chapter starts by illustrating the variants of the base cases, where the load is assumed to be covered by power from the grid directly. As stated earlier, these cases are hypothetical and not realistic, but are used as a benchmark to measure the feasibility of the cases involving battery energy storage systems. Further, the outputs of the different scenarios of the sizing model are analyzed. The state of the power grid is also considered for this model. Knowing the power and capacity characteristics of the BESS, the operation model is simulated for many of the same scenarios of the sizing model, in addition to a few more. The results from these cases are also presented and discussed. Lastly, some general remarks and interesting observations are brought up.

The base cases are solved and analyzed by using Excel, while the optimization models are solved by using a program made in Julia. Being run on a general-purpose laptop (Lenovo Yoga C930[34]), the program required 12 to 37 minutes to solve the different scenarios of the sizing model. For the operation model, 60 to 90 minutes were needed for each scenario. The case including the degradation cost in the objective function, for the operation model, required the longest run-time. All of the problem scenarios are *locally solved*, meaning that the solver (Ipopt) finds locally optimal solutions. These may also be globally optimal, but the program is not able to prove so.

5.1 Base Cases (No BESS)

The base cases from table 12 are investigated and compared with respect to net present costs, NPCs, as for the other cases in this chapter. The resulting costs of the base cases are understood as the costs that would apply if the adapted load, having a new peak power of 1.5 MW, were to be covered by power from the grid, directly. Figure 28 shows and compares the net present costs of operation after four years, and the operation costs of the first year, for scenarios with different energy costs. These include three different elspot prices and the case of an increased power cost in the grid tariff. The first year operation costs are not discounted. It is shown that there are significant differences in the energy costs for the three different elspot prices that are investigated.

---

[34]Processor: Intel(R) Core(TM) i7-8550U CPU @ 1.80GHz 1.99 GHz; 16.0 GB RAM; Windows 11 Home, x64-based processor.
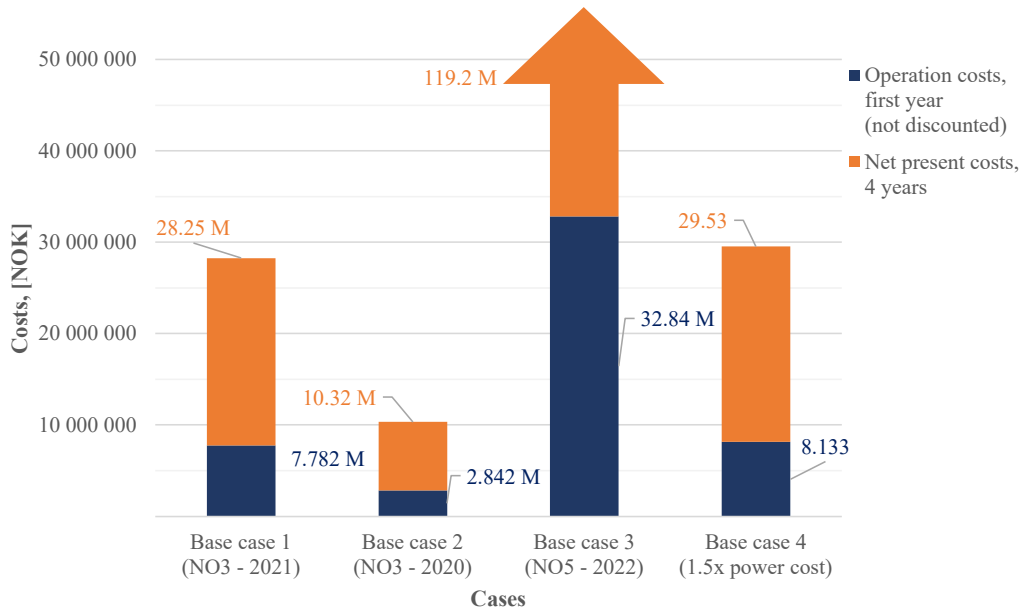
Figure 28: Net present costs of operation for the base cases (only grid connection, no BESS).

It is only the energy costs that vary for the first three scenarios. The power costs and transformer loss costs stay the same, being 702 400 NOK and 59 745 NOK for the first year, respectively. This is because the load is assumed inflexible, requiring the same, monthly, peak power for all years and all cases. The monthly power peaks, in addition to the original power costs of the grid tariff, are illustrated in figure 29. Note that the highest power peaks are during the spring, while the power costs are generally the highest during the winter months. This is due to the pricing scheme of the grid tariff, where the price of power is higher during the winter months (from November to, and including, April). Based on this, it could be an idea to reduce the peak of the power imported in April.
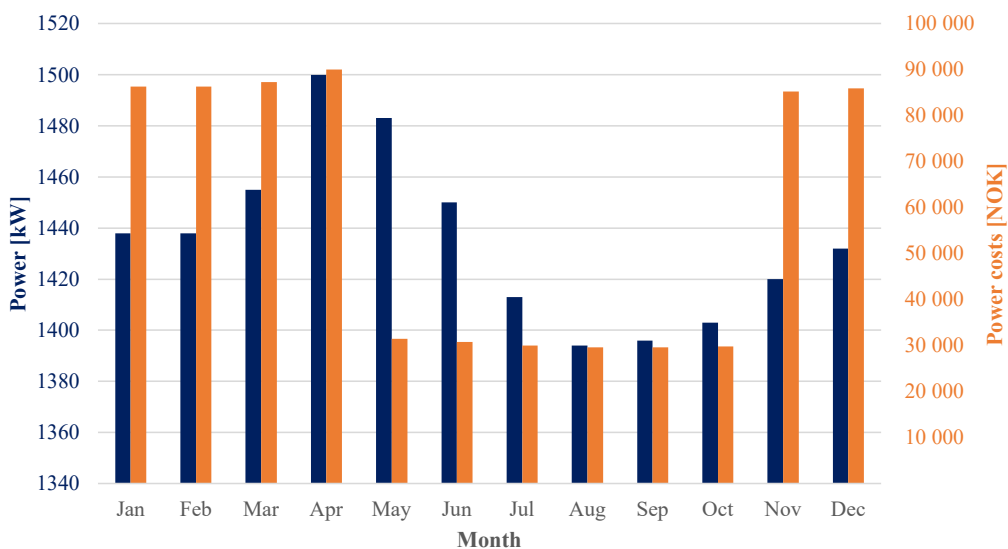
Figure 29: Monthly power peaks and power costs for the base cases (only grid, no BESS).

Table 15 shows a breakdown of the NPC calculation for base case 1. The actual costs, based on the monetary value of 2022, include energy and power costs that are static, and a cost of transformer losses which increases for each year as presented in table 16. The sum of these cost elements are discounted to give the present cost of the respective year, and the total net present cost for all years of interest. After four years, the NPC of base case 1 is found to be approximately 28.25 MNOK. For base case 0, assuming a fixed electricity price for every hour throughout the year, the NPC is slightly higher, being around 28.29 MNOK.

Table 15: Breakdown of NPC calculation for base case 1 (no BESS).

Year	Discount factor	Costs, 2022 level [NOK]	Discounted costs (Present value) [NOK]	NPC [NOK]
1	0.9615	7 782 100	7 482 800	7 482 800
2	0.9246	7 783 100	7 195 900	14 678 700
3	0.8890	7 784 100	6 920 000	21 598 700
4	0.8548	7 785 200	6 654 800	28 253 500

Table 16: Transformer loss costs for the base cases (no BESS).

Year (y)	Reference year	Costs of T3 losses, in year (y) [NOK]
1	2024	59 745
2	2025	60 767
3	2026	61 782
4	2027	62 829

The figures and result data presented above are used as benchmarks for comparison with the cases involving battery energy storage systems. These are described in the subsequent subsections.

5.2 Results From the Sizing Model

The goal of the sizing model is primarily to find the optimal BESS sizing, given the investment costs, possible savings in energy costs from energy arbitrage, and the restrictions on available power. But, as it also include a model of the grid side, it also aims to ensure that the implementation of a BESS, with the new power demand of the end user, is technically achievable.

5.2.1 Optimal Sizing

The optimal sizing of a BESS depend on several aspects, such as the system constraints, investment costs and the possibilities of cost savings from demand side management or grid services. The latter is not a focus for the cases of this thesis, as the battery is considered installed behind-the-meter (BTM).

Sizing case 0: Fixed Electricity Price

The first scenario to consider is sizing case 0, which is based on a fixed electricity price throughout the whole year of operation. This case is included to isolate the effect that the restrictions on available power and grid capability have on the BESS sizing. Figure 30b shows the energy throughput (cumulative charged and discharged energy) for every month throughout the year. It clearly illustrates that the BESS is used extensively for February, in contrast to the rest of the months. The use in February is more closely illustrated in figure 30a, which shows a plot of the battery power versus time. Discharged power is positive, while charging is negative. The figure indicates which times the battery is required, considering the available power from the grid, as there are no economical incentives for discharging these amounts of power with a flat electricity price.
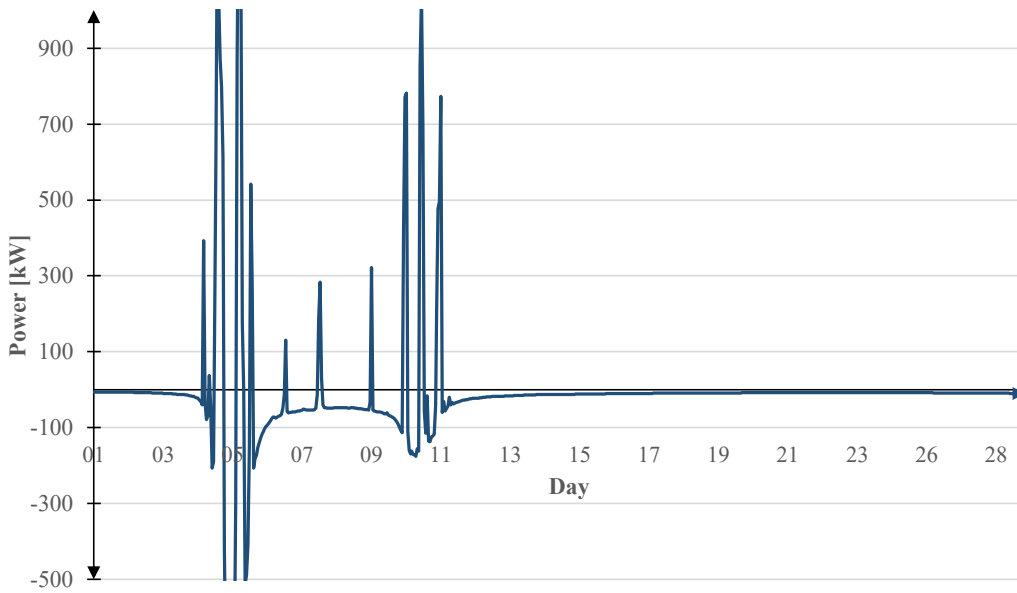
(a) Battery power, $P_B(t)$, for February. Sizing case 0
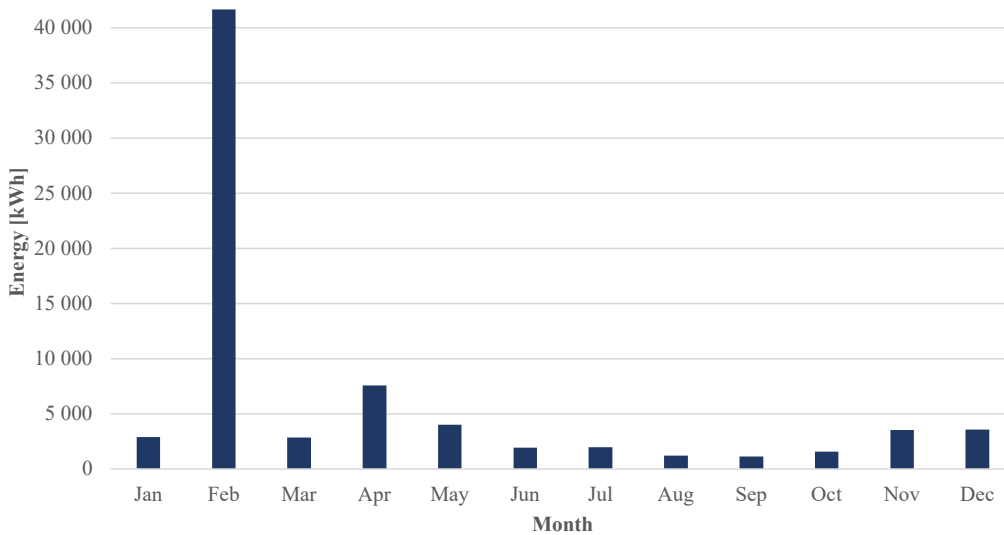
(b) Battery energy throughput (sum of charging and discharging) for each month. Sizing case 0

Figure 30: Battery use for sizing case 0 (fixed electricity price).

The heavy use of the battery during February can be understood when considering the power demand of the region in this period, illustrated by figure 27a. At this time of the year, the regional transformer (T2) is known to operate at its capacity limits, as the local power generation is not sufficient to cover the total demand. Therefore, the battery must be used in order to cover the load of the end user. It is the capacity and power requirements of this period that decides the BESS sizing in this scenario.

During the rest of the year, the battery is used to a small extent. As there is no motivation for energy arbitrage, the only way of reducing operating costs (being a part of the objective function), is to

reduce the peaks of the imported power (peak shaving / load shifting). It is observed that the BESS charges and discharges small amounts of energy in order to achieve this during the rest of the year, and especially during the winter months where the grid tariff is most expensive. This is especially notable for April, having the highest power costs in base case 1 (figure 29). The peak power of this month is reduced by approximately 40 kW when including the battery system.

Optimal Sizing for the Different Cases

Sizing case 0 gave a nominal capacity of 8603 kWh and a power capability (of the converter / inverter) of 1330 kW. As stated above, this is found to be the required capacity and power in order to cover the load given the constraints of the model. However, when including varying (real) elspot prices, which is further described in subsection 5.2.2, the optimal BESS sizing is found to be the same. There are also no changes in optimal sizing with the cases of cheap and expensive BESS investment costs (sizing case 7 and 8). The latter is logical, as the sizing model is only solved for one year of operation. In order to investigate the benefits or drawbacks of investments in extra battery capacity, a longer time horizon would be required to include future savings.

This means that the optimal BESS sizing for the case of this thesis are also the minimum capabilities that are required due to the limitations of the power grid only. Table 17 summarizes the sizing parameters that was found to be optimal (and minimum), for the different scenarios of the sizing model. These results are commented on in the subsequent paragraphs.

Table 17: Optimal BESS sizes, for the different sizing cases.

Sizing case	BESS optimal capacity (Nominal capacity[*]) [kWh]	BESS optimal power capability (converter power) [kW]
BESS sizing case 0	8603 kWh	1330 kW
BESS sizing case 3	12 208 kWh	1330 kW
BESS sizing case 4	53 kWh	33 kW
All other sizing cases	8603 kWh	1330 kW

(*) Degradation not accounted for.

5.2.2   BESS Sizing and Usage for Different Electricity Spot Prices

Even though the battery sizing is found to be the same for all of the scenarios with different elspot prices, the battery system is used differently in these cases. This is discussed more in-depth in section 5.3, but is introduced here as it is also related to the grid side of the model. The yearly electricity costs of sizing case 1 to 4 are all somewhat lower than those of the base cases with corresponding energy costs. This is because the BESS is used actively for energy arbitrage and load shifting, in order to minimize operating costs. This is observed from figures 31 and 32, showing the energy throughput for the whole year as well as the battery power and variations in elspot prices for February, for NO3 in 2021 and NO5 in 2022, respectively.

Compared to sizing case 0, the battery is used more extensively in February in the case of the electricity spot price in NO3 from 2021. This is displayed in figure 31a, where it is evident that the battery is charged (negative power) during times of low electricity prices (e.g. February 23. and 26.), and discharged during times of high prices. This comes in addition to the required battery usage due to limitations of the power grid.
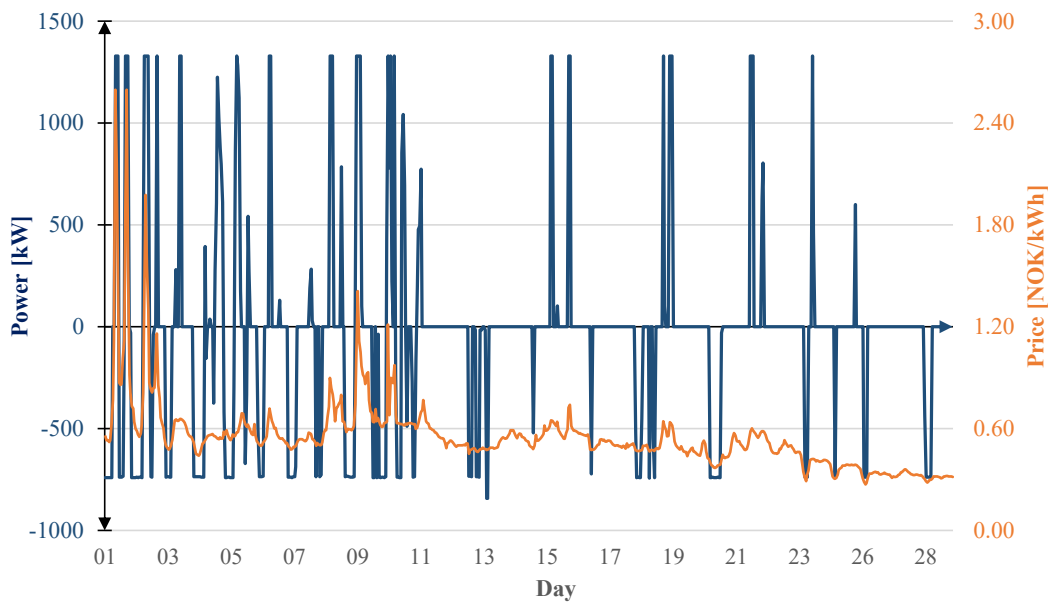
(a) Battery power, $P_B(t)$, for February. Sizing case 1
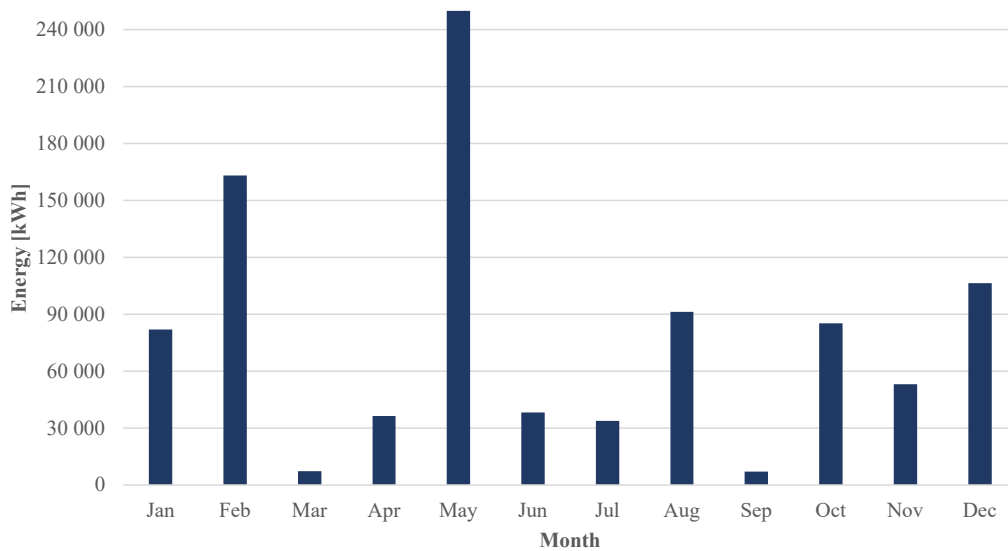
(b) Battery energy throughput (sum of charging and discharging) for each month. Sizing case 1

Figure 31: Battery use in sizing case 1 (NO3 elspot of 2021).

Furthermore, considering figure 31b, February is no longer the month where the battery is used the most. The highest energy throughput of the battery is now observed for the month of May. This can for instance be explained by the fact that the electricity prices of this period are characterized by a lot of variation (see the orange graph of figure 24), that can be exploited by the BESS. It is also defined as the first "summer month" for the grid tariff, meaning that the costs of peak power are lower than for instance those of April. Because of this, the battery can charge at a higher power rate, for the same or lower total costs compared to the winter months.

In the case of the electricity spot price from NO5 in 2022, the battery usage is quite different. During February, the BESS is used to a small extent as illustrated by figure 32a. Looking at figure 32b, it is observed that the battery is used substantially more frequent from September to December. Again, considering the elspot prices from figure 24 (the graph in gray color), this can be explained by the high variations for these months, which allow for significant savings from energy arbitrage.
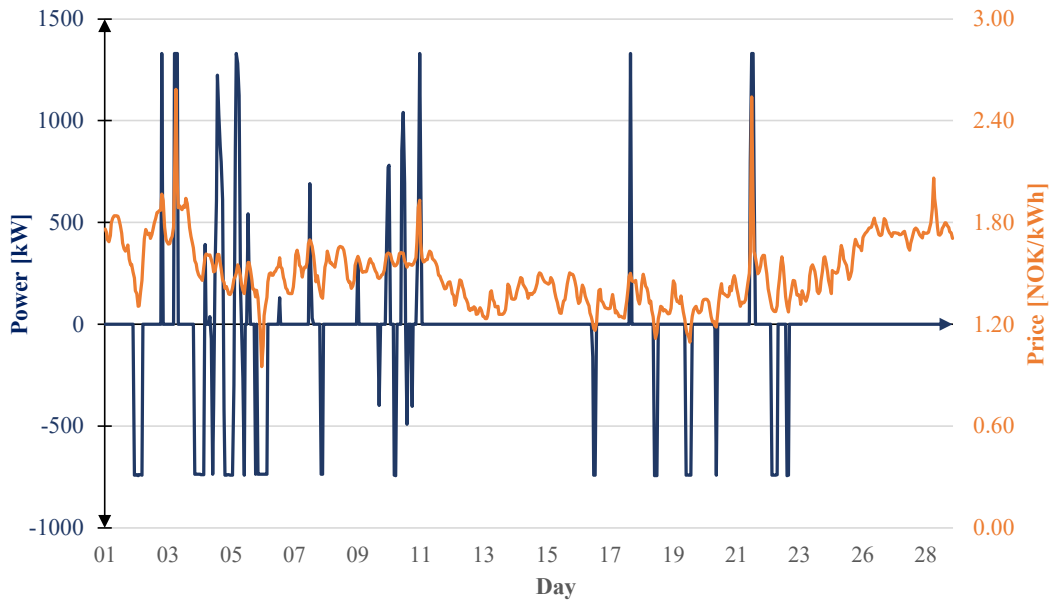
(a) Battery power, $P_B(t)$, for February. Sizing case 5
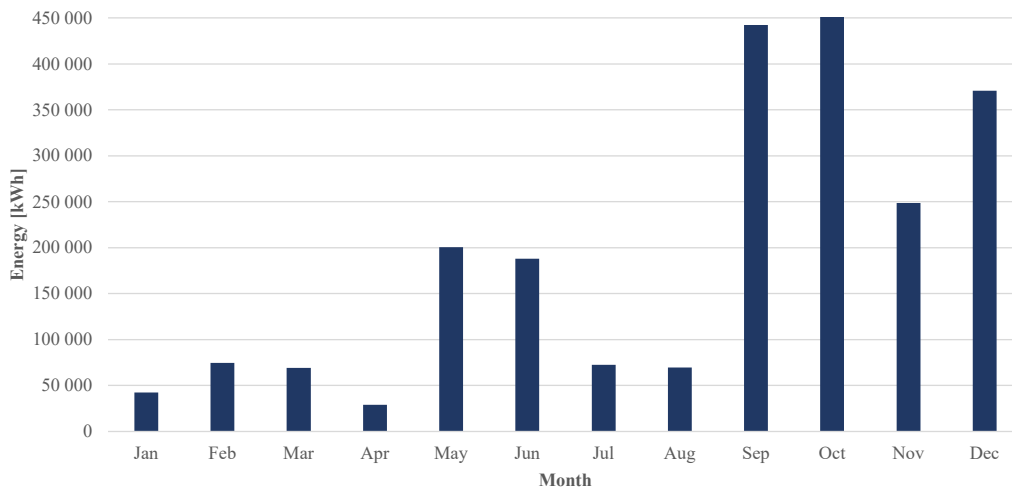
(b) Battery energy throughput (sum of charging and discharging) for each month. Sizing case 5

Figure 32: Battery use in sizing case 5 (NO5 elspot of 2022).

5.2.3   BESS Sizing for Different Scenarios of Regional Demand

The sizing model is also investigated for scenarios where the total power consumption of the region, on the 22 kV side of transformer T2, is increased according to the descriptions from section 4.4. This affects the available power for the end user, as the power production of the region and the power capability of T2 remain the same. Because of this, the battery usage and the states of the power grid are also influenced. For sizing case 2, the output sizing parameters remain the same as for sizing case 0, with slightly different use of the battery. In this scenario, T2 is observed to import energy at an average power that is higher than 22.5 MW for 388 hours, mostly during January and February, but also during November and December. For sizing case 0 and 1, the same is only observed for 102 hours in January and February. This indicates that there is less available power to charge and discharge the BESS for the new load situation.

For sizing case 3, representing the highest regional power demand, the situation is different. In this scenario, T2 imports energy at an average power that is above 22.5 MW for 734 hours. This also occurs in the months of March, May and October, and causes the required battery capacity to increase to a nominal capacity of 12 208 kWh (an increase of almost 42 %). The optimal power capability remains the same (1330 kW). In other words, a large amount of battery packs are required in order to exploit the available power for a situation as this, where the regional load increases due to for instance electrification and new industry.

Load shedding - Reducing the Load of the End User

In sizing case 4, the end user is assumed to reduce its power demand back to the original load of 2021 for the periods where the power imported through T2 exceeds 22.5 MW. In this case, the power demand of the end user is reduced for 32 instants (hours). This approach reduces the need for battery energy storage, having a resulting optimal capacity of 53 kWh and a power capability of 33 kW. Analyzing the output data, the sizing of this BESS is still based on the requirement of covering the load, which is now reduced compared to the main case. However, this sizing also allows for reductions in monthly power peaks for several winter months.

Figure 33 shows the battery usage for sizing case 4, similarly as for the previous scenarios. The usage pattern is quite different for this case, characterized by a lower volume of energy throughput and a lower monthly variability. This is likely because the BESS is mainly used for energy arbitrage and load shifting in a small scale, compared to the above-mentioned scenarios.
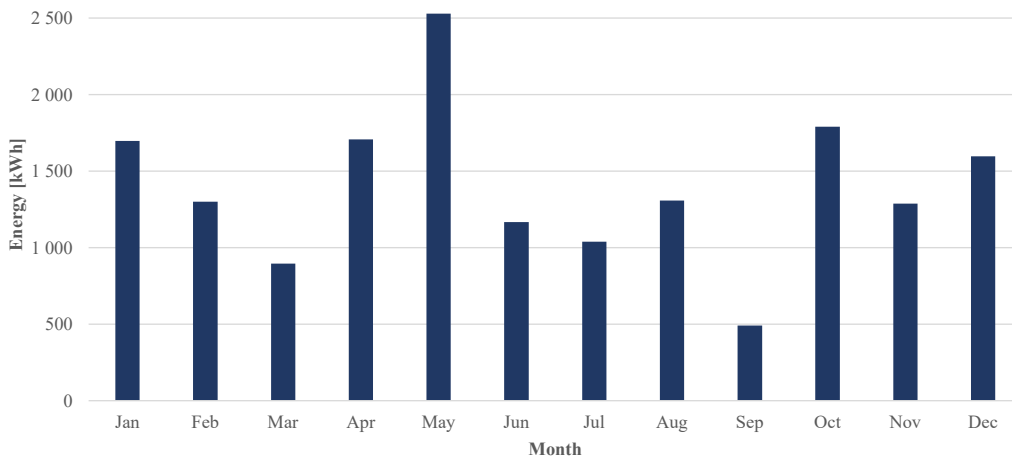
Figure 33: Battery use in sizing case 4 (when end user cuts load).

For the sizing cases (1 to 6), a relatively extensive use of the battery is observed. However, the optimal battery usages, involving energy arbitrage and reductions of power peaks, are not providing for enough savings in energy costs to motivate for larger BESS sizing. The optimal battery sizing is also the minimum sizing for the given constraints, as the model is formulated as a minimization problem for one year only. Within this short time horizon, it will not be possible to cover significant parts of the investment costs with the savings from energy arbitrage. Another approach, formulating the model as a maximization problem with the objective of maximizing energy cost savings for a longer period, could give different results. However, while the grid requirements remain the same, a large BESS with correspondingly high investment costs would be the outcome for the realistic investment costs that are investigated.

5.2.4 System States (Grid Side)

The sizing model also includes a grid model, with power flows, line currents and voltages for the part of the distribution grid that will be affected by a BESS installation and an increased load. Figure 34 and 35 show snapshots of the states of the power grid for two different time steps (hours) based on sizing case 1 and 5, respectively. The output variable values, as well as the known power generations for the corresponding time step, are indicated by green labels.

At the time of the snapshot in figure 34, the power flow is from point B to $T3$, and the battery is charging at a power of 739 kW ($c_{rate} < 0.1$). Most of the power required to cover the regional power demand is in this case imported from the regional grid through transformer T2 (approximately 22 MW).
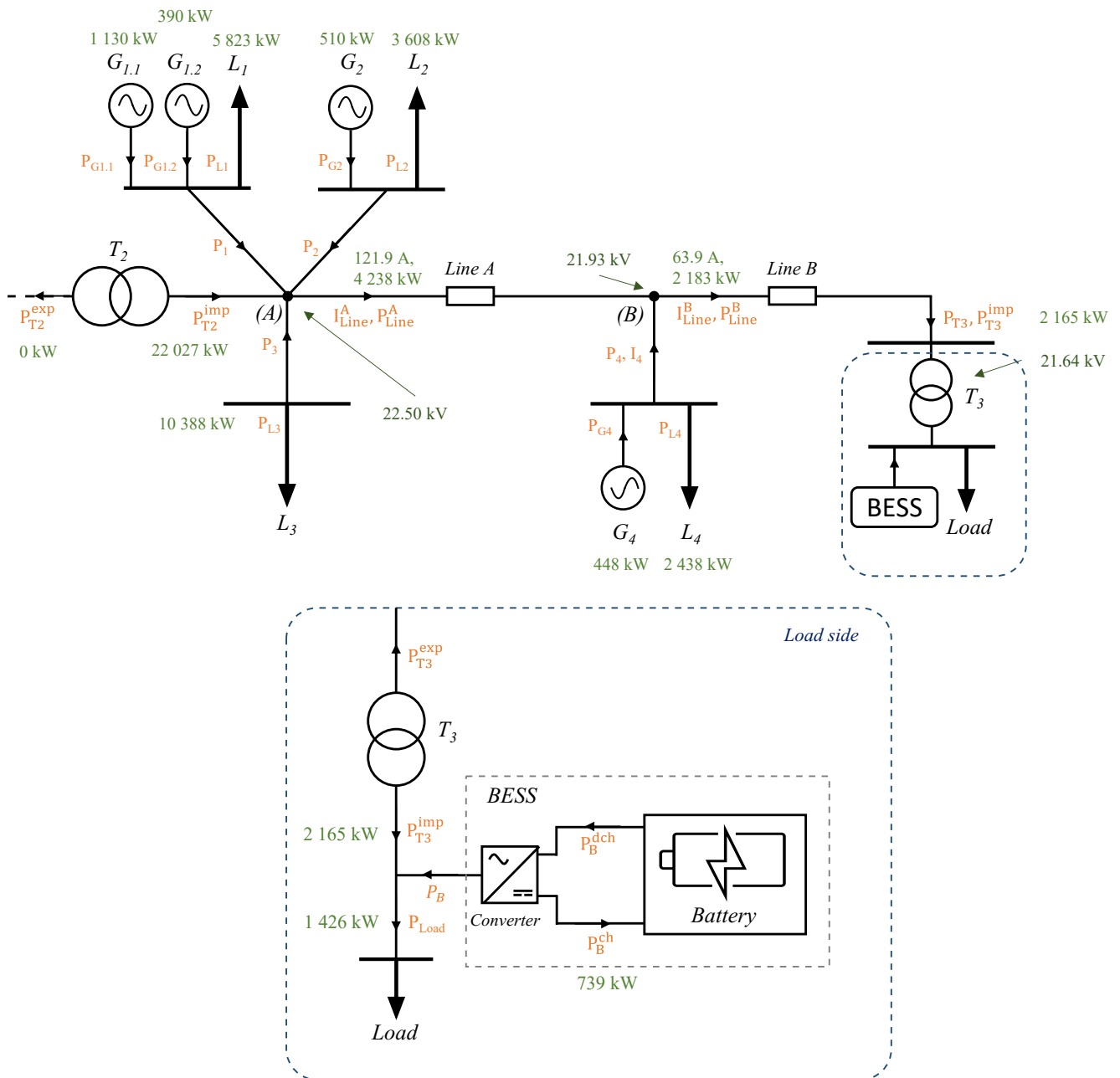
Figure 34: Snapshot of system state (grid and load). Sizing case 1 (NO3 el. spot prices of 2021), on February 10, at 15.00.

At the time of the snapshot in figure 35, the power flow is in the opposite direction. That is, from $T3$ to point B, and from point B to point A. The BESS is discharging a power of 1329 kW, which is 13 kW more than required by the load at this time. The surplus power is therefore exported to the grid, and flows toward point B. At this instant, there is a surplus of power on the 22 kV side of T2, resulting in the export of 9.5 MW out of the region.
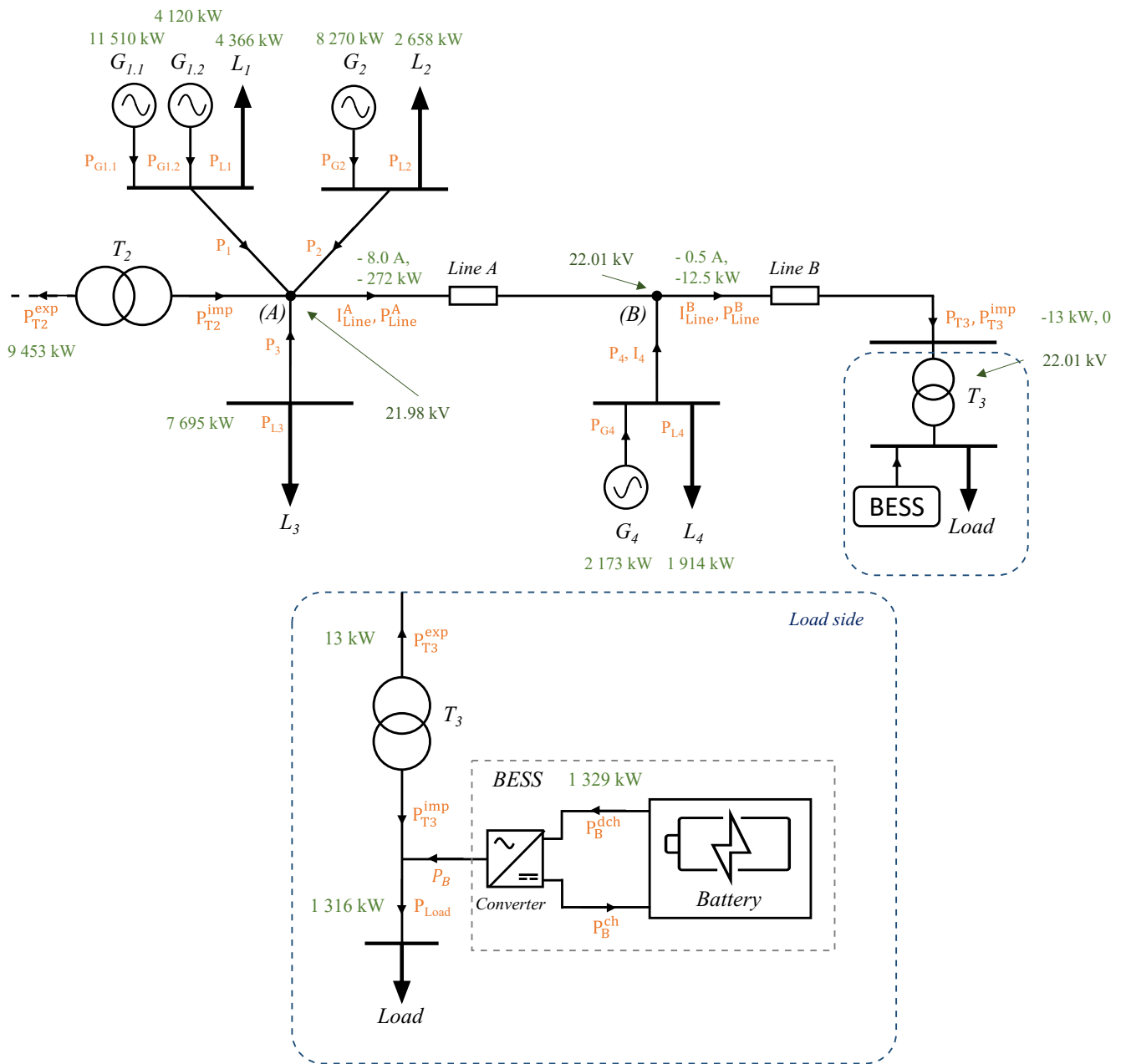
Figure 35: Snapshot of system state (grid and load). Sizing case 5 (NO5 el. spot prices of 2022), on October 7, at 10.00.

The snapshots show the working of the sizing model. The power is flowing according to the rules defined by the constraints of the model, which aim to ensure realistic operating conditions. Recalling that the constraints involve limits on currents and voltages, it is possible to say something on the achievability of the BESS implementation and the increase of power consumption by investigating these. Considering the current carrying capacity of the power lines, being 629 A for *line A* and 266 A for *line B*, the new situation will not cause too high loading on the power lines as the maximum registered currents are 179 A and 85 A for *line A* and *B,* respectively. This occurs for sizing case 3, which represent the highest loads of the region. In other words, the constraints on current limitations are never binding.

Considering the voltages, registered for point *A*, *B* and *T*3, these are also found to be within the required minimum and maximum limits of $\pm$ 5 % of nominal voltage (22.0 kV), for all times. However, the voltage constraints are binding for several time steps. Figure 36 shows the variations in voltages for the three different scenarios of regional load. The figures are based on daily average, and the actual magnitude of the variations are therefore actually higher. Nevertheless, for the case of the highest loads, plotted in figure36c, a voltage dip down to 20.9 kV (being the minimum limit of the voltage) is registered for *T*3 in February.

It is observed that all voltages, for all three scenarios, drop at this time. This can be seen in connection with the peak in the regional power demand, which occur in the same time period. Although the voltages stay within the requirements, the situation is not optimal. A possible solution is to adjust the tap settings[35] on the regional transformer (T2), in order to increase the voltage of point *A*.

---

[35]The transformer taps are mechanisms that can be adjusted in order to change the turns ratio and voltage levels.
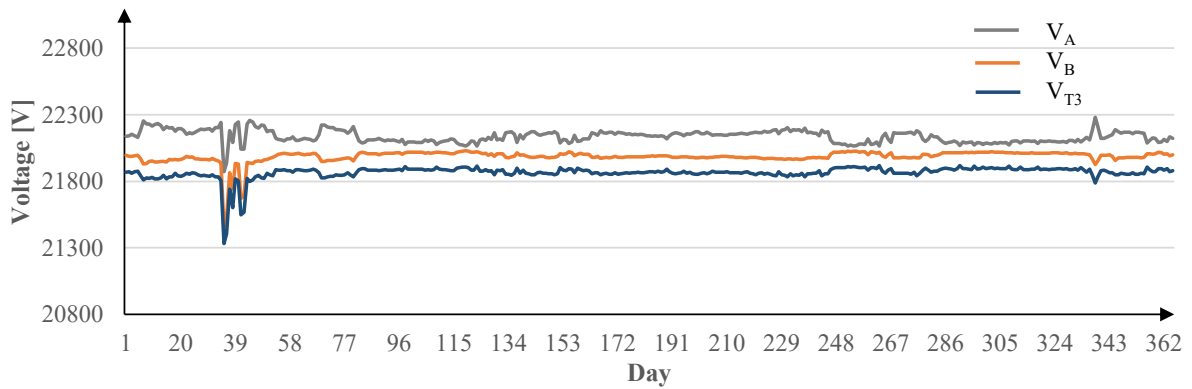
(a) Sizing case 1 (2021 regional load).
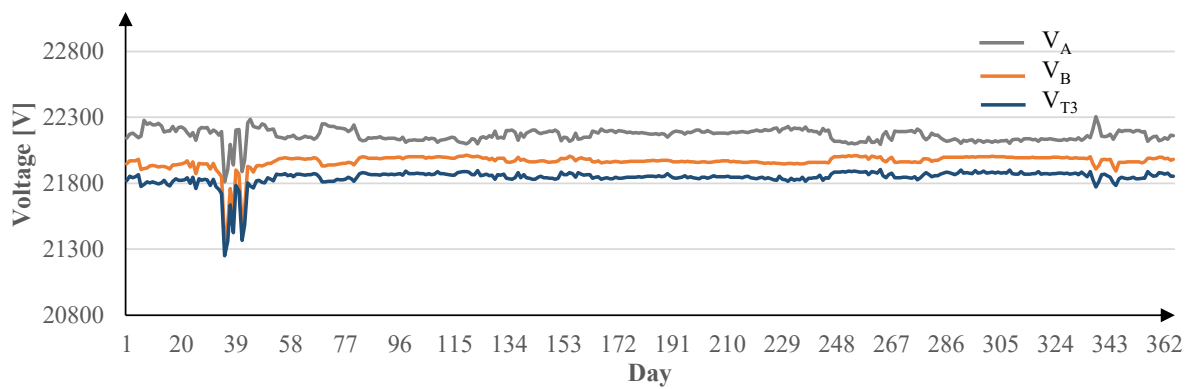
(b) Sizing case 2 (regional load adapted).
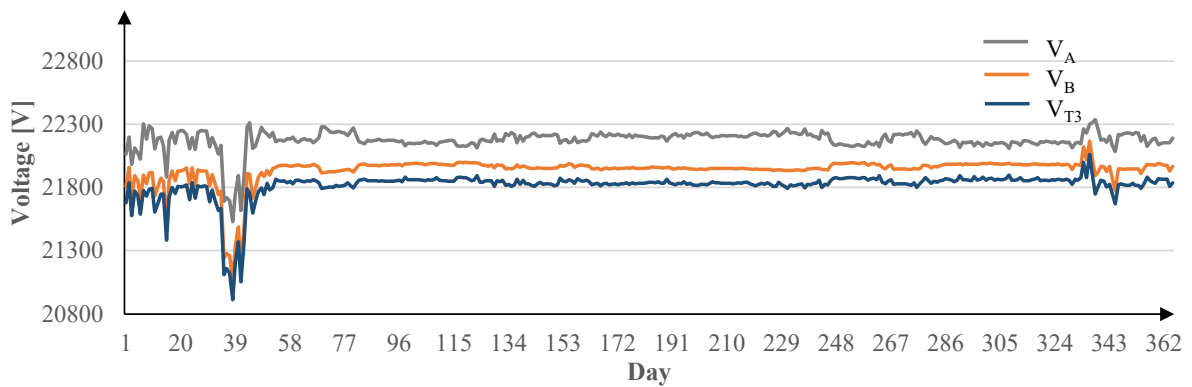
(c) Sizing case 3 (regional load adapted).

Figure 36: Voltages (daily average) for each node of interest, for three regional load scenarios.

5.2.5 Setting the BESS Size for the Operation Model

Having obtained the optimal BESS sizing parameters, these are used as basis for the operation model. However, as the operation model includes degradation, this must be take into account before moving on. According to the Wang Model for degradation, which is used for this thesis, the calendric aging

can reduce the battery capacity by 20 % for four years, according to figure 18b (for 15 °C). In order to allow for some margin, and the effect of cyclic aging, a degradation of 30 % is assumed when setting the required battery capacity for four years of operation. This results in the following BESS capacities, adapted from table 17:

$$E_{B,1}^{nom} = \frac{8603\,kWh}{0.7} = 12290\,kWh \Rightarrow \underline{12500\,kWh}$$

$$E_{B,2}^{nom} = \frac{12208\,kWh}{0.7} = 17440\,kWh \Rightarrow \underline{18000\,kWh}$$

For most of the operation scenarios, a nominal battery capacity of 12 500 kWh is therefore set as a fixed parameter. For the case of the highest regional power demand, *regional load case 3*, a capacity of 18 000 kWh is set. For all cases, a power capability of 1500 kW, allowing for some margin and power fade, is set. This means that the maximum possible c-rate for this system is 0.12.

5.3 Results From the Operation Model

In the following part, the results from the operation model is presented, analyzed and discussed. In contrast to the sizing model, the operation model is used for the whole period that requires battery operation, being four years. The nominal BESS power and capacity is set based on the outputs of the sizing model, and the degradation of the battery capacity is included. So are also the operation and maintenance (O&M) costs and costs of transformer losses for substation T3. It is for the operation model that the economical aspects, with potential costs savings, are investigated.

Table 18 summarizes the total net present costs (NPCs) obtained for the different scenarios of the operation model. It includes the investment cost of the BESS, as well as the discounted operating costs for the four subsequent years of operation. For most of the cases, a BESS with capacity of 12 500 kWh is required, giving an investment cost of about 54.08 Million NOK. Per unit of capacity, this is 4 326 NOK/kWh. For BESS OPR 2.2 and BESS OPR 4.2, larger battery capacities are required, with investment costs assumed to be 4 150 and 4 200 NOK/kWh, respectively.

Table 18: A summary of the NPC of investment and operation of the BESS, for different scenarios.

Operation case	Nominal capacity of the BESS [kWh]	Investment costs[1] [Million NOK]	NPC of operation costs, after 4 years [Million NOK]	Total NPC, after 4 years[2] [Million NOK]
BESS OPR 0	12 500	54.08	28.72	87.65
BESS OPR 1.1	12 500	54.08	28.19	87.11
BESS OPR 1.2	12 500	54.08	28.22	87.15
BESS OPR 2.1	12 500	54.08	28.23	87.16
BESS OPR 2.2	18 000	74.70	27.97	109.4
BESS OPR 3.1	12 500	54.08	10.70	69.63
BESS OPR 3.2	12 500	54.08	116.3	175.3
BESS OPR 3.3	12 500	54.08	29.61	88.53
BESS OPR 4.1	12 500	54.08	28.16	87.09
BESS OPR 4.2	16 000	67.20	28.13	101.4
BESS OPR 4.3	12 500	54.08	28.10	87.03

(1) Total investment costs, including materials and installation. Excluding taxes.
(2) Net present value of investment costs and operating costs, discounted for four years. Taxes included.

The calculation of the NPC of operation case 1.1 (BESS OPR 1.1) is further shown in table 19, representing a breakdown of the cost items. The investment is assumed to be a cost at year zero, and the operating costs of the subsequent years are discounted and summed. Lastly, the residual value of the system after end of operation is subtracted, giving the total NPC. This value includes a value added tax (VAT) of 25 %.

Table 19: Breakdown of the NPC calculation for BESS OPR 1.1.

Year (y)	Disc. factor $\alpha_r(y)$	Energy costs, [2022-NOK]	Power costs, [2022-NOK]	T3 costs of losses [2022-NOK]	Discounted costs (Present value) [NOK]	NPC of operation [NOK]
0	1.0	*Investment, excl. VAT [NOK]*				*54 075 000*
1	0.9615	6 819 100	794 900	61 700	7 452 700	7 450 600
2	0.9246	6 826 400	799 400	62 700	7 177 800	14 630 400
3	0.8890	6 832 100	800 700	63 700	6 908 800	21 539 200
4	0.8548	6 834 500	801 900	64 700	6 647 000	28 186 100
		Residual value, excl. VAT [NOK]				*-6 933 500*
		Total NPC, incl. VAT [NOK]				87 112 900

5.3.1 Variations in Electricity Prices

From investigating the effect of different electricity prices, the results show significant variations. This is understood from looking at the net present costs of operation in table 20. This table includes some key findings for operation with four different electricity prices and one case with higher power tariff (BESS OPR 3.3). Compared to the base cases, based on the same energy cost scenarios, the inclusion of a BESS is found to both increase and reduce the total energy costs after four years. For a flat price, in the case of BESS OPR 0, the BESS solution gives a net present operating cost that is 435 100 NOK, or 1.54 %, higher than that of the hypothetical case of only grid power. For the elspot price of 2020, generally characterized by low prices of very little daily variation, the case of a BESS is found to be 3.64 % more expensive. The higher costs are due to the O&M and costs of losses.

Table 20: Comparison of NPC of operating costs, for different elspot prices.

Case	Elspot	SoH after 4 years [%]	Total amount of equivalent cycles, N_{eq} [#]	NPC of opr. costs, after 4 years [NOK]	Difference from base case of corresp. elspot [NOK]	[%]
BESS OPR 0	NO3, 2021 (fixed avrg.)	79.40	19.78	28 721 900	435 100	1.54
BESS OPR 1.1	NO3, 2021 (med. cost)	79.34	263.2	28 186 100	- 67 400	- 0.239
BESS OPR 3.1	NO3, 2020 (low cost)	79.40	59.8	10 700 400	376 100	3.64
BESS OPR 3.2	NO5, 2022 (high cost)	79.22	606.9	116 332 200	- 2 874 500	- 2.41
BESS OPR 3.3	(1.5x power cost)	79.37	188.2	29 606 000	- 77 600	- 0.263

However, for the case of higher elspot prices with significant, daily, variations, the BESS is found to generate savings in the energy costs, compared to the base cases. This applies to BESS OPR 1.1 and 3.2, which is based on the elspot prices of 2021 (NO3) and 2022 (NO5), respectively. In the case of an increased power tariff, some extra savings are also observed. The differences in net present costs of operation are found to be between 0.239 and 2.41 %, compared to the base cases of corresponding elspot and power pricing. The electricity spot price of 2021 is assumed to be more realistic for future scenarios than those of 2020 and 2022, because of the effects from geopolitical situations (as stated in section 3.2).

Other observations from this table are the amount of equivalent cycles that the battery goes through during the phase of operation. For the cases of low elspot prices, with small variations, the battery is utilized very little as it ends up with a total number of equivalent cycles being between 20 and 60. For the other scenarios, the battery is used more, with the resulting number of 188 to 607 equivalent cycles. Nevertheless, the battery degradation is almost the same for all of these cases, which indicate that the battery usage in these scenarios have little impact on the aging.

The net present costs of operation for the cases with varying elspot are also illustrated in figure 37, for comparison. This also includes the first year operation costs, that are not discounted, which are further split into cost elements in figure 38. The latter illustrate that the energy costs, mostly being the electricity spot prices, constitute the largest cost item, followed by the power cost of the grid tariff. The operation and maintenance costs are assumed fixed, constituting 75 000 NOK/year, and the transformer loss costs are between 60 000 - 70 000 NOK for all cases.
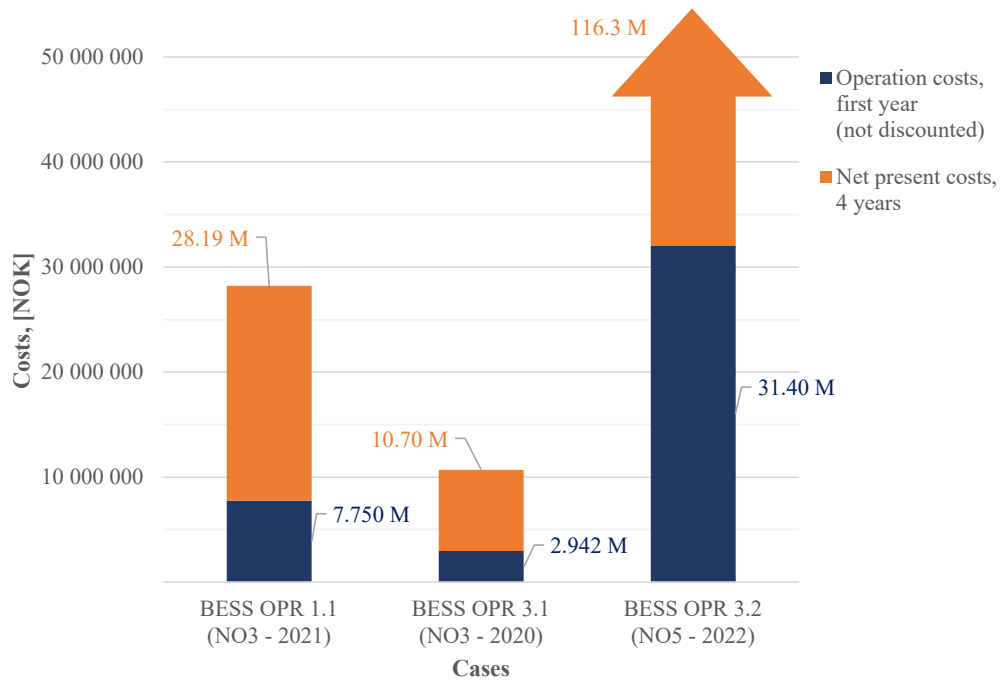
Figure 37: NPC of operation for the operation cases with different elspot.

(a) BESS OPR 1.1.

(b) BESS OPR 3.1.

(c) BESS OPR 3.2.
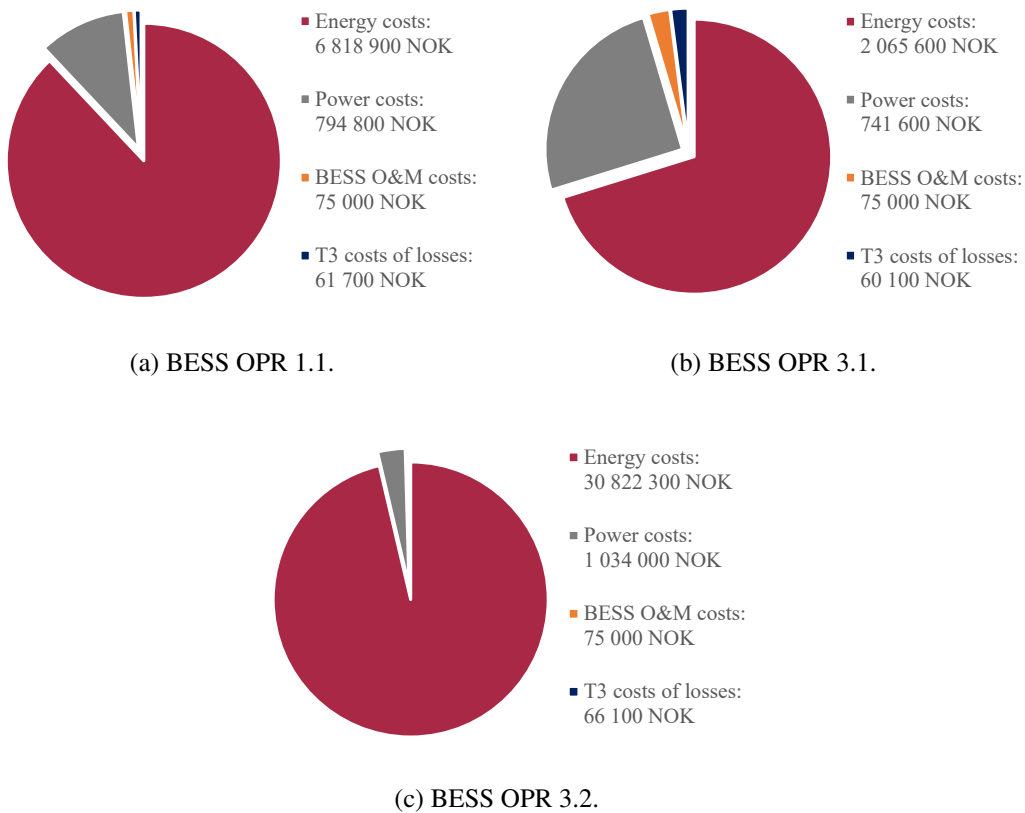
Figure 38: Cost compositions of first year operating costs, for the scenarios of different elspot prices.

Even though the power costs have a relatively small contribution to the total operating costs, it is interesting to observe how the BESS implementation affect the peak of the power imported from the grid. The power peaks of every month during the period of operation are shown in figure 39a, 39b and 39c, for BESS OPR 1.1, 3.2 and 3.3, respectively. Firstly, it can be noted that the power peaks are generally higher here than for the base cases, shown in figure 29. In addition, the power peaks increase slightly from year to year, which is probably due to the degradation of the battery causing the need for more rapid charging and discharging. But for the last scenario, the peaks are significantly lower than the others, meaning that the higher costs of power reduce the benefits from energy arbitrage. This observation is further supported by the battery usage. Having only 188 full equivalent cycles after four years, the battery is used less than for the case of a normal grid tariff.
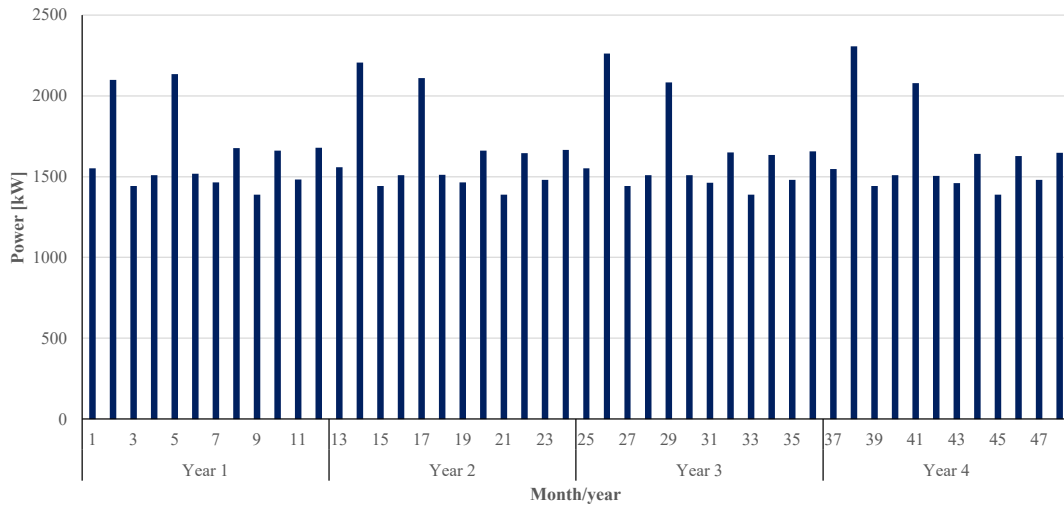
(a) BESS OPR 1.1.
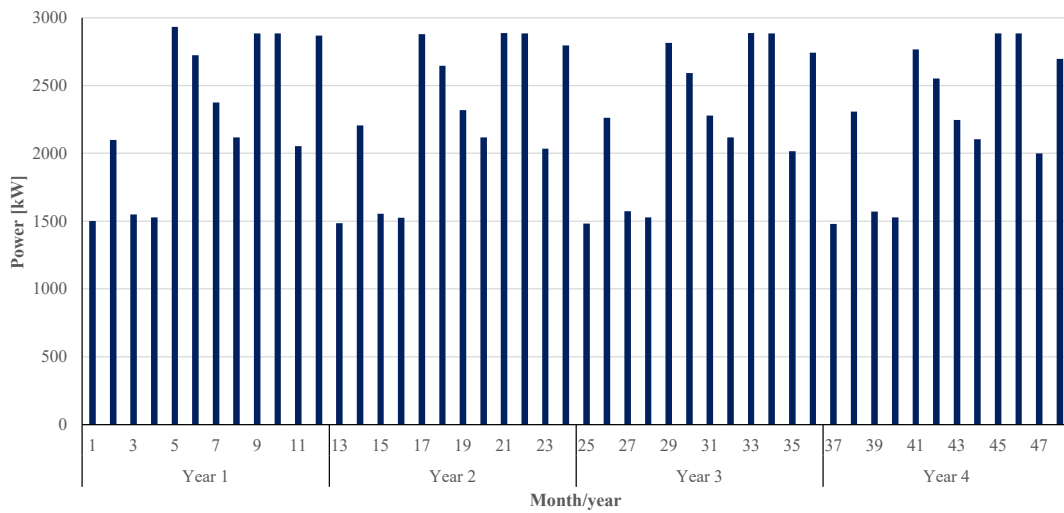
(b) BESS OPR 3.2.
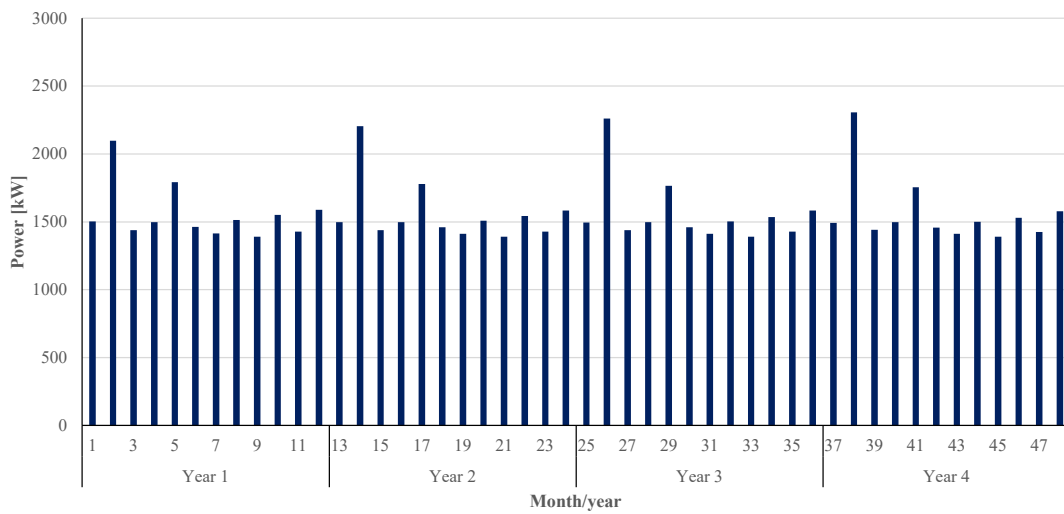
(c) BESS OPR 3.3.

Figure 39: Monthly peaks of imported grid power, for variations in electricity prices.

For BESS OPR 1.1, the highest peaks are observed for February, being the month in which battery use is required. This is followed by May, being the first month of lower grid tariff which also has significant variations in the elspot price. For BESS OPR 3.2, with the highest and the most variable elspot prices, the power peaks are much higher. This indicates that it is more beneficial to import power at a high rate, to use it for energy arbitrage, than to reduce costs of power peaks. The motivation for high power costs as a price signal from the DSO to reduce the loading on the distribution grid, is therefore not successful for this scenario.

The operation model is constructed such that the BESS is used to cover the load, given the restrictions in available power, but also to reduce the operating costs through price arbitrage and load shifting. Figure 40 illustrates the working of the BESS operation, for one week in February, where the charging and discharging of the BESS is influenced by signals on elspot prices and available power[36].
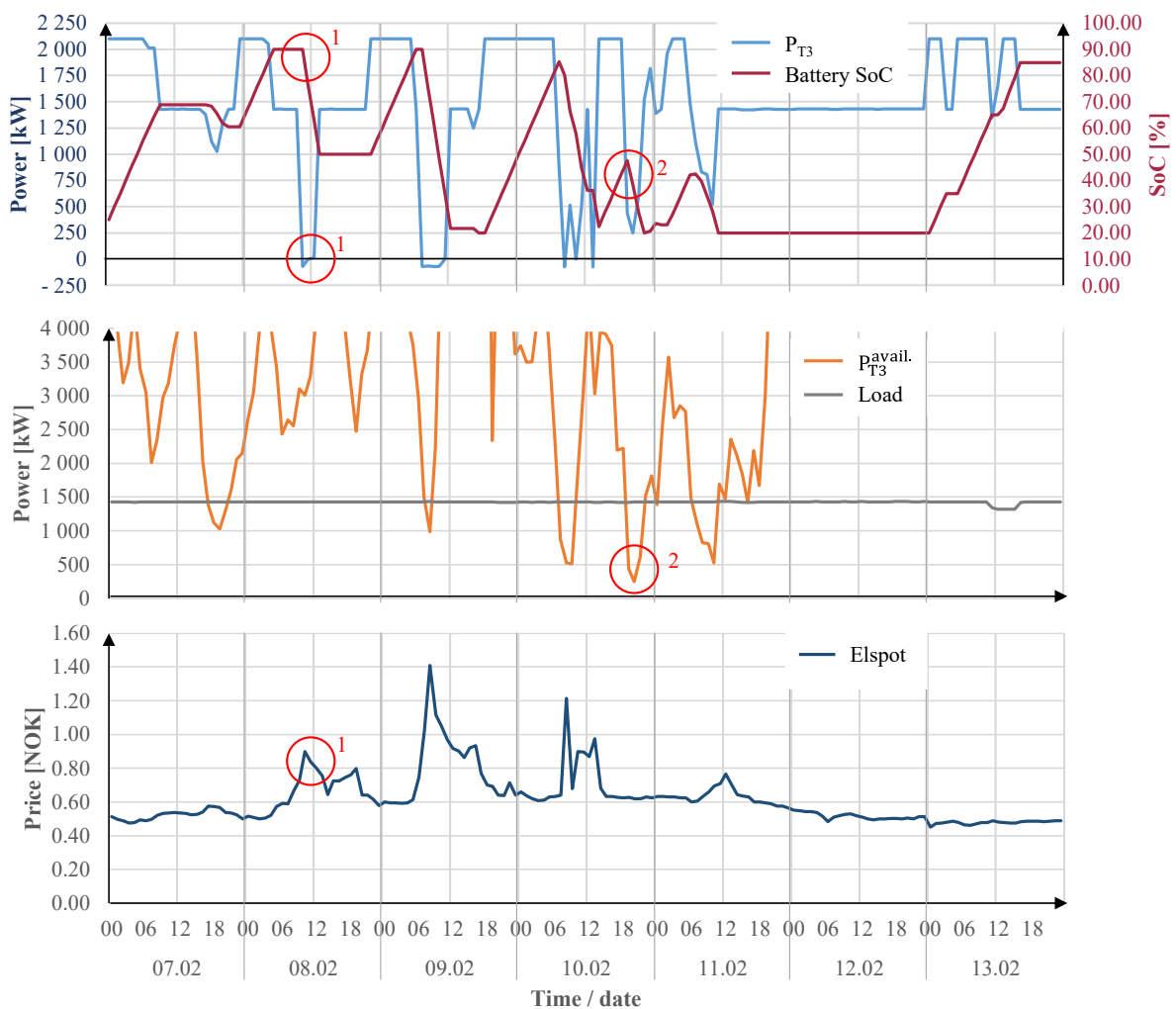
Figure 40: Plots of grid power, batter level (SoC), available power, load and elspot, for a week in February. (BESS OPR 1.1).

---

[36]The cost of power (grid tariff), is also a price signal but is not included in the illustration as it is not affected by the operation during the week of focus.

Two points in time are marked by red circles in the plots. For point 1, a peak in the elspot causes the battery to discharge in order to cover the power demand at a lower cost. In this case, a small amount of surplus power is also exported to the power grid which generates a small revenue. At point 2, the battery is discharged to cover the load as the available power from the grid is less than the power required by the load. At this time, and for the subsequent day, there are no economical motivations for using the battery as the variations in elspot prices are very small. Therefore, the battery SoC remains he same, at minimum, for this period.

As mentioned, some power is exported and sold to the grid (at spot price), in cases where the discharged power is higher than the one required by the load. More power is exported in the operation model compared to the sizing model, as the power rating is increased from the optimal value of 1330 kW to 1500 kW, to include some margin. However, energy arbitrage for self usage is prioritized. This can be concluded as there are only 23 hours with maximum export (at 100 kW) and 127 hours of any power export, during the first year of operation for BESS OPR 1.1. For the case of high elspot prices, BESS OPR 3.2, there are more hours of export (283 hours of 100 kW and 537 hours in total), but self usage is still most important. Furthermore, it is also observed that less power is exported during the fourth year than during the first year, which is probably because the degradation of the battery reduces the amount of energy that is available for export.

5.3.2 Different Scenarios for the Regional Demand

The operating costs are very similar for the different cases of regional power demand. This is illustrated in figure 41. Compared to the base cases with corresponding electricity price, being the elspot of NO3 from 2021, all of the scenarios generate some cost savings. These, in addition to the states of health (SoH) and amount of equivalent cycles, are summarized in table 21. It can be noted that the savings are the smallest for BESS OPR 2.1, representing the scenario with moderate increase of the regional loads. The savings are actually the highest for the case of the largest increase in regional loads, BESS OPR 2.2. However, this can be explained because a larger BESS (18 000 kWh) is required, which also allows for energy arbitrage with larger volumes, but at the expense of higher investment costs.
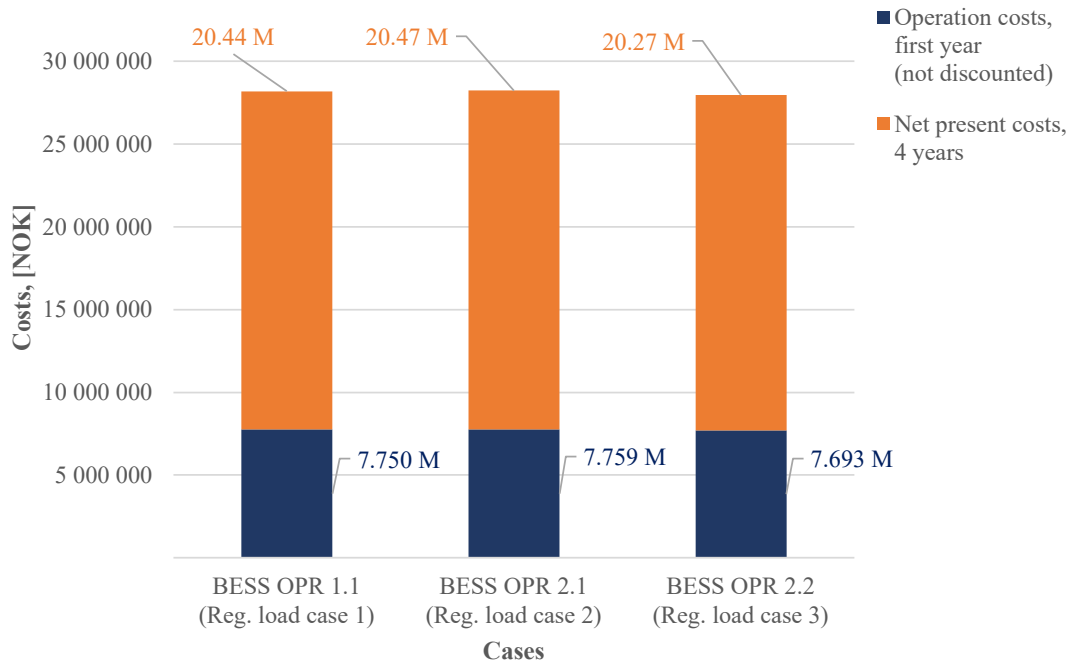
Figure 41: NPC of operating costs for the scenarios with different regional load.

Table 21: Comparison of NPC of operating costs, for different regional load.

Case	Elspot	SoH after 4 years [%]	Total amount of equivalent cycles, N_{eq} [#]	NPC of opr. costs, after 4 years [NOK]	Difference from base case of corresp. elspot	
					[NOK]	[%]
BESS OPR 1.1	NO3, 2021	79.34	263.2	28 186 100	- 67 400	- 0.239
BESS OPR 2.1	NO3, 2021	79.34	264.1	28 230 700	- 22 800	- 0.081
BESS OPR 2.2	NO3, 2021	79.36	216.5	27 968 400	- 285 100	- 1.01

The peaks of power imported from the grid are similar for regional load case 1 and 2 (figure 39a), but are very different for regional load case 3. The latter is presented in figure 42, with the notable high peaks for the months of May. As for several of the above-mentioned scenarios, this can likely be explained by the combination of varying spot prices and lower power prices for this period. The power peaks are in general lower for the other months, because of less available power from the grid.
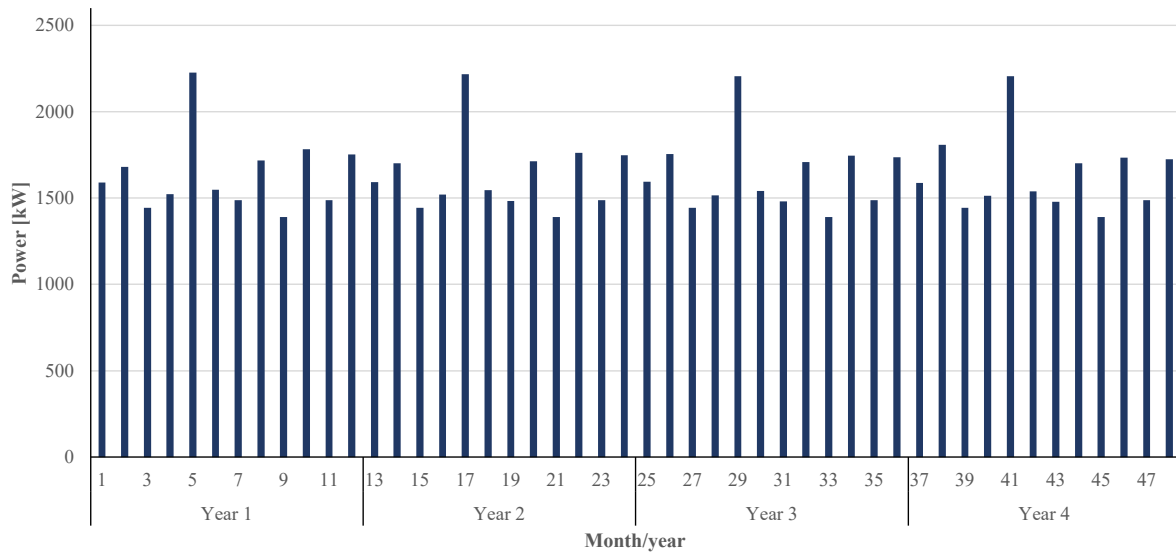
Figure 42: Monthly peaks of imported grid power, for high regional load: BESS OPR 2.2.

Load Shedding

Recalling that the BESS is only really required for some periods in February, for regional load case 1, it is interesting to consider the consumption during this month specifically. BESS OPR 2.3 involves an adaptation of the load, where it is reduced during the periods of limited available grid power, according to the descriptions given in the introduction of section 4.4. The idea is that it could be advantageous to invest in a smaller BESS and rather reduce the loads of some periods.

From the sizing model it was found that a battery capacity of 53 kWh, without considering degradation, could be sufficient. A small battery of this size can also be used for some energy arbitrage, and to reduce the peaks of imported power. However, when including maintenance costs and costs of transformer losses, a small battery system is found to generate higher operating cost than that of the corresponding base case.

Table 22 shows the resulting differences between the operating costs for the scenarios with load shedding, and the operating costs of base case 1. Both are based on the same electricity spot price (NO3, 2021). The cost variations are investigated for different standard combinations of power and capacity, being 1, 2, 4 and 6 hour batteries. All of the combinations result in higher operating costs when including a BESS, except from the 6h battery of 1000 kW. The latter gives a operation cost that is close to a break even. This means that, for the case of this thesis, a relatively large battery is required to give savings in energy costs, even with load shedding. The high operating costs are results of maintenance costs and costs of transformer losses, the latter not being included in the objective function.

Table 22: Different BESS sizes for BESS OPR 2.3, with corresponding reduced/increased operation costs.

BESS size/ configuration	Difference from base case 1, (NO3 2021 elspot), 1. year operating costs.
500 kW / 500 kWh	44 370 NOK
500 kW / 1000 kWh	36 000 NOK
500 kW / 2000 kWh	22 500 NOK
500 kW / 3000 kWh	11 800 NOK
1000 kW / 4000 kWh	19 700 NOK
1000 kW / 6000 kWh	-577 NOK

5.3.3 The Impact of Degradation

The degradation is an important part of the operation model, as the available capacity fades with time and use. Figure 43 shows the resulting degradation of the battery capacity, for the main case of this thesis with variations in temperatures. It is evident that the calendric degradation is the main reason for the capacity fade, which is also highly dependent on temperature. For instance, when the battery is operated at a temperature of 5 °C, the SoH ends up at 85 % after four years, compared to about 79.4 % and 60 % for temperatures of 15 and 35 °C, respectively. The cyclic aging mechanisms are found to have almost no effect on the total degradation.
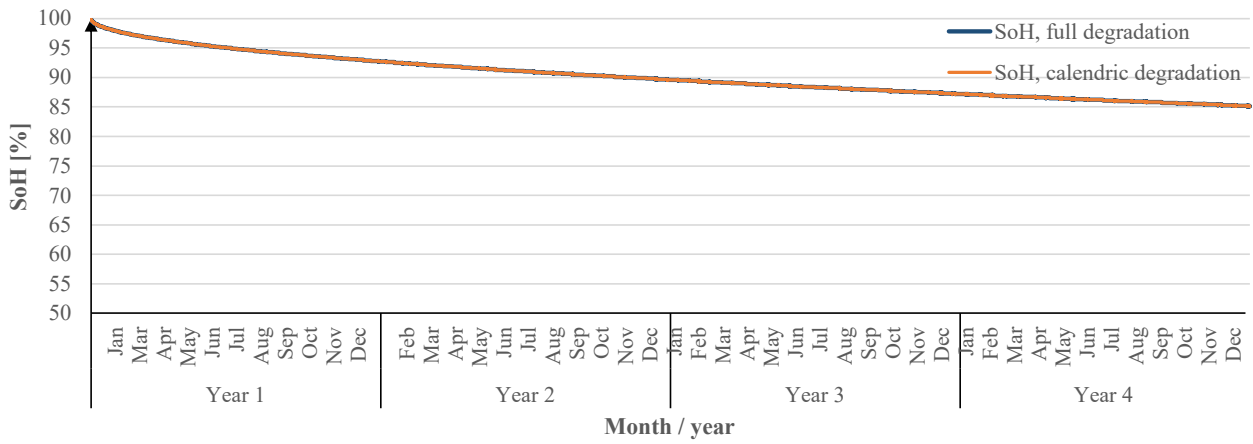
(a) Temperature: 5 °C: BESS OPR 4.1.
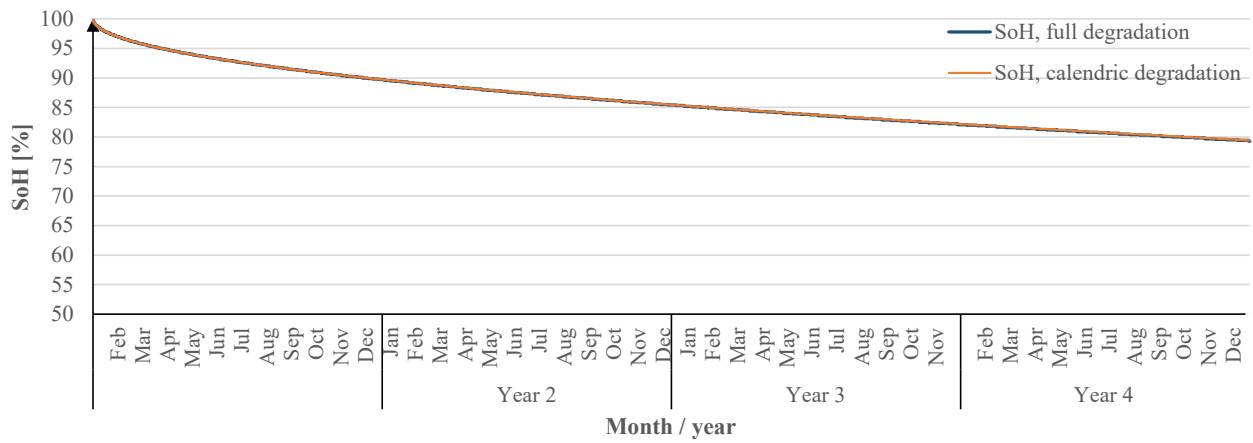
(b) Temperature: 15 °C: BESS OPR 1.1.
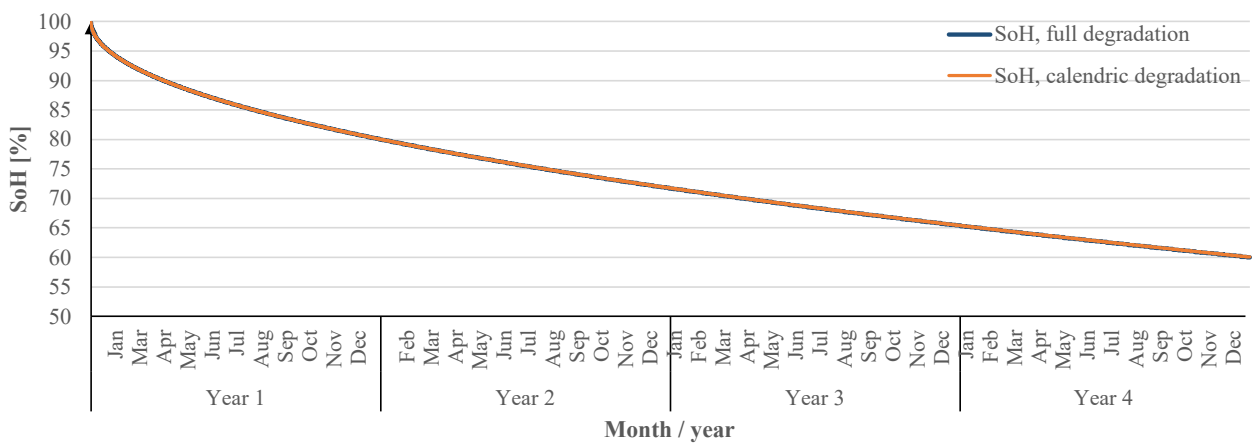
(c) Temperature: 35 °C: BESS OPR 4.2.

Figure 43: Degradation of the battery for the period of operation, for different temperatures.

Table 23 summarizes the key findings for the operation cases based on different assumptions on degradation. Firstly, BESS OPR 1.1 and BESS OPR 1.2 include the exact same conditions of operation, but the latter includes the degradation cost in the objective function (C_{deg}^{tot}). The results show that the battery is used less for BESS OPR 1.2, with a total number of equivalent cycles of 134 compared to 263 without the degradation cost. However, this only reduces the degradation with 0.04 %. In addition, it reduces the potential savings significantly. Therefore, it is found that the use of a degradation cost in the objective function have a counterproductive effect on the BESS operation, for the case of this thesis.

Table 23: Comparison of the different operation scenarios with degradation.

Case	Elspot	SoH after 4 years [%]	Total amount of equivalent cycles, N_{eq} [#]	NPC of opr. costs, after 4 years [NOK]	Difference from base case of corresp. elspot	
					[NOK]	[%]
BESS OPR 1.1	NO3, 2021	79.34	263.2	28 186 100	- 67 400	- 0.239
BESS OPR 1.2	NO3, 2021	79.38	134.3	28 219 600	- 33 900	- 0.12
BESS OPR 4.1	NO3, 2021	85.12	268.2	28 161 800	- 91 700	- 0.325
BESS OPR 4.2	NO3, 2021	59.99	213.1	28 130 600	- 123 000	- 0.435
BESS OPR 4.3	NO3, 2021	100	285.9	28 103 800	- 149 700	- 0.53

It can be observed that the operation at low temperature, resulting in the minimum degradation, gives larger savings in operating costs compared to the main scenario. This is also the case when having no degradation, which generates the highest savings, as energy arbitrage is possible for larger volumes of energy. Considering the case with the most degradation, BESS OPR 4.2, high savings are observed because this case includes a larger BESS capacity (16 000 kWh). This size is required in order for the BESS to be able to cover the load even at the fourth year of operation. However, this comes with a higher investment costs.

Due to relatively small variations in potential savings, it is found that the degradation is not so important with respect to the operation costs. However, the different degradation assumptions significantly affects the investment costs of the BESS. This is, as stated in section 5.2.5, because the degradation must be accounted for when sizing the system. In the above-mentioned scenarios, only BESS OPR 4.2 involves an adapted BESS size in order to be technically feasible. However, the battery capacity for the scenario of the lowest degradation, BESS OPR 4.1, could be adapted similarly. The required capacity of this case, given the constraints of the operation model and some margin, would be 11 000 kWh (allowing for 20 % degradation and some margin). This capacity reduction represents savings of 3.75 Million NOK in investment costs. Although this is a lot, the reduced volume that is available for energy arbitrage and the costs associated with temperature management must also be evaluated, as this will affect the total costs.

5.4 Notes on Assumptions and General Remarks

In the following parts, some general remarks that cover several of the above-mentioned observations are commented on and discussed.

5.4.1 BESS Investment Costs

The investment costs of the BESS are probably the most uncertain assumptions for all of the cases. The costs are divided in power and capacity cost elements in order to be able to choose the optimal configuration. Being based on figures obtained from various literature on different BESS projects and estimates on future costs development, there are several elements of uncertainty. For instance, the contents covered by a certain number are not always well-defined in the literature. Furthermore the cost data depend on factors such as scale (size), location, battery chemistry, country of installation and currency, that need to be accounted for and converted to fit the case of this thesis. However, by considering average values that fit the requirements of this case, it is assumed that the obtained investment costs of 2 500 NOK/kWh and 3 200 NOK/kW are possible and realistic, but perhaps somewhat optimistic.

5.4.2 General Assumptions for the Cases

Load Distribution

The scenarios investigated, for both the sizing model and the operation model, include other assumptions in addition to the investment costs. First, the sizing model include some assumptions for the grid side of the model. The most important one is maybe the load distribution, defined in table 7. Even though the location and magnitudes of these loads are presumed to be realistic, unknown loads may give a different picture and affect the power flows. In addition, no other loads are assumed connected to T3 or on the line between point B and $T3$ (see figure 26). If large loads are connected here, the power that is available for the BESS to charge can be affected, because of possible saturation of the power lines and high voltage drops. However, as the maximum currents that are registered are far below the current carrying capacities of the lines, it is assumed that the increased power of the end user, including a BESS, will be achievable even with other loads connected to $T3$ or *line B*.

Available Power

For the sizing case, a limit of 23.9 MW is set for the regional transformer, T2, for all year. This may not be the case, as for instance temperature and reactive power requirements may limit the possible

power throughput. Considering the capacities of the power lines, on the other hand, these should include large margins as described in table 8. The limit on available power also assumes that the regional grid (transmission grid), at 66 kV, will be capable of providing up to 23.9 MW at all time.

Input Data (Time Series)

The input time series, such as data on power generation, transformer power, load and elspot prices, are repeated for all years for both the base cases and the operation model. The volumes of energy, the usage patterns (load and production profiles) and the characteristics of price variations are assumed to be realistic for the future, with a horizon of four years. However, the actual conditions will for sure be somewhat dissimilar, and may result in different operation of the battery system with correspondingly different costs. This is especially likely for the case of elspot variations. Based on the differences in electricity prices from 2020 to 2022 for NO3 and NO5 (figure 24), it is possible and probable with significant variations during a period of four years. Additionally, the power tariff is set to be equal for all years of interest, while it for instance could increase. Nevertheless, the contribution from variations in electricity spot prices are assumed to be of higher importance than the grid tariff for the case of this thesis.

Degradation Model

The degradation model that is used for this thesis is based on the Wang Model, described in section 2.3.1. Results from the operation model points out that the calendric degradation contribute the most, by far, to the capacity reduction of the BESS during four years. The model is accepted as appropriate and realistic for the battery type of this thesis, but could also be somewhat pessimistic. The latter point of reflection can for instance be seen in relation with other works that involve battery degradation, such as [20]. For that case, the degradation of a NMC battery was found to be around 7.5 % after one year of operation, compared to approximately 10 % for the main case of this thesis. The degradation model of the cited work is bases on DoD and not the c-rate, which is used to measure cyclic degradation in this thesis. By including the effect of different depths of discharge, the degradation could look differently. Anyways, the LMO-NMC blend is known for having poor calendric life time, that is highly dependent on temperature, compared to other types of Li-ion.

Time Resolution

All input data and variables are based on an hourly time resolution. This means that for instance short-term power peaks, and other fast variations that can affect the battery usage, are not included. In [22], it was found that input data and solving in minute resolution could affect the operation, and especially degradation, significantly. However, knowing that calendric degradation is the main driver for capacity fading in this thesis, the smaller time resolution would probably not affect the outcomes that much.

5.4.3 Considerations for Installation

In the models of this thesis, the battery is presumed installed behind-the-meter, on the low voltage side of substation T3 (22/0.415 kV). This is mainly done for simplicity, regarding the regulations for ownership of energy storage systems, and in order to include the costs of transformer losses. However, this is not necessarily the most feasible solution, both technically and economically. Localizing the BESS on the HV side, or having separate transformer systems for the BESS and the load side could be an alternative.

5.4.4 EOL and Environmental Considerations

The battery energy storage system is only set to operate for four years in the cases of this thesis. For most of the scenarios, the BESS ends up with a SoH of around 80 % after this time. This means that it cannot longer cover the load after this point in time when considering the constraints of the model. Although it can still be used for energy arbitrage and load shifting for several more years, this is not investigated. But a residual value of 15.0 %, which is also discounted, is set in order to put a value on the battery investment after the end of the operation phase. Considering the possible scale of savings and the SoH at this point, the residual value is assumed to be in the correct order of magnitude. If the battery is to be disassembled, the recycling process should be reviewed for both economical and environmental considerations, but these are out of scope of this thesis.

5.4.5 The Feasibility of BESS As a Solution

If the requirements of load and available grid power remain as assumed for the main cases of this thesis, a very large BESS (12 500 kWh / 1 500 kW) would be required. This would be larger than any other battery installation in Norway at the time of writing, and does also involve a power / energy ratio (P/E-ratio) that is highly uncommon for battery storage systems.

Considering the space requirements for such an installation, referring to table 6, six 20 ft. containers or three 40 ft. containers would probably be required. The components only would therefore need an area of at least 100 m^2. As the most important property of a battery in this case is capacity, the use of second life batteries that still have enough capacity left could be interesting. As these batteries would already have been degraded, for instance by 20 %, more such batteries would be needed which would require more space. But, considering the location of the end user, the space in this order of magnitude is probably available.

The operating costs of the different BESS scenarios, including energy costs, power costs, maintenance costs and transformer loss costs, are in general lower than those of the corresponding, hypothetical,

cases of only grid power and no BESS. However, these are far from being able to cover the initial investment costs. For instance, the scenario entailing the largest savings have a net present cost of operation that is about 2.87 Million NOK less than the corresponding base case, after four years. This applies to BESS OPR 3.2, which is based on the expensive and highly varying elspot prices of NO5 in 2022. With these savings, the BESS investment will never be accounted for within its life time (less than 20 years).

Therefore, the economical feasibility of the BESS is rather a question on the investment costs, and what revenues (e.g. from increased production and sales) that can be expected for the increased energy consumption that the battery system will allow for. Recalling that the BESS is only really required for some periods in February, for the main case, an alternative solution can involve load shedding for these instants. For the rest of the year, it is assumed that the power consumption (peaking at 1.5 MW) can be covered by the grid directly. In other words, the value of high power consumption during the periods of limited grid power must be weighted against the investment costs of the BESS.

At the end of the operation period, being four years, it is assumed that grid reinforcements are in place such that the power can be drawn directly from the power grid. At this point, the transformer T2 would be the limiting element if having the same power rating as used in the scenarios of this thesis. It could be possible to postpone the investment of a new regional transformer, and still be using the BESS. However, the battery degradation would have to be considered, and more battery packs would likely be required. The investment of a new transformer is assumed to cost up to 7 Million NOK, for power ratings up to 50 MVA (see appendix E, [54]), which is substantially less than the investment costs for the required BESS system. In order for a BESS to be financially attractive in this case, the investment cost should be below 800 NOK/kWh[37].

One of the reasons why the battery energy storage systems are not able to provide for more savings is due to the flat load profile of the end user. The load profile, per month of 2021, is presented in appendix F. The BESS operation is mainly limiting the operation costs by performing load shifting and energy arbitrage with the elspot as a price signal. In a case with loads of higher power peaks, the battery could help reducing the costs of the grid tariff, but this is not the issue of the end user in focus of this study. Actually, as observed for most of the operation scenarios, the battery usage actually increases the overall power costs as more power is imported for charging the battery compared to the base cases.

The feasibility of the BESS could probably be improved if it was also used for providing grid services, such as frequency regulation and voltage support. The latter is made possible to investigate in the sizing model, but without any economical benefits. The model also show that, for the investigated load situations, voltage support may not be needed. One approach for such cases is to include the

---

[37]Assuming a NPV of total savings being minimum 3.0 MNOK.

battery system in the balancing market. But if this is to be an extra field of application, in addition to covering the load, a larger battery with greater power capability would be required. Although it is possible to check for other grid services, this would require a time resolution of minutes and seconds, which was not possible for this study. Furthermore, the localization and sizing of the battery storage systems would be different for the above-mentioned purposes.

Feasibility of Other Battery Solutions

The cases of this thesis is based on Li-ion batteries with the LMO-NMC chemistry. Although this battery type have versatile characteristics, it is known to have poor calendric life time, which entails the investment of more battery packs (capacity). Therefore, it could be beneficial to investigate other battery types, such as other Li-ion chemistries and lead-acid, and evaluate factors such as investment costs, field of applications and degradation. Given the area of use for the case of this thesis, being mainly load shifting and capacity reserves, most types of batteries can be evaluated (as shown in figure 10).

For the required power and energy ratio that was found to be optimal (and minimum), the Vanadium redox flow (VRFB) type is an especially interesting alternative. With a long life time, almost no degradation, nearly 100 % useful capacity and the possibility of large capacity compared to power capability, the flow battery has many characteristics that can be suitable for the case of this thesis. Assuming no degradation, 90 % useful capacity and some margin, the required capacity of a flow battery for the main cases of this thesis would be around 7 000 kWh[38]. This is 5 500 kWh less than for the Li-ion battery, which can represent a significant reduction in the investment costs.

The footprint of a Vanadium redox flow battery is however much larger than that of a Li-ion battery. Assuming 7.5 MWh capacity, and the footprint data from table 6, an area of 550 to 600 m^2 could be required. This is significantly more than for the Li-ion BESS. In addition, weight and volume would require higher costs and more analysis of the physical foundation.

BESS Combined with Local Energy Production

Another factor that could increase the feasibility of the BESS system, or be an alternative solution to the problem case, is the implementation of local energy production from for instance wind power or solar power. As the BESS strictly speaking is only required for some periods during winter time, when there is little solar energy to exploit, wind power would probably be the one fitting best. However, a PV installation would be useful during summer time as the load is assumed to be high all year. Combined with a BESS, a PV solution can prove to be feasible. As the topic is out of scope of this thesis, a short summary of such a solution is only provided in appendix G.

---

[38]Calculation, assuming 70 % available capacity for Li-ion ($SoC_{max} - SOC_{min} = 0.7$): $8603 \cdot \frac{0.7_{Li-ion}}{0.9_{VRFB}} \approx 6691 kWh$

Lastly, it must be noted that the scenarios of this thesis are solved to find optimal conditions when knowing all data in advance of solving. This include the electricity spot prices, power demand both for the end user and the region, and local power generation during the whole year. A BESS operated in the real world would not have access to such data, but would have to rely on estimates and forecast on future conditions. Therefore, the exact same optimal operation found in the scenarios presented here are not possible to achieve. However, good control and forecast systems could still generate approximately the same savings in energy costs.

6   Conclusions

The problem case of this thesis has been to investigate the feasibility of a BESS as a solution for capacity expansion, for a location in Fosen (Trøndelag) where the transmission grid faces limitations today. The study concentrates on one single end user (grid customer) that is connected to the distribution grid of Fosen. In the main case, the end user is assumed to increase its load from having a peak of 200 kW to having a peak of 1.5 MW. The load profile, based on data from 2021, is assumed to be the same for all scenarios of this thesis. The power consumption is high and steady (flat) during the whole year.

In order to give an answer to the research question of this problem, optimization models for sizing and operation of a BESS are made. These include constraints that define the situations of loads and available grid power. The objectives are to minimize operating costs, including the costs of energy, power, maintenance and energy losses. Furthermore, the cases are based on a system consisting of Li-ion battery packs, having the chemistry of the LMO-NMC blend. This is known to be a relatively cheap and versatile type of Li-ion batteries, and a degradation model has also been possible to include for this type of chemistry.

Several scenarios have been investigated with the optimization models. The most significant results are found for variations in the electricity spot prices. For a period of four years, the net present costs of operation with BESS are found to be 2.41 % lower to 3.64 % higher than the hypothetical scenarios of only grid power (with corresponding elspot prices). The worst case is found for the electricity prices of NO3 from 2020, being low and with little variation, while the best case is found for the elspot of NO5 from 2022, characterized by prices that are high and particularly varying. It is observed that variations in the elspot prices are the most important factor for cost savings in this study. This is due to the opportunity of energy arbitrage with the BESS. It is concluded that it is likely that a BESS can give some reductions in the yearly energy costs of the end user of focus in this thesis.

Given the restrictions on available grid power and the fact that the high load of the end user must be met, a large battery system would be required. In order for it to be technically feasible, a nominal capacity of 12 500 kWh and a power capability of 1330 (1500) kW, is set for the Li-ion battery. The sizing is only motivated by the requirement of covering the load during the periods when the grid is not capable of doing so alone. In the main case, based on data from 2021, this only occurs for some periods in February. Furthermore, the sizing is to a large extent affected by degradation. During four years of operation the capacity is found to fade by approximately 20 % (mostly due to calendric aging). This entails the need for more battery packs.

It is concluded that the economical feasibility of the BESS is mostly dependent on the investment costs, as the savings in operation costs are small in comparison. For the above-mentioned BESS

installation, it is assumed an investment cost of more than 54 Million NOK (4 326 NOK/kWh, excluding VAT). In order to be economically feasible, the estimated revenue from increasing the power consumption, must be weighted up against the investment cost of the BESS.

If it would be possible to cut, or reduce, the load of the end user for some periods, a smaller battery installation would be sufficient. However, the operating costs are found to be somewhat higher than for the case of only grid power, which indicate that a smaller battery would not be economically feasible. Due to the load profile of the end user, the only way for the BESS to reduce the energy costs are to conduct energy arbitrage. More savings are generated with this method for systems of higher capacity and power ratings, but with higher investment costs. The reduction of peaks in power imported from the grid is not a possibility for the case of this grid customer.

Other fields of applications could increase the feasibility of the BESS, by generating income for services such as frequency regulation, voltage support, backup power and other grid purposes. However, these scenarios are not investigated, as such technical issues are likely not representing challenges for the region of interest in this study.

To summarize, the economical feasibility of BESS as a solution is totally dependent on the investment costs and the revenue that is expected from an increased power consumption. Nevertheless, due to the type of load profile and probable electricity prices of the future, a BESS is probably not an economically feasible solution for the problem case of this thesis.

7 Further Work

The work of this master's thesis provides an overview of the required sizing, possible costs and probable cost savings that can apply when choosing a BESS as a solution to the case problem. However, there are also other approaches, solutions and considerations that should be evaluated. Some examples on further work are therefore given below.

Updating The Existing Model - With BESS as a Solution

- More certain load data, especially on the distribution of regional loads, can improve the realism of the grid part of the sizing model. Different load situations for the end user could also be investigated, for sensitivity analysis.

- The grid model of the sizing model could also include reactive power flow, to give an even more realistic overview of the grid loading.

- The location of the BESS could be re-evaluated. It is located BTM and on the LV side of substation T3 for the case in this thesis, but it could also be installed FTM, and on the HV side of T3. The latter also allows for investigating other applications for the BESS, such as grid support.

- The sizing model could be updated with more certain BESS investment costs, and account for usage for a longer time horizon than one year, to better incorporate the correlation between investment costs and potential cost savings.

- Both the sizing and operation model could be adapted for other battery, or energy storage, technologies (considering different degradation, operation constraints etc.). This may for instance include lead-acid batteries, redox flow batteries (e.g. VRFB) and hydrogen energy storage.

Investigating Other Possible Solutions

- As mentioned above, it may turn out that the use of a BESS for other applications than demand side management, such as providing grid services, may increase the feasibility of the BESS. Scenarios such as frequency regulation, voltage support and participation in the balancing market can be investigated.

- The implementation of local energy production can likely be a suitable and more feasible solution than having an energy storage system. Additionally, a BESS could be used in symbiosis with local energy generation from renewable energy resources.

Next Steps Toward Realization

If the BESS solution or other approaches are to be carried out, there are several steps to consider.

- It could be relevant to conduct some load flow studies considering the BESS and state of the grid, for instance in a hypothetical max load situation, in order to control that a solution is feasible with a different approach.

- The technical solution, with required material, electrical wiring, control systems and safety measures, must be planned.

- A control system, with a control program, must be designed. The control must include live data on the load, power flow in the region (having communication with transformer T2), the day-ahead prices and some forecast on future load in order to decide whether the system should to charge or discharge.

- If a third party is going to own the battery, in stead of the grid customer, a business model must be developed. One example of a business model, based on rental / leasing, is *Peak Shaper* by Eidsiva [61].

- A plan for EOL management must be made, in order to ease the decommissioning and to ensure for the lowest possible environmental footprint. It must also be evaluated how long the BESS can be used, for energy arbitrage and demand side management, before maintenance costs become higher than the savings.

References

[1] IEA. World total energy supply by source.

[2] Abraham Alem Kebede, Theodoros Kalogiannis, Joeri Van Mierlo, and Maitane Berecibar. A comprehensive review of stationary energy storage devices for large scale renewable energy sources grid integration. *Renewable and Sustainable Energy Reviews*, 159:112213, 2022.

[3] TENSIO Bengt Eidem. Varsel om begrensninger i det regionale strømnettet i ørland kommune. Letter from TENSIO to Ørland municipality, May.

[4] Ingrid E. Haukelig and others (NVE). Langsiktig kraftmarkedsanalyse. Technical Report 202115981, NVE: Norges vassdrags- og energidirektorat, Middelthunsgate 29, Oslo, October 2021.

[5] Camilla Aabakken and others (NVE). Veileder til leveringskvalitetsforskriften. Technical Report 7-2018, NVE: Norges vassdrags- og energidirektorat, Middelthunsgate 29, Oslo, December 2018.

[6] Kjersti Berg. Bruk av batterier i strømnettet. 2019.

[7] Peter Ahcin, Kjersti Berg, Idar Petersen, and Pedro Crespo del Granado. Når er batterier lønnsomme? Technical Report 502001599, SINTEF, Postboks 4761 Torgarden 7465 Trondheim, August 2019.

[8] Ingvild Birkeland, Ingvild Fløtre, Linn-Anita Bergland, and Oda Skeie. Batterier i distribusjonsnettet sommerprosjekt 2020. Technical Report 202011402, NVE: Norges vassdrags- og energidirektorat, Middelthunsgate 29, Oslo, August 2020.

[9] IRENA. Utility-scale batteries innovation landscape brief. Technical Report ISBN 978-92-9260-139-3, IRENA, IRENA - International Renewable Energy Agency, September 2019.

[10] ABB. Introduction to energy storage solutions: Elds, packaging and solutions, 2021. Accessed: 2022-10-24.

[11] EU. Directive (eu) 2019/944 of the european parliament and of the council of 5 june 2019 on common rules for the internal market for electricity and amending directive 2012/27/eu (recast). `https://eur-lex.europa.eu/legal-content/EN/ALL/?uri=celex:32019L0944`, 2019. Accessed: 2022-01-05.

[12] Gaurav Gaur, Nishtha Mehta, Rintu Khanna, and Sandeep Kaur. Demand side management in a smart grid environment. In *2017 IEEE International Conference on Smart Grid and Smart Cities (ICSGSC)*, pages 227–231, 2017.

References

[13] Kjell Sand, Kjersti Berg, Andreas Hammer, and Karoline Ingebrigtsen. Veileder for kost/nytteâvurderinger ved integrasjon av batteri i distribusjonsnettet. Technical Report 502001599, SINTEF, Postboks 4761 Torgarden 7465 Trondheim, November 2020.

[14] Tore Langset and Hege Holte (NVE) Nielsen. National report 2021. Technical Report 202116067, NVE, The Norwegian Energy Regulatory Authority, October 2022.

[15] Max Schoenfisch and others (IEA). Grid-scale storage. `https://new.abb.com/medium-voltage/packaging-and-solutions/energy-storage-solutions`, 2022. Accessed: 2022-10-30.

[16] BloombergNEF. Battery pack prices cited below $100/kwh for the first time in 2020, while market average sits at $137/kwh.

[17] Andy Colthorpe and BloombergNEF. Bloombergnef: Average battery pack prices to drop below usd100/kwh by 2024 despite near-term spikes. internet, December.

[18] Nettselskapet AS. Data on grid, power flow and electricity consumption. Data provided for the case by e-mail., September.

[19] Thaddaus Weniger, Kjersti Berg, and Matthias Resch. Techno-economic analysis of skagerak energylab. Technical Report 502001599, SINTEF, Postboks 4761 Torgarden 7465 Trondheim, February 2020.

[20] Frida Berglund. Optimal operation of battery storage for peak shaving applications. Master's thesis, NTNU: Norwegian University of Science and Technology, Trondheim, Norway, 2018.

[21] Usama Bin Irshad, Mohammad Sohrab Hasan Nizami, Sohaib Rafique, M. Jahangir Hossain, and Subhas Chandra Mukhopadhyay. A battery energy storage sizing method for parking lot equipped with ev chargers. *IEEE Systems Journal*, 15(3):4459–4469, 2021.

[22] Eirik Haugen. Optimization of battery energy storage system: A case study for an electric vehicle fast-charging station. Master's thesis, NTNU: Norwegian University of Science and Technology, Trondheim, Norway, 2020.

[23] David Feldman, Vignesh Ramasamy, Ran Fu, Ashwin Ramdas, Jal Desai, and Robert Margolis. U.s. solar photovoltaic system and energy storage cost benchmark (q1 2020).

[24] R M Dell and D A J Rand. *Understanding Batteries*. RSC Paperbacks. The Royal Society of Chemistry, 2001.

[25] Souleman N. Motapon, Enric Lachance, Louis-A. Dessaint, and Kamal Al-Haddad. A generic cycle life model for lithium-ion batteries based on fatigue theory and equivalent cycle counting. *IEEE Open Journal of the Industrial Electronics Society*, 1:207–217, 2020.

References

[26] Héricles Eduardo Oliveira Farias and Luciane Neves Canha. Battery energy storage systems (bess) overview of key market technologies. In *2018 IEEE PES Transmission Distribution Conference and Exhibition - Latin America (TD-LA)*, pages 1–5, 2018.

[27] Ellen (Bryte batteries) Loxley. Bryte batteries. e-mail, presentation. Dec 2022.

[28] IRENA. Solution x: Utility-scale battery solutions. pages 1–9, 2019.

[29] Andrew W. Thompson. Economic implications of lithium ion battery degradation for vehicle-to-grid (v2x) services. *Journal of Power Sources*, 396:691–709, 2018.

[30] Terrence Xu, Wei Wang, Mikhail Gordin, Donghai Wang, and Daiwon Choi. Lithium-ion batteries for stationary energy storage. *JOM*, 62:24–30, 09 2010.

[31] Ruifeng Zhang, Bizhong Xia, Baohua Li, Libo Cao, Yongzhi Lai, Weiwei Zheng, Huawen Wang, and Wei Wang. State of the art of lithium-ion battery soc estimation for electrical vehicles. *Energies*, 11:1820, 07 2018.

[32] Bolun Xu, Alexandre Oudalov, Andreas Ulbig, Göran Andersson, and D.s Kirschen. Modeling of lithium-ion battery degradation for cell life assessment. *IEEE Transactions on Smart Grid*, 99:1–1, 06 2016.

[33] Peter Keil. *Aging of Lithium-Ion Batteries in Electric Vehicles*. PhD thesis, Technische Universität München, Lehrstuhl für Elektrische Energiespeichertechnik. Fakultät für Elektrotechnik und Informationstechnik, 2017.

[34] Maik Naumann. *Techno-economic evaluation of stationary battery energy storage systems with special consideration of aging*. PhD thesis, Technische Universität München, Lehrstuhl für Elektrische Energiespeichertechnik. Fakultät für Elektrotechnik und Informationstechnik, 2018.

[35] Khalid Abdulla, Julian de Hoog, Valentin Muenzel, Frank Suits, Kent Steer, Andrew Wirth, and Saman Halgamuge. Optimal operation of energy storage systems considering forecasts and battery degradation. *IEEE Transactions on Smart Grid*, 9(3):2086–2096, 2018.

[36] Seyed Mohammad Rezvanizaniani, Zongchang Liu, Yan Chen, and Jay Lee. Review and recent advances in battery health monitoring and prognostics technologies for electric vehicle (ev) safety and mobility. *Journal of Power Sources*, 256:110â124, 06 2014.

[37] Ying Wang, Zhi Zhou, Audun Botterud, Kaifeng Zhang, and Qia Ding. Stochastic coordinated operation of wind and battery energy storage system considering battery degradation. *Journal of Modern Power Systems and Clean Energy*, 4(4):581–592, 2016.

References

[38] Guannan He, Qixin Chen, Chongqing Kang, Pierre Pinson, and Qing Xia. Optimal bidding strategy of battery storage in power markets considering performance-based regulation and battery cycle life. *IEEE Transactions on Smart Grid*, 7(5):2359–2367, 2016.

[39] Smith Earleywine K. et al. Comparison of plug-in hybrid electric vehicle battery life across geographies and drive cycles. In *SAE Technical Paper*, 2012.

[40] Gyan, P., Aubret, P., Hafsaoui, J., Sellier, F., Bourlot, S., Zinola, S., and Badin, F. Experimental assessment of battery cycle life within the simstock research program. *Oil Gas Sci. Technol. - Rev. IFP Energies nouvelles*, 68(1):137–147, 2013.

[41] Justin Purewal, John Wang, et al. Degradation of lithium ion batteries employing graphite negatives and nickelâcobaltâmanganeseÂ oxide +Â spinel manganese oxide positives: Part 1, aging mechanisms and life estimation. *Journal of Power Sources*, 272:937–948, 2014.

[42] Sofiane Belaid, Remy Mingant, Martin Petit, Joseph Martin, and Julien Bernard. Strategies to extend the lifespan of automotive batteries through battery modeling and system simulation: The mobicus project. In *2017 IEEE Vehicle Power and Propulsion Conference (VPPC)*, pages 1–9, 2017.

[43] Cole Wesley, Frazier A. Will, and Augustine Chad. Cost projections for utility-scale battery storage: 2021 update. Technical Report DE-AC36-08GO28308, NREL, 15013 Denver West Parkway Golden, CO 80401, 2021.

[44] PNNL: Pacific Northwest National Laboratory. Lithium-ion battery (lfp and nmc). `https://www.pnnl.gov/lithium-ion-battery-lfp-and-nmc`, 2021. Accessed: 2022-09-28.

[45] Zeenat Hameed, Seyedmostafa Hashemi, Hans Henrik Ipsen, and Chresten Træholt. A business-oriented approach for battery energy storage placement in power systems. *Applied Energy*, 298:117186, 2021.

[46] Ryutaka Yudhistira, Dilip Khatiwada, and Fernando Sanchez. A comparative life cycle assessment of lithium-ion and lead-acid batteries for grid energy storage. *Journal of Cleaner Production*, 358:131999, 2022.

[47] NREL. Life cycle greenhouse gas emissions from electricity generation. `https://www.nrel.gov/analysis/life-cycle-assessment.html`, 2021. Accessed: 2022-10-24.

[48] S. Frederick Hillier and J. Gerald Lieberman. *Introduction to Operations Research*. McGraw-Hill, New York, NY, 2010.

[49] Ivar Wangensteen. *Power System Economics - the Nordic Electricity Market*. Fagbokforlaget, Bergen, 2019.

[50] Statnett. Systemdrifts- og markedsutviklingsplan. `https://www.statnett.no/globalassets/for-aktorer-i-kraftsystemet/utvikling-av-kraftsystemet/smup/systemdrifts--og-markedsutviklingsplan-2022-2030.pdf`, 2021. Accessed: 2023-01-18.

[51] Nord Pool AS. Day-ahead prices. `https://www.nordpoolgroup.com/en/Market-data1/Dayahead/Area-Prices/ALL1/Hourly/?view=table`, Access to historical spot prices provided in october 2022, October.

[52] Statnett. Om strømpriser. `https://www.statnett.no/om-statnett/bli-bedre-kjent-med-statnett/om-strompriser/`, 2022.

[53] Nettselskapet AS. Nettleie. `https://nettselskapet.as/nettleie-2022/`.

[54] REN / SINTEF Energi. Planbok for kraftnett. `https://www.sintef.no/prosjekter/1993/planleggingsbok-for-kraftnett/`, 2019. Accessed: 2022-09-26.

[55] NVE. Reinvesterings- og fremskyndingskostnader. `https://www.nve.no/reguleringsmyndigheten/regulering/nettvirksomhet/anleggsbidrag/beregning-av-anleggsbidrag/reinvesterings-og-fremskyndingskostnader/`, 2021. Accessed: 2023-01-16.

[56] Møre Trafo AS. Standard transformatorer. `https://moretrafo.no/produkter/500-kva/`, 2020. Accessed: 2022-11-16.

[57] Julia. Julia 1.8 documentation. `https://docs.julialang.org/en/v1/`, 2022. Documentation on Julia programming language.

[58] Iain Dunning, Joey Huchette, and Miles Lubin. Jump: A modeling language for mathematical optimization. *SIAM Review*, 59(2):295–320, 2017.

[59] COIN-OR. Ipopt documentation. `https://coin-or.github.io/Ipopt/index.html`, 2022. Documentation on IPOPT solver.

[60] Apoorv Lal. Interior-point method for nlp. *Cornell University*, 2021.

[61] Eidsiva. Peak shaper: Batteritjenesten som løser kapasitetsutfordringer i nettet. `https://www.eidsiva.no/vekst/peak-shaper/`, 2022. Accessed: 2023-01-24.

[62] Trevor M Letcher. *Managing Global Warming - An Interface of Technology and Human Issues*. Academic Press, Elseviever, 125 London Wall, London EC2Y 5AS, United Kingdom, 2019.

[63] Marcus King, Anjali Jain, Rohit Bhakar, Jyotirmay Mathur, and Jihong Wang. Overview of current compressed air energy storage projects and analysis of the potential underground storage capacity in india and the uk. *Renewable and Sustainable Energy Reviews*, 139:110705, 2021.

[64] Jarand Hole and Hallgeir Horne. Batterier vil bli en del av kraftsystemet. `https://publikasjoner.nve.no/faktaark/2019/faktaark2019_14.pdf`, 2019. Accessed: 2022-09-21.

[65] Ieee guide for design, operation, and maintenance of battery energy storage systems, both stationary and mobile, and applications integrated with electric power systems. *IEEE Std 2030.2.1-2019*, pages 1–45, 2019.

[66] NEK Standard Norge. Standarder for sikkerhet ved installasjon og drift av batterier og energilagringssystemer. internet, 2019. Accessed: 2023-01-16.

[67] DNV. 2020 battery performance scorecard. Technical report, DNV, 2020.

[68] DNV. Dnv-rp-0043 safety, operation and performance of grid-connected energy storage systems - revised. Technical report, DNV, 2021.

[69] SSB. Electricity prices in the end-user market, by type of contract (øre/kwh) 2012 - 2021.

[70] SSB. Consumer price index.

[71] The European Commission PVGIS. Photovoltaic geographical information system (pvgis). `https://re.jrc.ec.europa.eu/pvg_tools/en/tools.html`, (Tool for estimation of PV energy production), 2022. PVGIS tool.

[72] PEIMAR. *OR10H545M: Half cell line*. PEIMAR: Italian photovoltaic modules.

A Properties of Different Energy Storage Technologies

Table A.1: A comparison of different energy storage technology categories with sub-technologies [2, 26, 62].

Energy storage category	Sub-technology	Use / location	Energy capacity	Power capacity	Storage period (short term / long term)[1]	Discharge time	Response time	Lifespan [years][2]
Electro-chemical	Li-ion	FTM/BTM	<100 MWh	1.0 kW - 50 MW	Short term / med. term	Min. – hours	ms. - sec.	5 - 15 (20)
	NaS	FTM	<100 MWh	<10 MW	Med. term / long term	1.0 - 24 h	sec. - min.	<15
	Pb-Acid	FTM/BTM	<10 MWh	some MW	Short term / med. term	Min. – hours	ms.	5 - 15
	Ni-Cd	-	some MWh	some MW	Short term - long term	Sec. – hours	ms.	10 - 20
	Ni-MH	-	some MWh	some MW	-	-	-	5 - 15
	VRFB (flow)	FTM	<100 MWh	<10 MW	Long term	Sec. – hours	sec. - min.	10 - 20
	Zn Br (flow)	FTM	<100 MWh	<10 MW	Long term	-	-	5 - 10
Electrical	SCES	FTM	<10 kWh	0.1 - 5.0 MW	Short term	ms. - hours.	<10 ms.	8 - 20
	SMES	FTM	<5 kWh	0.1 - 5.0 MW	Short term	ms. - min.	<100 ms.	20 - 30
Thermal	STES	FTM/(BTM)	10 - 50 kWh/t	1.0 kW - 1.0 MW	Med. term - long term (day-months)	Minutes	days - months	10 - 30
	PCM*	FTM/BTM	50 - 150 kWh/t	1.0 kW - 1.0 MW	Short term - long term (hours - months)	Hours – days	<10 min.	20 - 40
	TCS*	FTM	12 - 250 kWh/t	1.0 kW - 1.0 MW	Short term / med. term (hours - days)	Hours – days	<10 min	10 - 30
Mechanical	CAES[(3)]	FTM	500 kWh - 16 GWh	<1.0 GW	Med. term / long term	Hours	<15 min	30 - 100
	PHS	FTM	<25 GWh	10 MW - 5.0 GW	Med. term / long term	Hours – days	Sec. - min.	~60
	FES	FTM	1.0 - 200 kWh	<20 MW	Short term (seconds)	ms. - min.	ms. - min.	>10 (10^5 cycles)

---

[1]Long term is typically seasonal.

[2]Dependent on usage. Assumed moderate operating conditions

(*) Denotes technologies currently under development.

Abbreviations:

CAES: Compressed Air Energy Storage. [3]

FES: Flywheel Energy Storage.

Li-ion: Lithium-ion.

NaS: Sodium-sulfur.

Ni-Cd: Nickel-cadmium.

Ni-MH: Nickel metal hydride.

Pb-Acid: Lead-acid.

PCM: Latent-phase Change Material.

PHS: Pumped Hydro Storage.

SCES: Supercapacitor Energy Storage.

SMES: Superconductive Magnetic Energy Storage.

STES: Sensible Thermal Energy Storage.

TCS: Thermochemical Storage.

VRFB: Vanadium Redox Flow Batteries.

Zn Br: Zinc Bromine Flow Batteries.

---

[3]

Largest facility: 16 GWh [63]

Table A.2: A comparison of characteristics for different battery technologies, for stationary applications [2, 26].

Battery type	Specific energy [Wh/kg]	Energy density [kWh/m^3]	Round-trip efficiency [%]	Daily self discharge [%]	Cycle life [# of cycles]*	Lifespan [years]	CAPEX** (capacity) [NOK/kWh]	CAPEX** (power) [NOK/kW]	OPEX** [NOK/kW/yr]
Li-ion	100 - 210	200 - 500	78 - 98	0.10 - 0.33	2 000 - 10 000	5.0 - 20	3 000 - 23 000	8 400 - 37 000	50 - 110
NaS	100 - 240	100 - 280	70 - 90	0.05 - 20.0	2 000 - 5 000	10 - 15 (20)	2 800 - 5 000	3 700 - 28 000	90 - 750
Pb-Acid	30 - 50	25.0 - 100	70 - 85	0.10 - 0.30	500 - 3 000	5.0 - 15	560 - 3 200	2 800 - 6 100	90 - 470
Ni-Cd	40 - 80	30.0 - 150	60 - 90	0.20 - 0.60	1 500 - 3 500	10 - 20	3 700 - 22 500	4 700 - 14 000	< 200
Ni-MH	30 - 90	100 - 300	50 - 80	0.30 - 1.00	1 000 - 3 500+	5 - 15	-	-	-
VRFB (flow)	10 - 35	1.0 - 34	60 - 80	0.01 - 0.20	12 000+	5 - 25	1 400 - 10 000	6 000 - 15 000	90 - 650

(*) Until battery capacity is at 80 % of initial capacity. Smallest number referring to high levels of DoD (80 %) while low numbers refer to low levels of DoD (<40 %).

(**) CAPEX and OPEX are very dependent on the scale of the BESS. The values of CAPEX are total investment costs divided by either capacity or power capability.

B Li-ion Battery Degradation Mechanisms

Figure B.1 shows different degradation mechanisms, sorted based on electrode, causing both power and capacity fade.
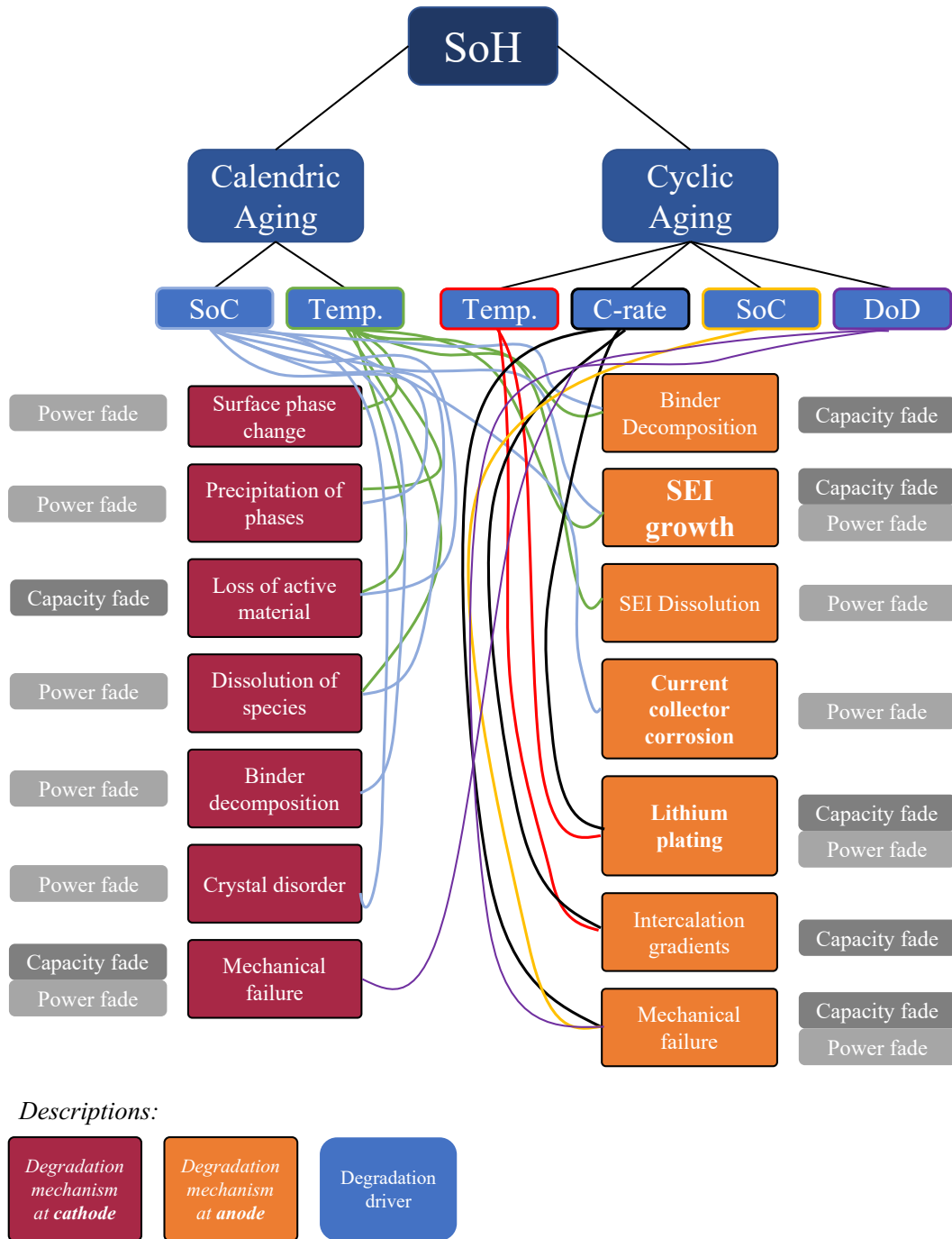

Figure B.1: Overview of the most important degradation mechanisms for Li-ion batteries, including degradation drivers Adapted from [29].

C   BESS Cost Data

Table C.1 shows a comparison of cost data for battery energy storage systems collected from several sources, converted to 2022-NOK[1]. The table contains data for different system sizes, capacities and power ranges, but are mostly reflecting costs for utility-scale applications. The values are total investment cost for a BESS, related to its storage capacity.

Table C.1: A comparison of BESS investment costs (CAPEX) obtained from literature, excluding taxes. The data is converted to 2022-NOK

Source name and citation	Bess size	Original currency and year[2]	Low estimate [NOK/kWh], (2022-NOK)*	High estimate [NOK/kWh], (2022-NOK)**	Comments
NVE [8, 64]	10 kWh, 9kW	NOK, 2019	3 100	4 800	1 hour operation, voltage support
Ying Wang (et al.) [37]	18 MWh, 6 MW	USD, 2015	3 000	6 000	3 hour operation
Usama Bin Irshad (et al.) [21]***	13.5 kWh, 5 - 7 kW	USD, 2020	⌣ 5 000		System with Tesla Powerwall
PNNL [44]	2 MWh, 1 MW	USD, 2021	4 300	5 300	Type: LFP 2 hour operation
PNNL [44]	2 MWh, 1 MW	USD, 2021	4 800	5 900	Type: NMC 2 hour operation
Wood Mackenzie: (Cole Wesley et al., NREL) [43]	-	USD, 2020	3 500	5 800	Converted to 4 hour operation
EPRI: (Cole Wesley et al., NREL) [43]	2 - 10 MWh, 1 - 5 MW	USD, 2021	2 800	4 900	Converted to 4 hour operation
PNNL: (Cole Wesley et al., NREL) [43]	4 MWh - 1 GWh, 1 - 100 MW	USD, 2020	2 700	4 000	Converted to 4 hour operation
Brattle: (Cole Wesley et al., NREL) [43]	20 - 40 MWh, 5 - 10 MW	USD, 2018	2 700	3 500	Converted to 4 hour operation

Table continues on next page

---

[1]Based on an inflation rate of 2.0 % and a linear cost reduction of 5.0 % per year until 2022.

[2]Cost data is converted to 2022-NOK using exchange rates from June 1, 2022, an inflation rate of 2 %/year and a decrease in costs of 5 %/year (from an assumed, linear cost reduction from 2020 to 2025 [43])

Appendices

Source name and citation	Bess size	Original currency and year	Low estimate [NOK/kWh], (2022-NOK)*	High estimate [NOK/kWh], (2022-NOK)**	Comments
Lazard: (Cole Wesley et al., NREL) [43]	-	USD, 2020	2 600	5 300	Converted to 4 hour operation
CPUC: (Cole Wesley et al., NREL) [43]	-	USD, 2019	2 300	4 000	Converted to 4 hour operation
David Feldman et al. [23]	30.0 - 240 MWh, 60.0 MW	USD, 2019	2 300	5 300	0.5 to 4 hour operation (utility scale)
David Feldman et al. [23]	300 kWh - 2.4 MWh, 600 kW	USD, 2020	3 000	12 700	0.5 to 4 hour operation (commercial)
David Feldman et al.[23]***	20 kWh, 5 kW	USD, 2020	∿ 5 000		4 hour operation (residential)
David Feldman et al. [23]***	6 kWh, 3 kW	USD, 2020	∿ 7 600		2 hour operation (residential)
Approximate average			*3 100*	*5 600*	*[NOK/kWh]*

System costs are assumed to include all required components for grid connection and installation labor.
Cost intervals reflect uncertainty and economy of scale.
For sources that do not provide cost intervals, an approximate cost is presented in the column of "Low estimate"

(*): Low estimate: Large-scale and/or low power capability. E.g. 3 000 NOK/kWh for 600 kW/2.4 MWh
(**): High estimate: Smaller scale and/or high power capability. E.g. 12 700 NOK/kWh for 600 kW/300 kWh
(***): Excluded in calculation of average.

D   BESS Regulations

There are several guides, standards and regulations to consider for designing, maintenance and operation of BESS installations. *IEEE Guide for Design, Operation, and Maintenance of Battery Energy Storage Systems, both Stationary and Mobile, and Applications Integrated with Electric Power Systems* ([65], 2019), describes approaches and methods for such cases. It also includes notes and guides on how to connect stationary or mobile battery storage systems to the power grid and to end users (grid customers) [13].

NEK, The Norwegian Electrotechnical Committee, has also published several standards that is about, or touching upon, battery energy storage systems [66]. Some of these are:

- **NEK 487:2022**: Safety requirements for secondary batteries and battery installations. Consisting of NEK 485:2022 and NEK 486:2021, for lead-acid and Li-ion batteries, respectively. These are translations of the international and european standards EN IEC 62485-2:2018 and EN IEC 62485-5:2020.

- **NEK IEC TS 62933-5-1:2017**: Electrical energy storage (EES) systems. Safety considerations for grid-integrated EES systems.

- **NEK EN 50549-1** and **NEK EN 50549-2:** Requirements for micro-generating plants and generating plants to be connected in parallel with distribution networks.

DNV has several reports on safety aspects of BESS installations. A Li-ion battery goes through thorough testing, involving heating, vibrations, resilience against pressure and high currents. Two very relevant publications on approvals, validations and safety performance for BESS installations, made by DNV, are:

- *2020 Battery Performance Scorecard, [67].*

- *Safety, operation and performance of grid-connected energy storage systems*, [68].

E   Electricity Cost Data and Notes on Economical Aspects

Costs Associated with Consumption of Electrical Energy in Norway

Figure E.1 shows historical electricity prices, excluding taxes and grid tariff. A significant increase in electricity costs are seen in the end of 2021, continuing in 2022, due to the state of the European electricity market.
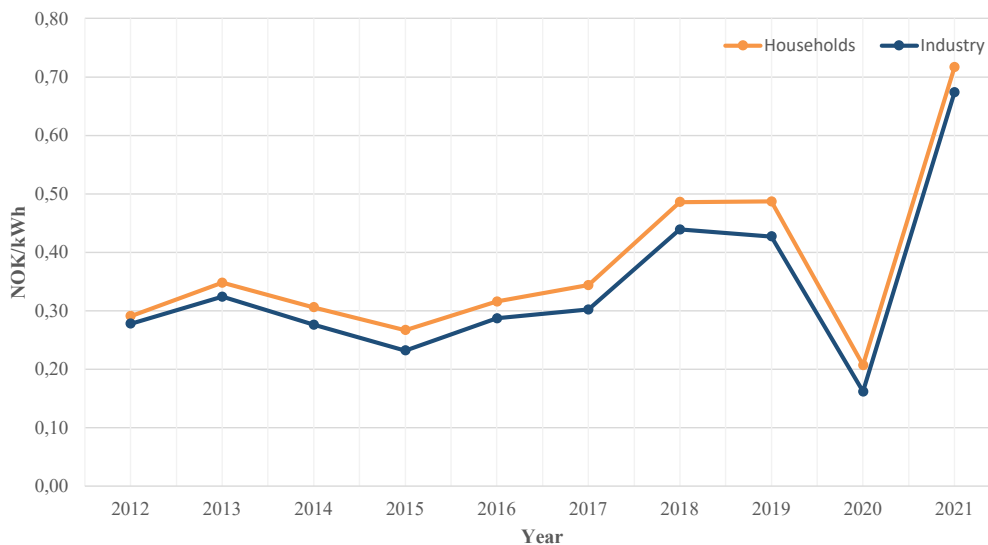
Figure E.1: Historical average electricity prices for Norway (all price zones), excluding taxes, grid tariffs and any support scheme. For households and industry, excluding power intensive industry, for all contract types [69].

Grid Tariff

Table E.1 shows the components of the grid tariff for big industries connected to the distribution grid of Nettselskapet AS[1], having an electricity consumption above 100 000 kWh per year. This model of grid tariff is known as power tariff, as opposed to capacity tariff which is used for end users with consumption below 100 000 kWh.

---

[1]The local DSO and grid owner in Fosen, Trøndelag

Table E.1: *Nettselskapet AS* grid tariffs for business / industry with consumption > 100 000 kWh/year and high voltage connection. Prices including 25 % VAT. [53]

Description	Price (value)	Unit
Fixed part	2087.5	NOK/month
Energy part	3.75	øre/kWh
Power part, winter[1]	60.0	NOK/kW/month
Power part, summer[2]	21.25	NOK/kW/month
General tax on electric power, low rate[3]	8.91	øre/kWh
General tax on electric power, high rate[4]	15.41	øre/kWh
Tax on electric power, reduced rate[5]	0.546	øre/kWh
Tax to the energy fund	1 000	NOK/year

The power part is based on the average of the three hours with highest consumption, happening at three different days, within a month.

(1): Winter period: 01.01 - 30.04 and 01.11 - 31.12

(2): Summer period: 01.05 - 31.10

(3): Low rate for the following period: 01.01 - 31.03

(4): High rate for the following period: 01.04 - 31.12

(5): Reduced rate for certain industries, equal throughout the whole year.

*For the case in this thesis, reduced rates are assumed. This is added to the energy part of the grid tariff.

Costs of Losses

In this part, a summary of the most relevant elements in calculations on costs of losses, taken from the *Planning Guide for the Power Grid* [54], are presented. The model to calculate costs of losses, described in this work, relies on some tabular data that are defined for certain ranges of years and for different locations and voltage levels in the power grid. The following data is for the grid layer where a substation is located between a 22 kV overhead line and a 230V (400V) overhead line system, for a location with low energy demand per area[2].

Table E.2b and E.2c show the cost equivalents k_{weqv} and k_p, respectively, for the time horizon and grid layer that is relevant for the case of this thesis.

---

[2]Typically sparsely populated areas, on the countryside.

Year	Value [NOK/kWh]
2024	0.495
2025	0.500
2026	0.504
2027	0.508
2028	0.512
2029	0.516
2030	0.520

Year	Value [NOK/kW/year]
2024	840
2025	862
2026	886
2027	911
2028	939
2029	969
2030	1002

(b) Equivalent yearly cost of losses, k_{weqv} [NOK/kWh] [54].

(c) Cost of maximum power losses (during max load), k_p [NOK/kW/year]* [54].

*Includes a discount rate of 4.0 (Both tables based on cost levels of 2021)

Investment Costs of Power Transformers

Power transformers and substations are expensive components in the power grid. The *Planning Guide for the Power Grid* [54] includes an overview of costs for components such as regional transformers Figures and data presented here are for cost levels of 2021.

The investment costs of substations (between 22 kV and 230 V/400 V) depend on the size/capacity of the transformer and the type of housing. The costs typically ranges from 280 000 NOK to 600 000 NOK for sizes between 315 kVA to 1600 kVA. The investment costs of larger power transformers are illustrated in figure E.2.
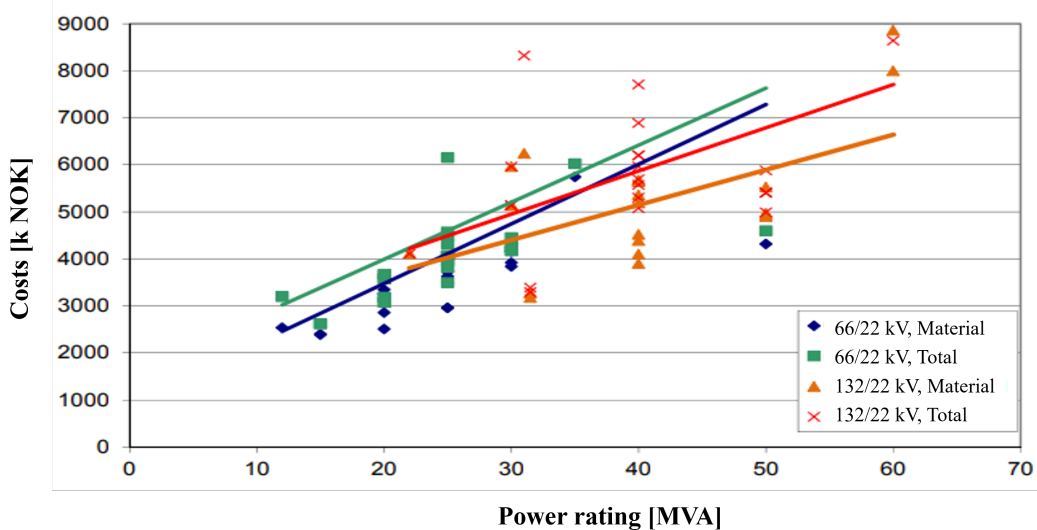

Figure E.2: Material and total costs for power transformers [54].

Economical and Financial Aspects

Several economical and financial aspects are considered in some of the calculations conducted in this thesis. Inflation is an important factor, describing the rate of increase in prices over a certain period of time. It is used to evaluate the value of money and cost data obtained from literature for different years. The consumer price index (CPI) is used as a measure on the inflation during a time interval. Figure E.3 shows the yearly changes in the consumer price index of Norway, excluding energy products and tax changes[3], from January 2015 to September 2022. The average inflation in this period is found to be **2.3 %**, which is used as basis for calculations in this thesis. Note that the inflation has increased significantly during 2022, which will affect price levels and cost data for future investments.


Figure E.3: Yearly changes of consumer price index (CPI-ATE) for each month from 2015 to 2022 [70].

---

[3]CPI-ATE is CPI adjusted for tax changes and excluding energy products, such as electricity costs. The variation in electricity prices is often causing incorrect illustration on general price development in the society, and is therefore often removed.

F   Future Load and Electricity Spot Prices

Figure F.1 shows the variations in the electricity consumption of the load / end user (active power) and electricity spot prices (NO3) for each hour throughout the whole year of 2021[1]. It is observed that the power consumption is high all year, with little variation. The load data is adapted based on the load profile registered for 2021. The electricity spot prices are provided by Nord Pool and exclude VAT as well as any surcharges [51].
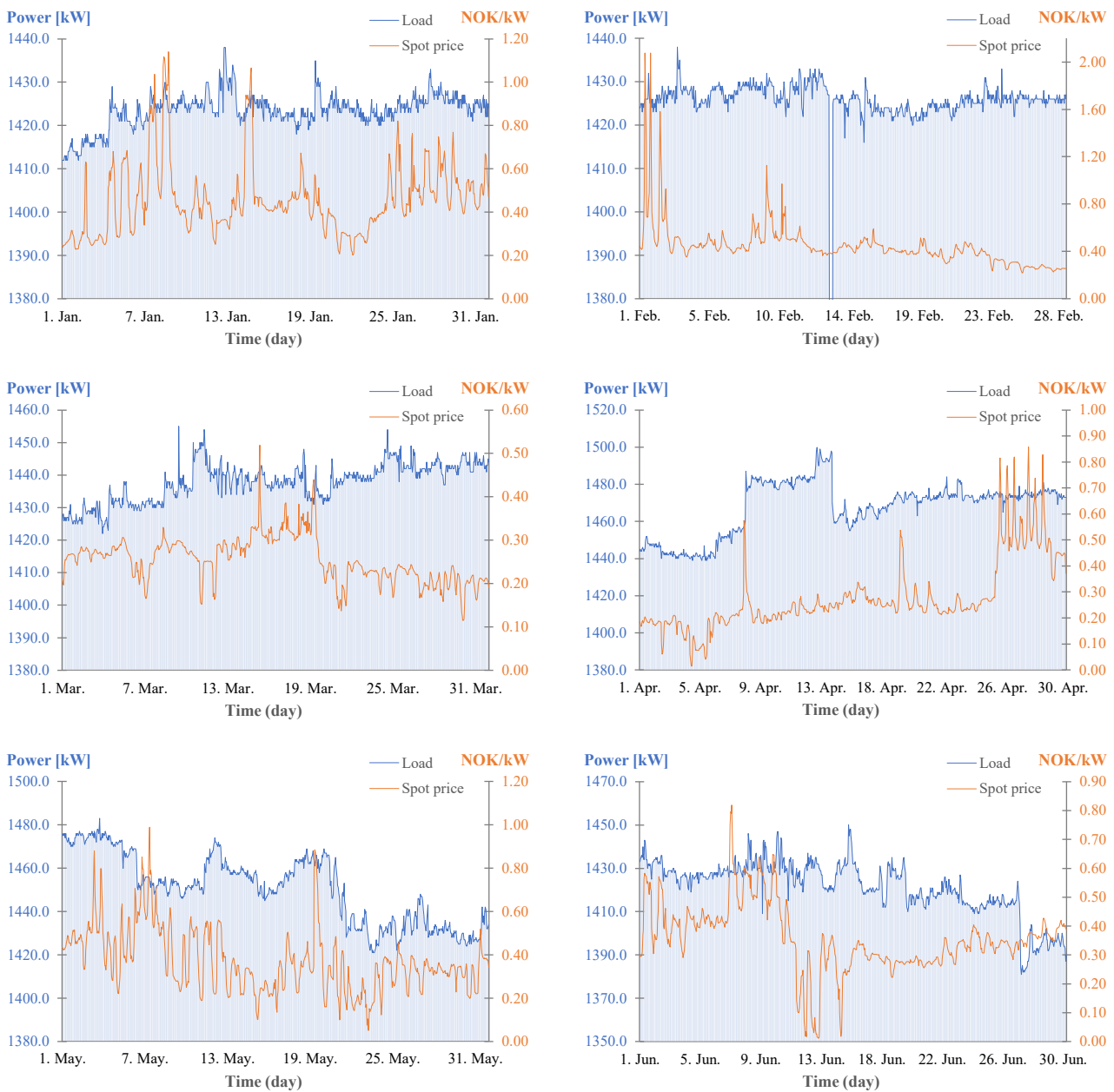
NB! Figure continues on next page
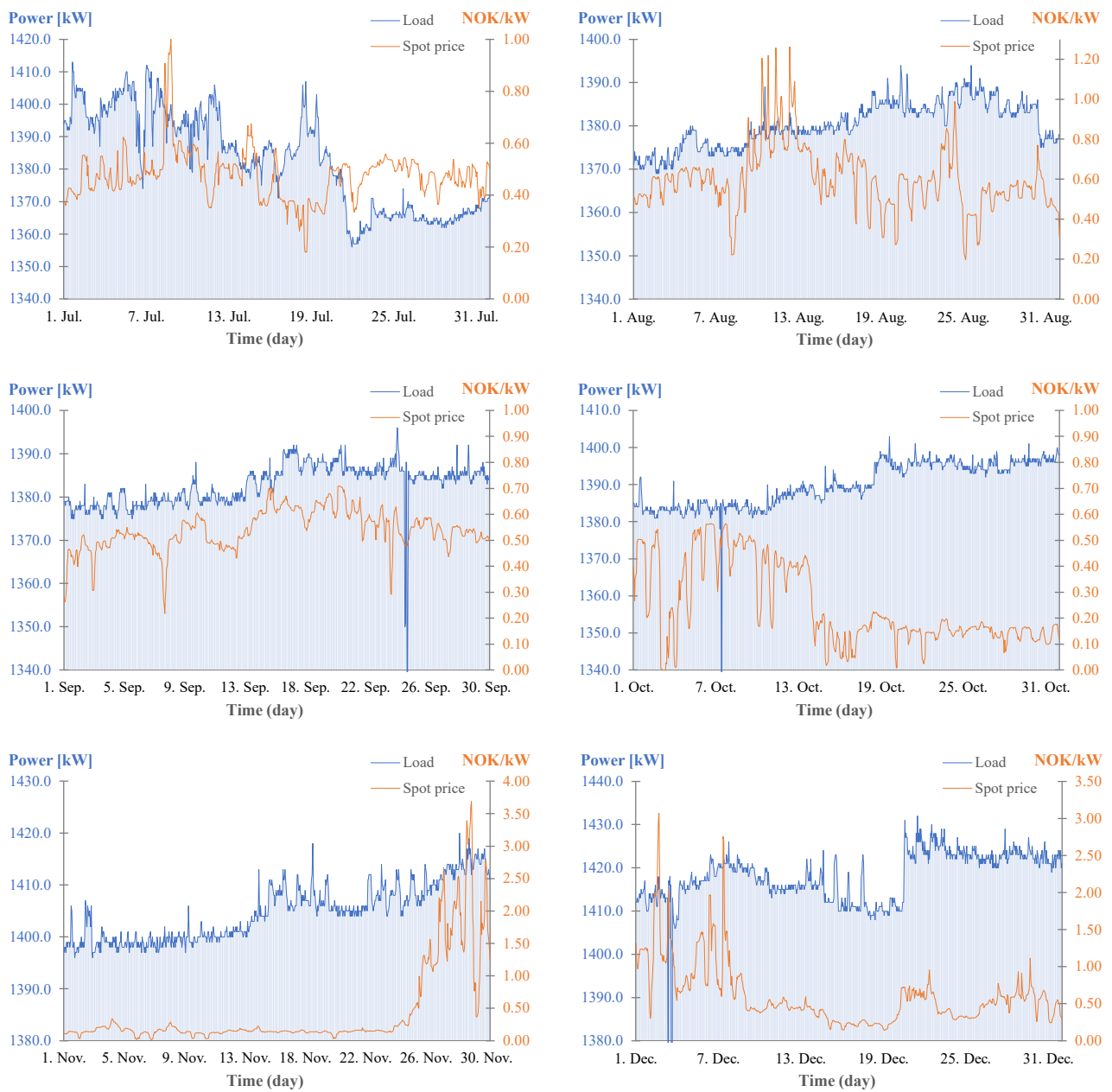
---

[1]Note the different scale of the axes.

Figure F.1: Load profile (adapted from 2021-profile) for the adapted load (end user) and elspot prices for NO3 (excl. VAT) [51, 18].

G Cases with PV and BESS

In this appendix, two extra cases that include a PV installation are described. First, the approaches and assumptions are stated, before the results of optimization are presented.

Case Approaches and Assumptions

The cases with PV assume that a rooftop PV system is installed at the location of the end user. Only the operation model, described by equations 58 to 59o, is simulated. The only difference from the original operation model, is that constraint 59b is updated to become equation 60, meaning that the load can be met by battery power, grid power and PV power. This also allows for charging the battery with power from the PV, instead of power from the grid. The updated load side, being the focus of the operation model, is illustrated in figure G.1. As depicted, the PV system and BESS are both connected to the AC bus in this case.

$$P_{load,t} = P_{T3}(t) + P_B(t) + P_{PV,t} \tag{60}$$
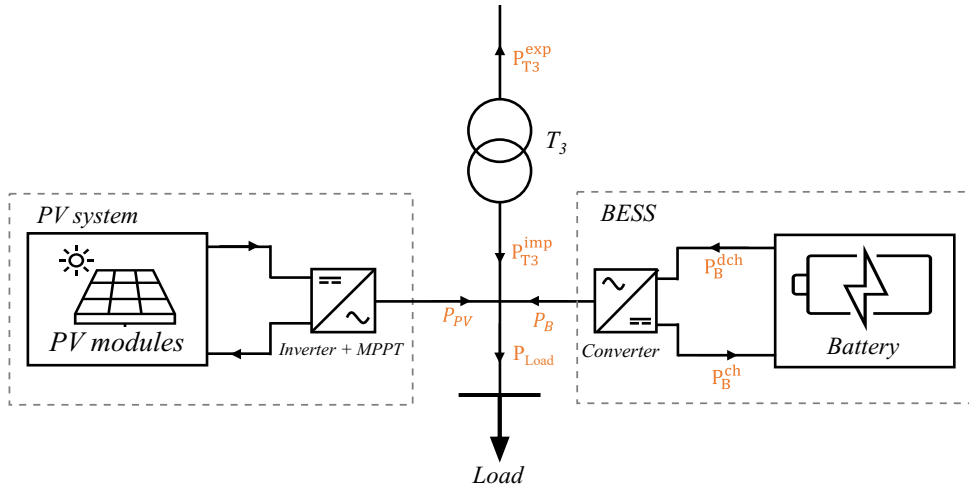
Figure G.1: A single line diagram of the case with PV and BESS.

A satellite photo of the end user is provided in figure G.2, which also indicates the rooftop area that is assumed available and suitable for PV modules. Based on the dimensions of the roof, an estimated azimuth angle (compass direction) and the ratings of an appropriate type of PV module, the hourly irradiance and electrical power output ($P_{PV,t}$) of the PV system is found by using PVGIS [71]. Relevant details on the PV system, and assumptions for the case, are given in table G.1.

Figure G.2: Overview of the area (roof) that is available for PV modules.

Table G.1: Parameter data and assumptions for the case with PV [71].

Data	Value	Description
Azimuth angle	43°	Compass direction: Southwest (90° = west, 0°= south).
Slope of the rooftop	20°	The steepness of the roof.
Radiation database	-	PVGIS-SARAH2[1]. Data from 2019.
System losses	14 %	System losses (converter, wiring, dirt etc.).
Type of PV modules	-	Peimar 545 Wp[2] [72] .
Number of modules mounted on area 1	128	Portrait mode: 2×64
Number of modules mounted on area 2	234	Portrait mode: 3×78
Total installed capacity of PV modules	197.29 kWp	PV power of the total system at STC[3]
PV electricity generation per year	137.8 MWh	Estimated electricity production per year, on the AC side, based on irradiance data of 2019.

[1]: Solar radiation based on satellite data.
[2]: PV modules with length = 2279 mm and width = 1134 mm
[3]: Standard Test Conditions: Irradiance = 1000 W/m^2, module temperature = 25 C, Air Mass = 1.5

The estimated monthly energy production from the PV system, per unit of installed capacity (kWp), is presented in figure G.3. The data is from 2019, which represent a relatively conservative estimate of the solar irradiation of the geographical location, compared to the average from 2005 to 2020. It can be observed that the highest energy production from the PV system of this case is assumed to be for April and July. There is almost no electricity production in the winter months, and especially little for December and January.
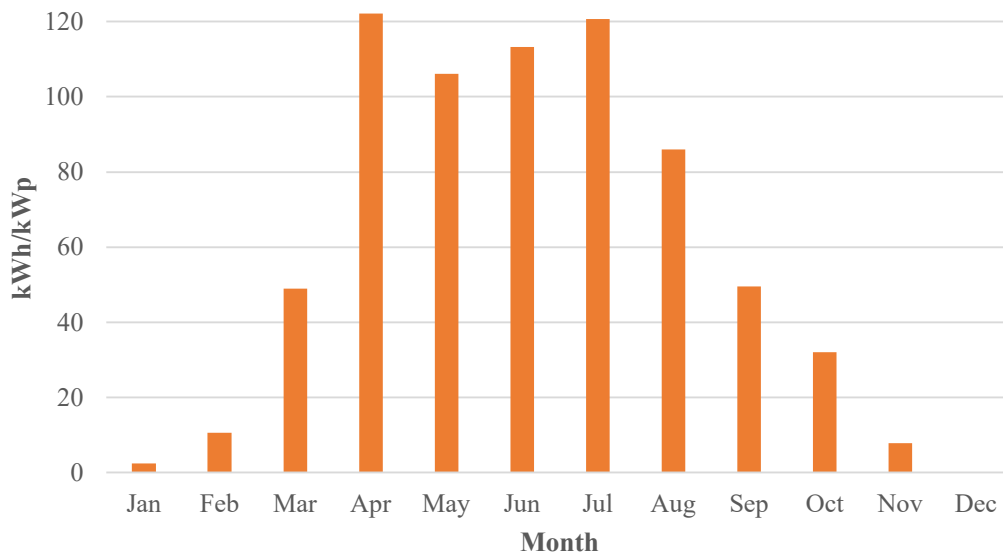

Figure G.3: Monthly energy output from the PV system, per kWp. Irradiance data from 2019 [71].

Scenarios For the Cases With PV

The PV system described above is included in both base cases without a BESS and cases with a BESS. As the life time of a PV system is assumed to be much longer than that of a BESS, including also the fact that the BESS in this case is only required for four years, the base cases assume power from the grid and PV system only. The cases with BESS and PV are simulated with the updated operation model, for four years. The assumptions and elements of the cases are in general the same as described in section **??**, with some extra information listed below:

- The load ($P_{Load,t}$) is adapted from 2021 data, giving a peak power of 1.5 MW.

- BESS sizing: 12 500 kWh, 1500 kW. Assumed investment cost: 54 MNOK (excl. VAT).

- Life time of the PV system: 30 years, with one replacement of the inverter.

- The BESS is only operated for the first four years. From the fifth year, the load is covered by the PV system and power grid only.

- Electricity spot prices of NO3, for 2021, and of NO5, for 2022, are used. These are repeated for every year of the cases.

Results

Figure G.4 shows the most relevant input data and output variables from the optimization model, for a week in May. On the bottom, the electricity spot price is plotted, which is for NO3 (2021). In the middle, the PV production and load are plotted. It shows that the PV production have peaks at the middle of the days, with some variations due to weather conditions. The load has a flat profile, with a relatively steady power which is just below 1.5 MW. On the top, the power flow through substation T3 (grid power) and the SoC of the battery is presented.
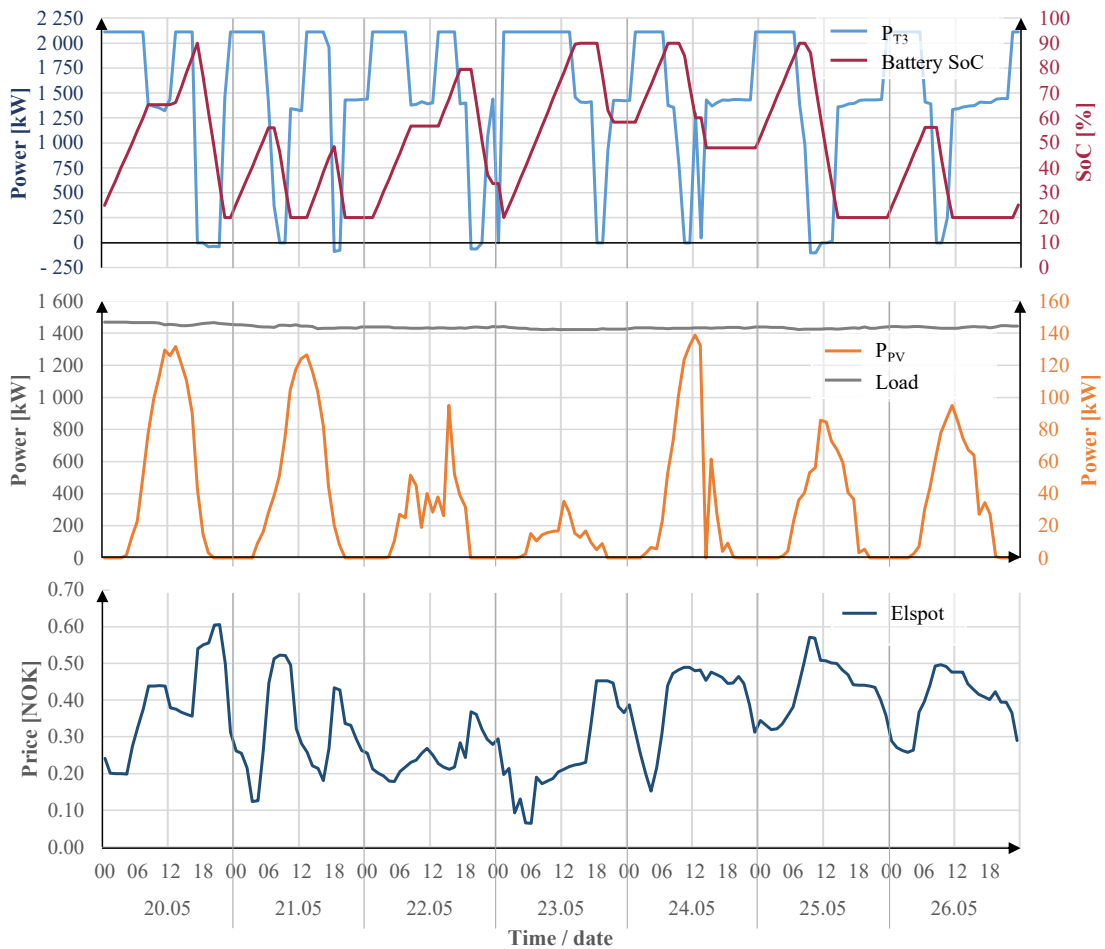

Figure G.4: Plots of PV power, load, BESS usage and elspot prices for a week in May.

It can be observed that for high elspot prices, for instance at the evening of the first day, the BESS is discharging to cover the load in stead of having to import power from the grid. At such instances, a small amount of power (maximum 100 kW) is also exported to the grid through T3. The combination of PV and BESS to reduce energy costs can also be seen during, for instance, the time of the highest PV power at day five. Here, the PV and BESS are used together to cover most of the load. The graphs indicate that the BESS is used actively to optimize the use of the PV power and the grid power.

As for the main cases of this thesis, the net present value (NPV) is used as a measure on the feasibility of the investment in a PV system together with the BESS. But for these cases, the NPV of savings in energy costs, compared to the case of no PV and no BESS (see figure 28), is expressed rather than the net present costs of operation. Table G.2 and G.3 show the breakdown of the net present cost calculations for some years until the life time of the PV system is reached (30 years)[1]. The first table is for the scenario with elspot prices of NO3 from 2021 while the second is for a scenario with elspot prices of NO5 from 2022. All operating costs, such as energy costs, power costs, costs of transformer losses and maintenance costs are included.

Table G.2a shows the net present values of cost savings after y years, when only having a PV installation and power from the grid. It also shows how big the total investment cost can be, per unit of installed PV capacity (NOK/W$_p$), in order to give a positive NPV after y years. For instance, the investment cost is required to be 5.60 NOK/Wp, or lower, to get a positive NPV after 18 years. The same results are provided in table G.2b for the case when a BESS is operated for the four first years. It is observed that the NPV of energy cost savings are 67 700 NOK higher for the case including a BESS, after four years. In other words, the battery installation increases the feasibility of the system, considering operation costs. However, due to the high investment costs of the BESS, the energy cost savings will not be able of covering the investment costs of the whole system.

Table G.2: Net present values of energy cost savings, for BESS + PV (NO3 elspot, 2021).

Year (y)	Present value [NOK]	Net present value, NPV [NOK]	Inv. cost for positive NPV in year (y) [NOK/Wp]	Year (y)	Present value [NOK]	Net present value, NPV [NOK]	Inv. cost for positive NPV in year (y) [NOK/Wp]
1	77 100	77 100	-	1	-	-	-
4	72 700	299 600	1.52	4	-	367 300	1.86
7	68 600	509 600	2.59	7	68 600	577 200	2.93
10	64 700	707 600	3.59	10	64 700	775 300	3.93
13	61 000	894 500	4.54	13	61 100	962 100	4.88
15	-21 300	933 100	4.74	*15*	-21 300	1 000 800	5.08
18	55 400	1 102 700	5.60	18	55 400	1 170 300	5.94
21	52 300	1 262 600	6.41	21	52 300	1 330 300	6.75
24	49 300	1 413 500	7.18	24	49 300	1 481 200	7.52
27	46 500	1 555 900	7.90	27	46 500	1 623 600	8.24
30	43 900	1 690 200	8.58	30	43 900	1 757 900	8.92

    (a) PV + power grid (no BESS).   (b) PV + power grid + BESS (4 years).

---

[1]NPV calculated according to equation 22, with a discount rate of 4.0 %. The calculations assume replacement of the PV inverter after 15 years, at a cost of 80 000 NOK (including discounting).

Table G.3a and G.3b contain similar results, for the scenario with an electricity spot price of NO5, from 2022. This elspot price is characterized by high values, and large daily variations. As indicated by the tables, the cost savings are significantly higher with the inclusion of a PV system in this case. The investment cost of the PV system can for instance be as high as 19.7 NOK/W$_p$ to give a positive NPV after 13 years, which is a very high price for such a system. Considering the inclusion of a BESS for the first four years as well, the same investment costs would result in a positive NPV before the end of the operation phase of the BESS (i.e. less than four years). After four years of BESS operation with PV, the NPV is more than 2.8 MNOK greater than that of only a PV system. This indicates that the BESS increases the economical feasibility of the system significantly, for this scenario. But the savings are not high enough to cover the investment costs of the combined system, having a value of 10.44 MNOK, compared to 54 MNOK for the BESS investment.

Table G.3: Net present values of energy cost savings, for BESS + PV (NO5 elspot, 2022).

Year (y)	Present value [NOK]	Net present value, NPV [NOK]	Inv. cost for positive NPV in year (y) [NOK/Wp]	Year (y)	Present value [NOK]	Net present value, NPV [NOK]	Inv. cost for positive NPV in year (y) [NOK/Wp]
1	334 800	334 800	1.70	1	-	-	-
4	315 900	1 301 100	6.60	4	-	4 138 200	21.0
7	298 000	2 212 700	11.2	7	298 000	5 049 800	25.6
10	281 100	3 072 700	15.6	10	281 100	5 909 800	30.0
13	265 200	3 884 000	19.7	14	265 211	6 721 200	34.1
15	175 100	4 319 200	21.9	*15*	175 100	7 156 400	36.3
18	240 700	5 055 500	25.7	18	240 700	7 892 700	40.1
21	227 000	5 750 100	29.2	21	227 100	8 587 300	43.6
24	214 200	6 405 400	32.5	24	214 200	9 242 600	46.9
27	202 000	7 023 600	35.7	27	202 100	9 860 800	50.1
30	190 700	7 606 800	38.6	30	190 700	10 444 000	53.0

(a) PV + power grid (no BESS). (b) PV + power grid + BESS (4 years).

The scenarios assume that the BESS only is operated for the first four years, and that the grid is capable of covering the load alone after that time. At the end of this period, the battery packs are found to have a SoH of 79.2 - 79.3 %, meaning that there still is a substantial amount of capacity left, that can be used for energy arbitrage and further cost savings. This can increase the feasibility of the system.